Max–Planck–Institut für Astrophysik

LMU TUM ORIGINS Excellence Cluster

SFB 1258 Neutrinos Dark Matter Messengers

SNνD 2023@LNGS

International Conference on Supernova Neutrino Detection

Gran Sasso National Laboratory, Assergi, L'Aquila, Italy; May 29–June 01, 2023

Core-Collapse Supernovae in 3D

From the Explosion Mechanism to Observational Properties

Hans-Thomas Janka

Max Planck Institute for Astrophysics

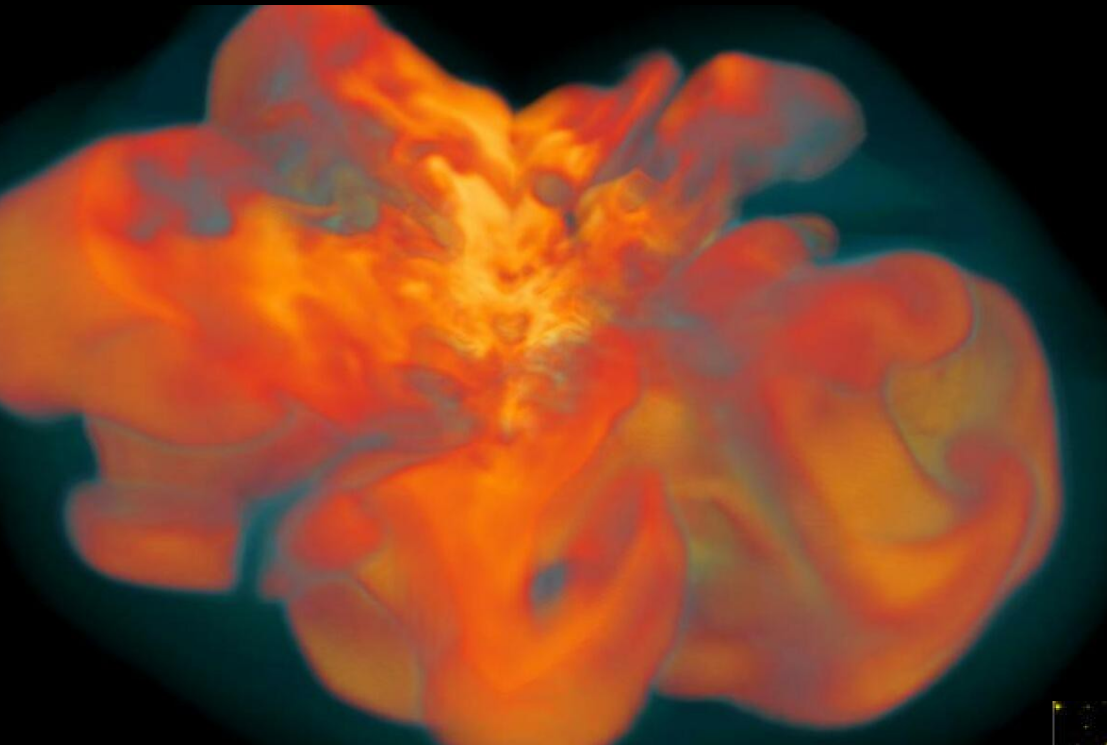
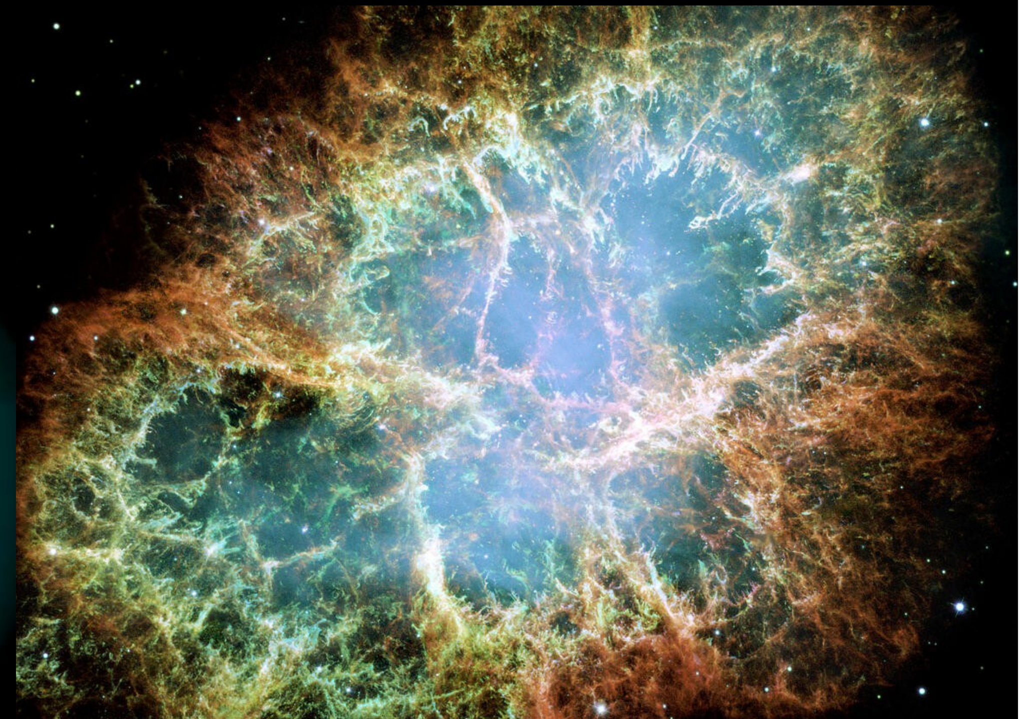
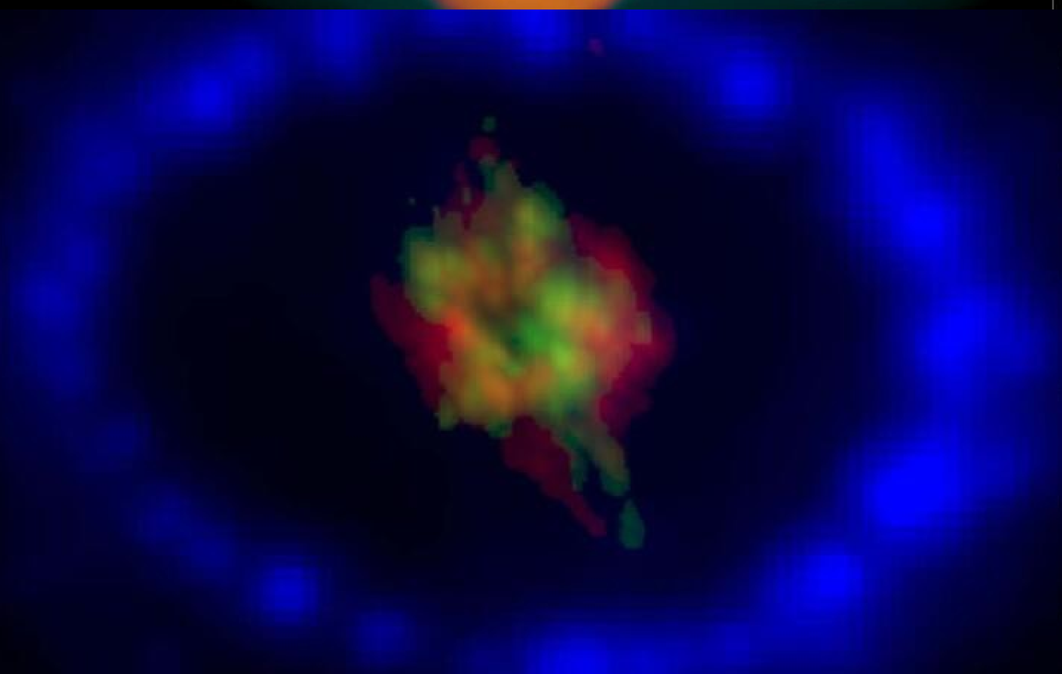
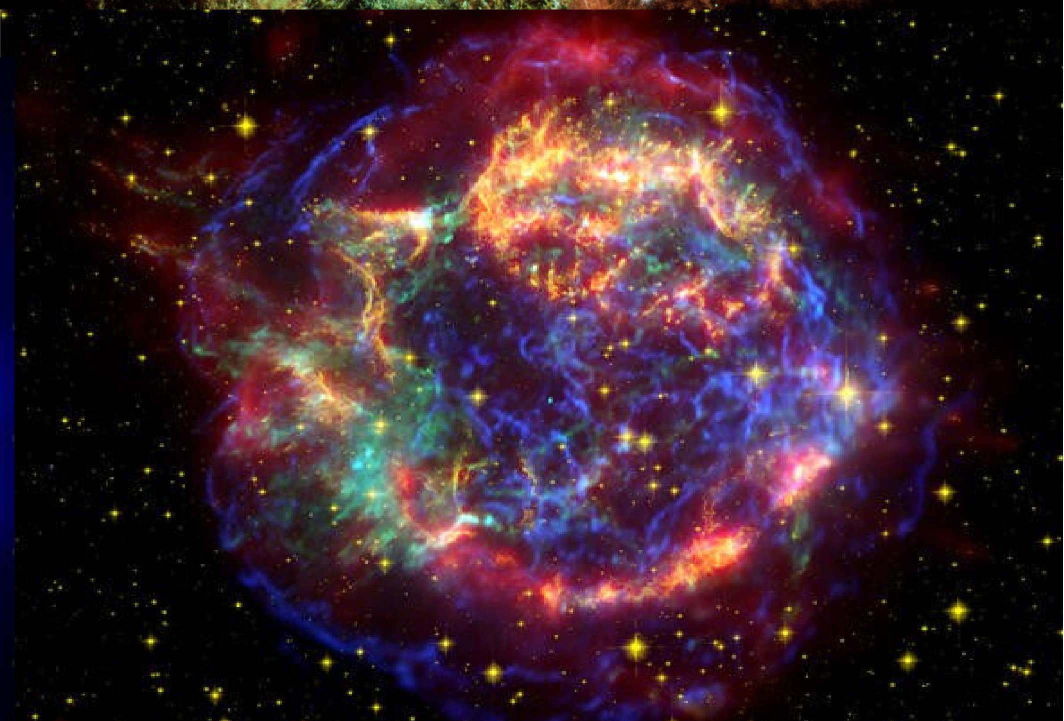

Source: HTJ & Bauswein, Handbook of Nuclear Physics
(Springer-Nature, 2023)

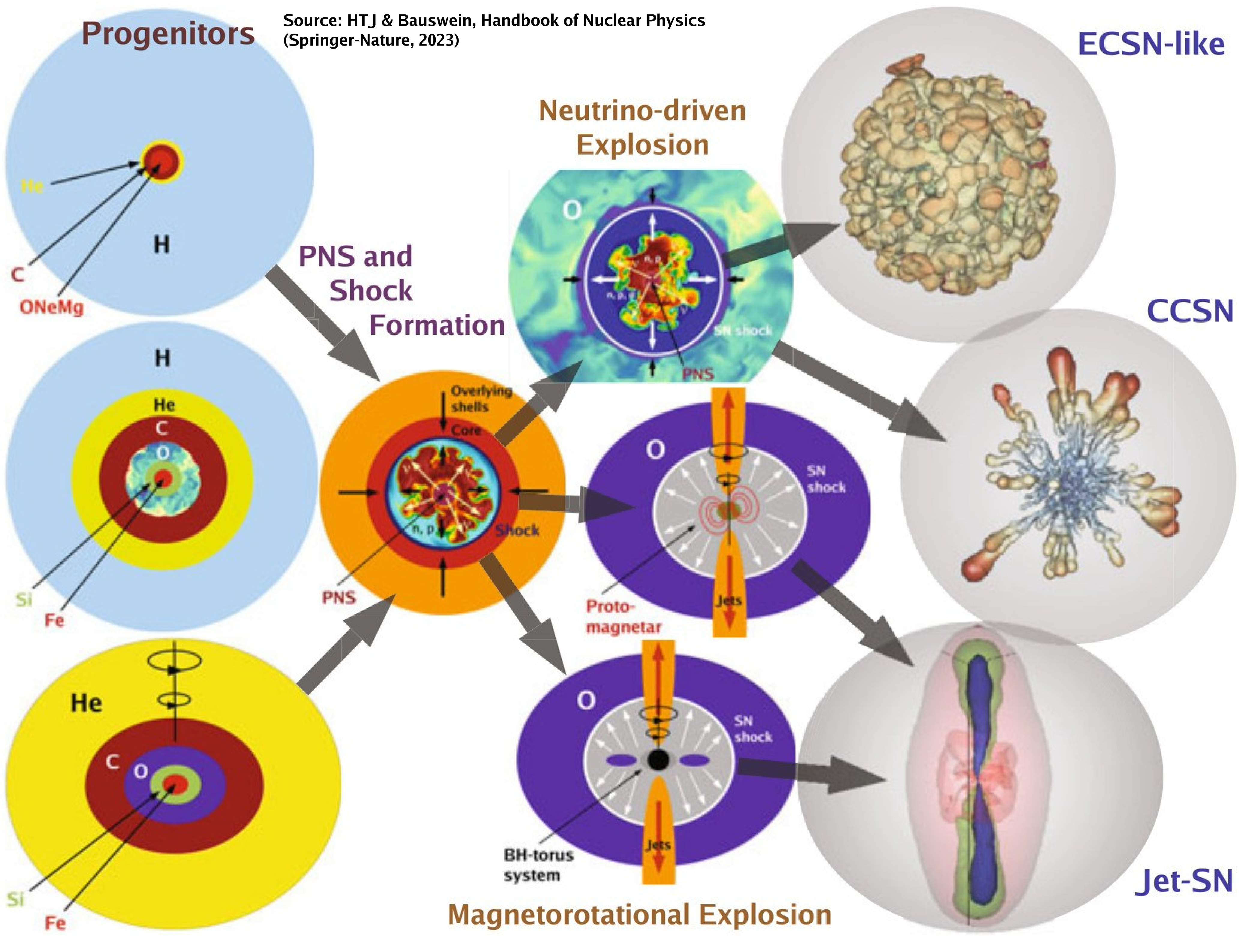

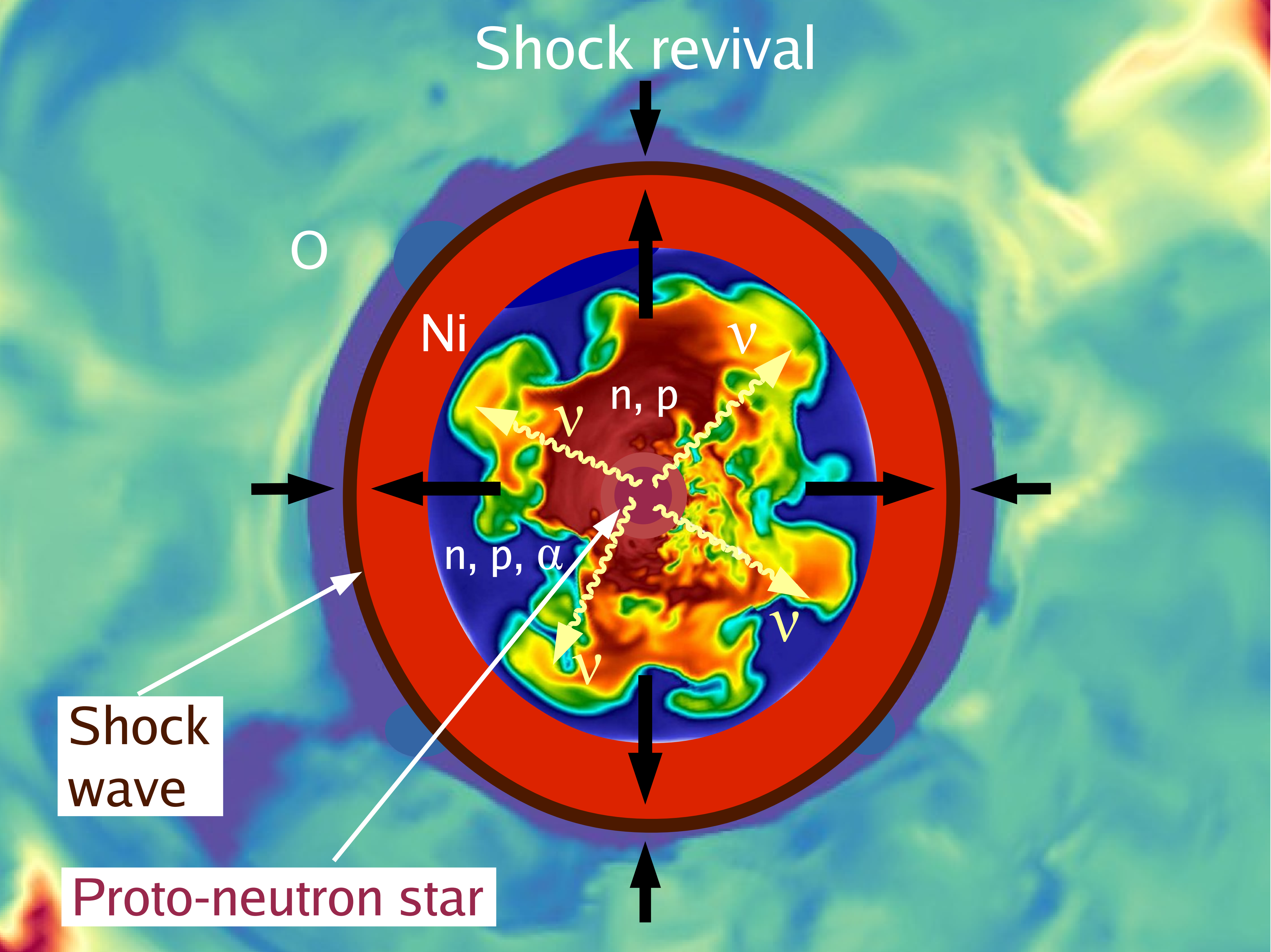

Shock revival
O
Ni
n, p
ν
ν
n, p, α
ν
ν
Shock wave
Proto-neutron star

Questions & Challenges

- **Core collapse SN explosion mechanism(s)**
- **SN explosion properties; explosion asymmetries, mixing, gaseous remnant properties**
- **NS/BH formation paths and probabilities (GW sources)**
- **NS/BH birth properties: masses, kicks, spins, magnetic fields**
- **Neutrino and gravitational-wave signals**
- **Neutrino flavor oscillations, sterile neutrinos, impact of Beyond Standard Model (BSM) physics**
- **Heavy-element formation; what are the sites of the r-process(es)?**
- **What is the equation of state (EOS) of ultra-dense matter?**

Predictions of Signals from SNe & NSs

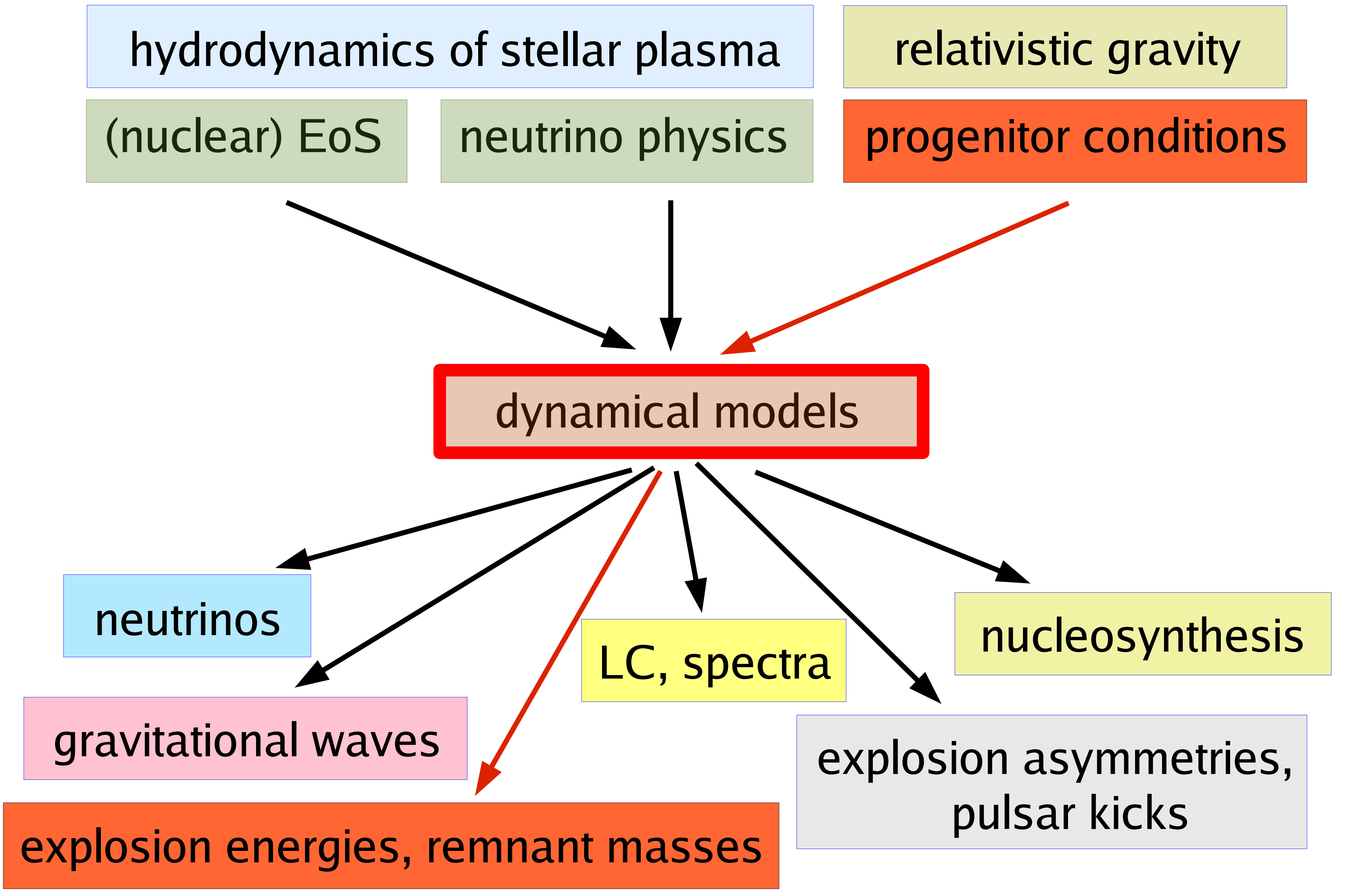

Improvements in Simulations since about 2000

- State-of-the-art neutrino transport methods (two-moment schemes with Eddington closure, Boltzmann solvers)
- General relativistic gravity or well-tested approximate GR
- Comprehensive set of neutrino interactions with more consistent and accurate treatment of the reaction rates
- Modern nuclear equations of state for hot neutron star matter, compatible with all experimental and astrophysical constraints
- Muons included in hot NS matter and neutrino interactions
- Modern progenitor models, partly 3D pre-collapse conditions
- 3D core-collapse and explosion modeling, Yin-Yang grid

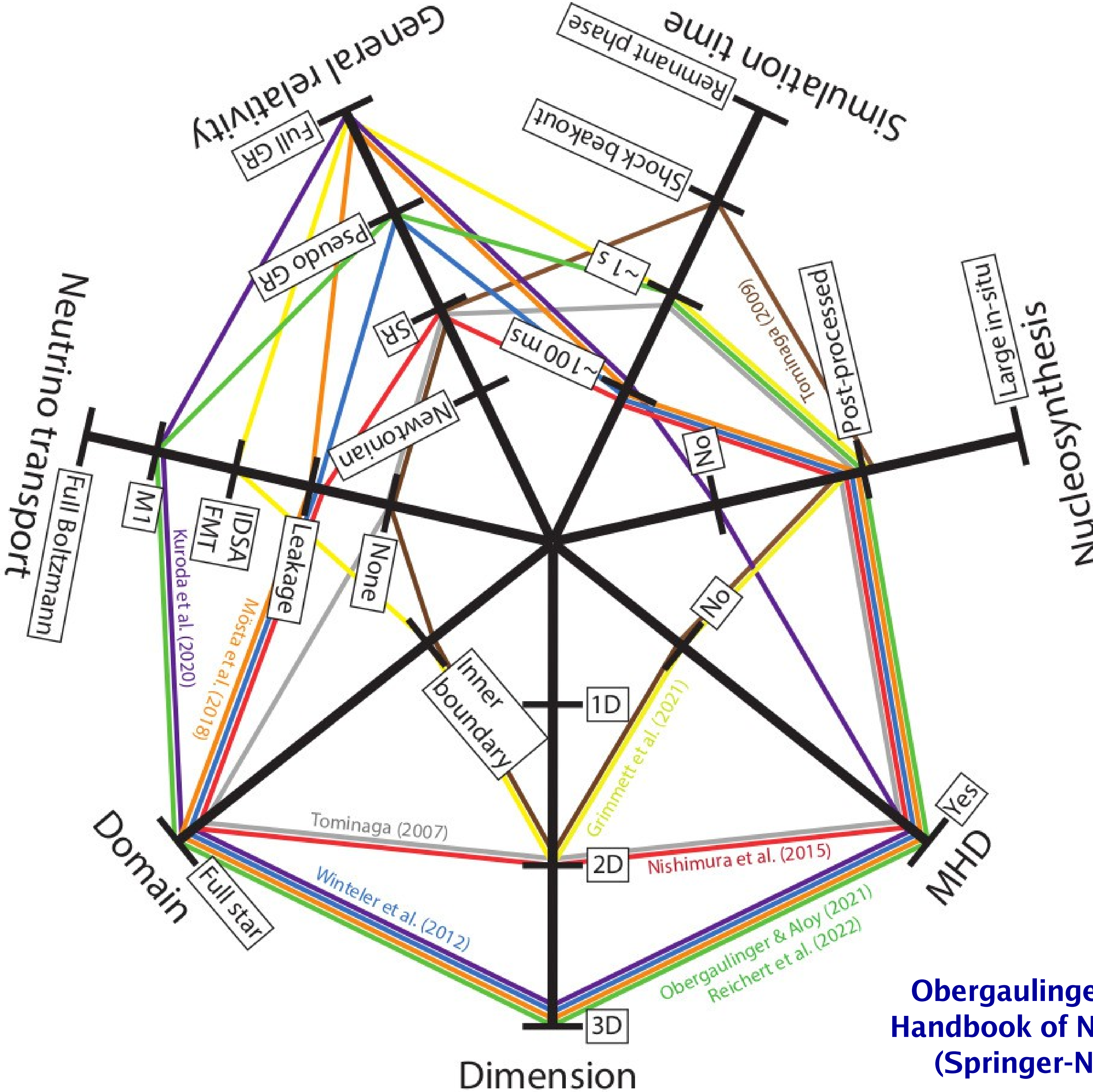

Obergaulinger & Reichert, Handbook of Nuclear Physics (Springer-Nature, 2023)

3D self-consistent, ab-initio simulations with state-of-the-art physics yield successful explosions

Some 3D Explosion Models of Garching Group

Neutrino-driven explosions of low-mass progenitors need no trigger; higher-mass progenitors explode with rotation or slight changes of neutrino opacity.

20 M_{sun}

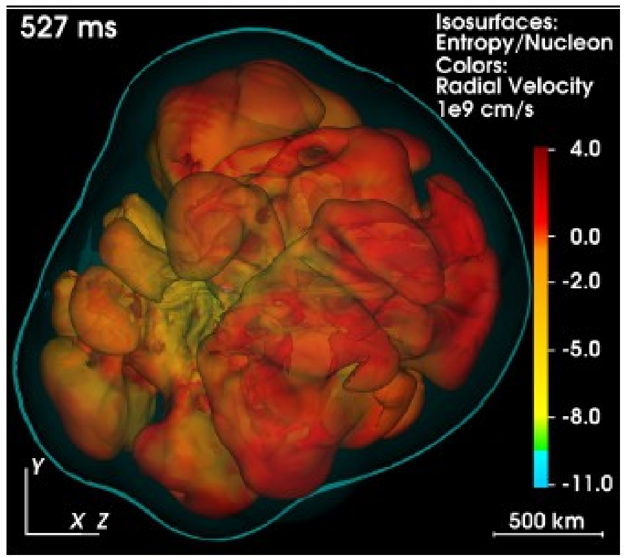

Melson et al., ApJL 808 (2015) L42

9.6 M_{sun}

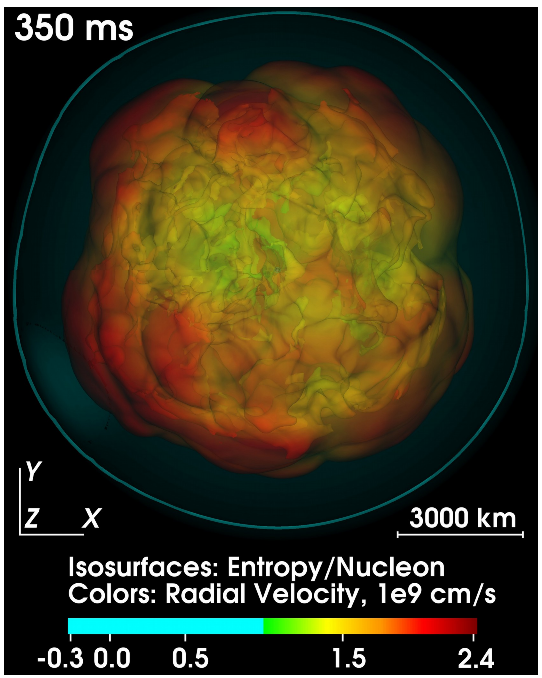

Melson et al., ApJL 801 (2015) L24

15 M_{sun}

Summa et al., ApJ 852 (2018) 28

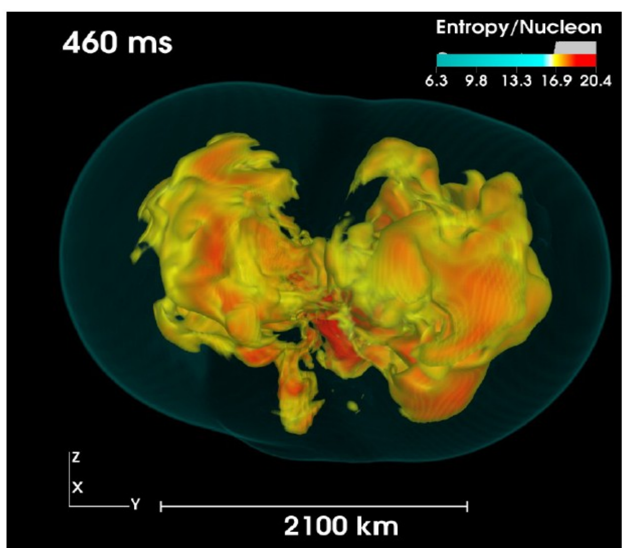

9.0 M_{sun}

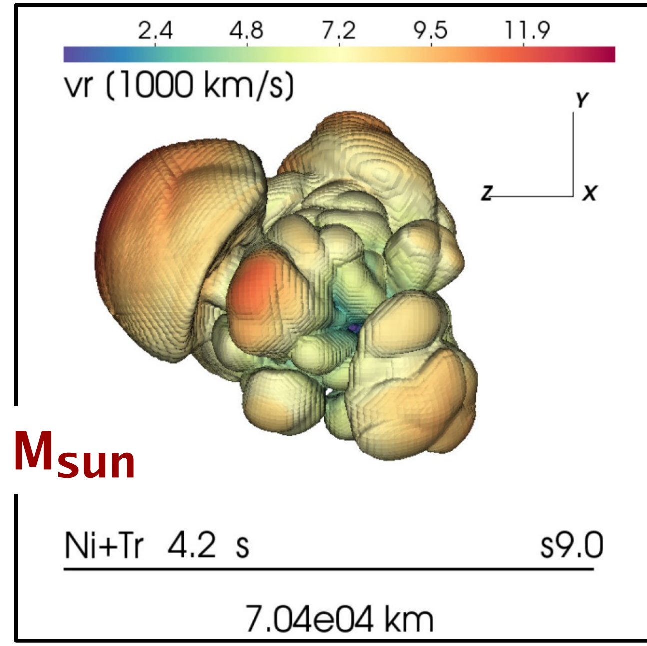

Stockinger et al., MNRAS 496 (2020) 2039

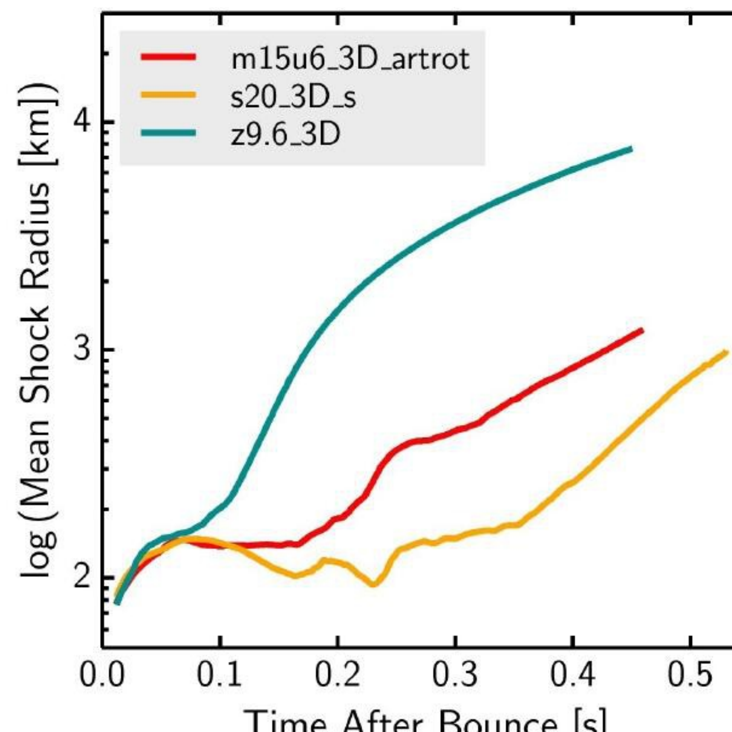

Janka, Melson & Summa, ARNPS 66 (2016)

BUT:

Pre-collapse 3D asymmetries in progenitor stars turned out to be crucial for the explosion

Supernovae as Time-scale Problem

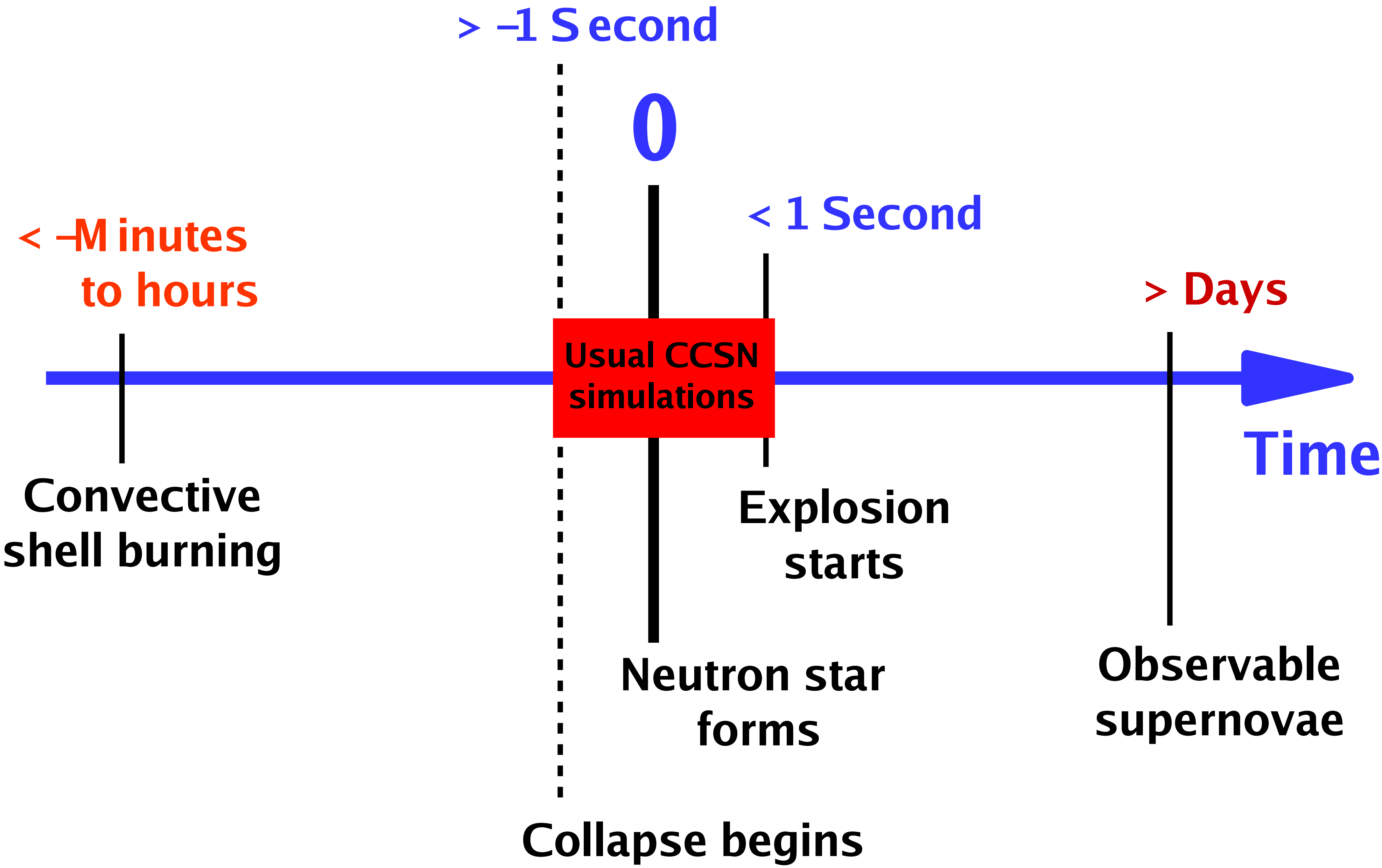

Neon-oxygen-shell Merger in a 3D Pre-collapse Star of ~19 M_{sun}

Flash of Ne+O burning creates large-scale asymmetries in density, velocity, Si/Ne composition

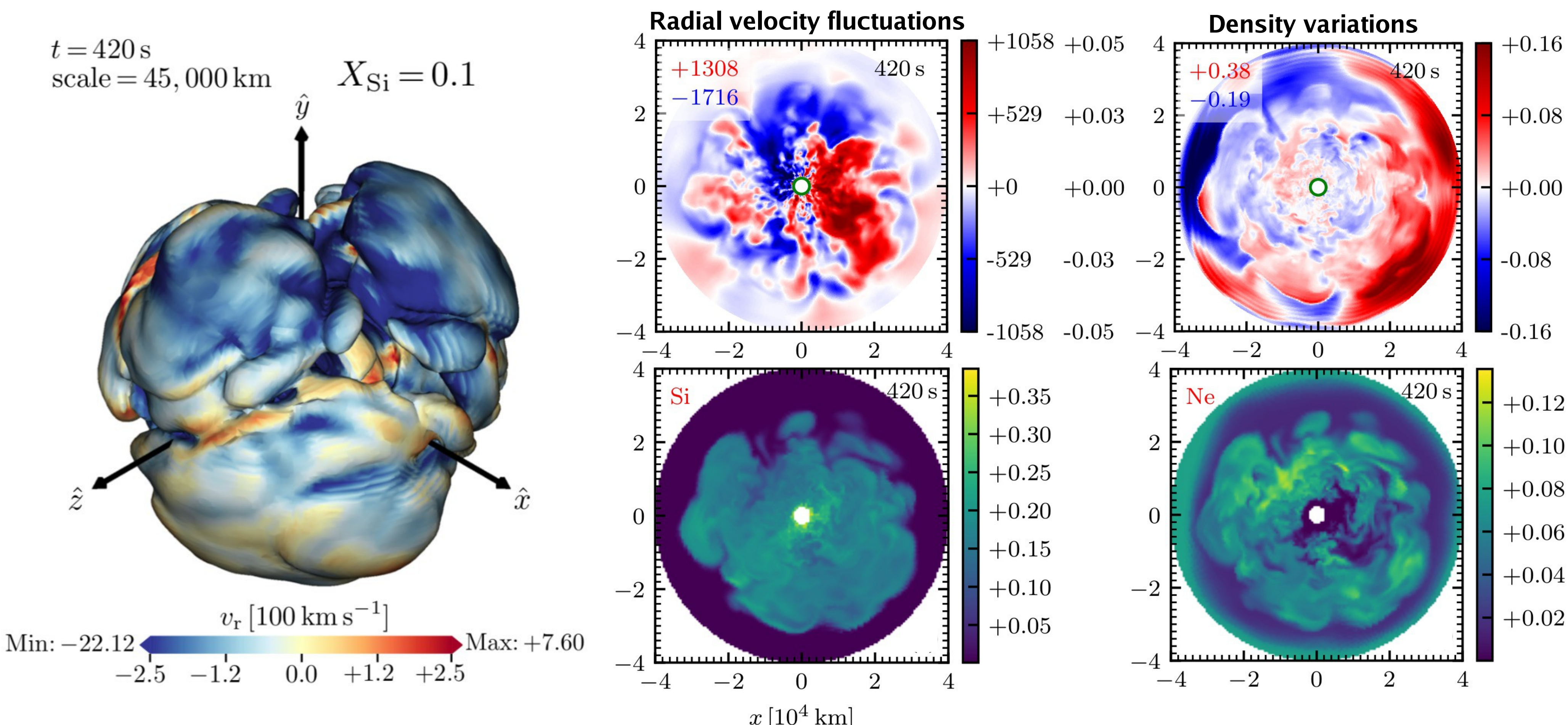

Yadav, Müller et al., ApJ 890 (2020) 94

3D Explosion of ~19 M_{sun} Star

Explosion energy saturates at 10^{51} ergs after 7 seconds

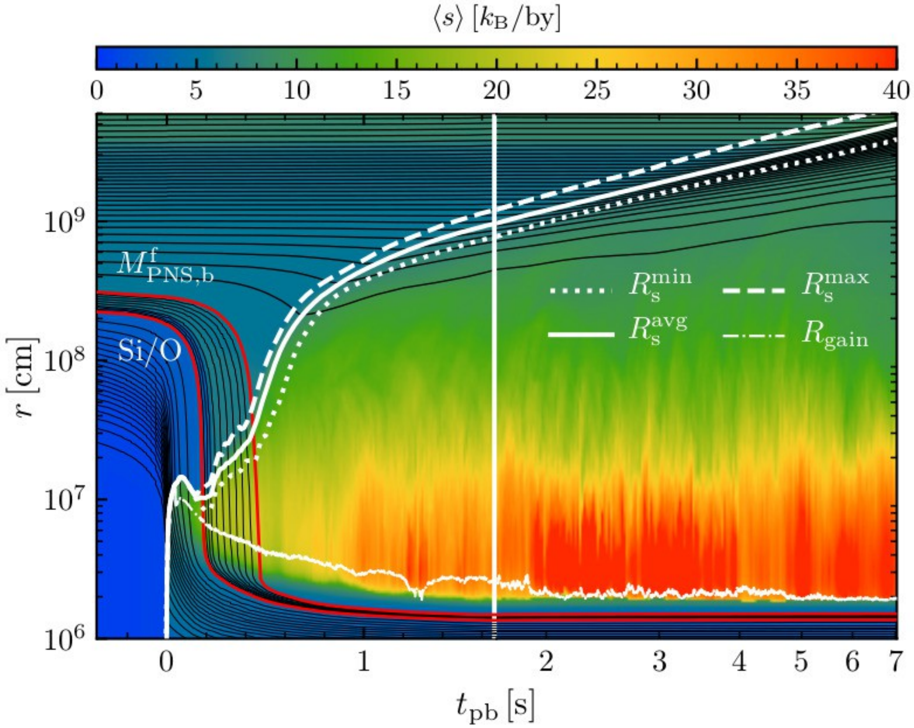

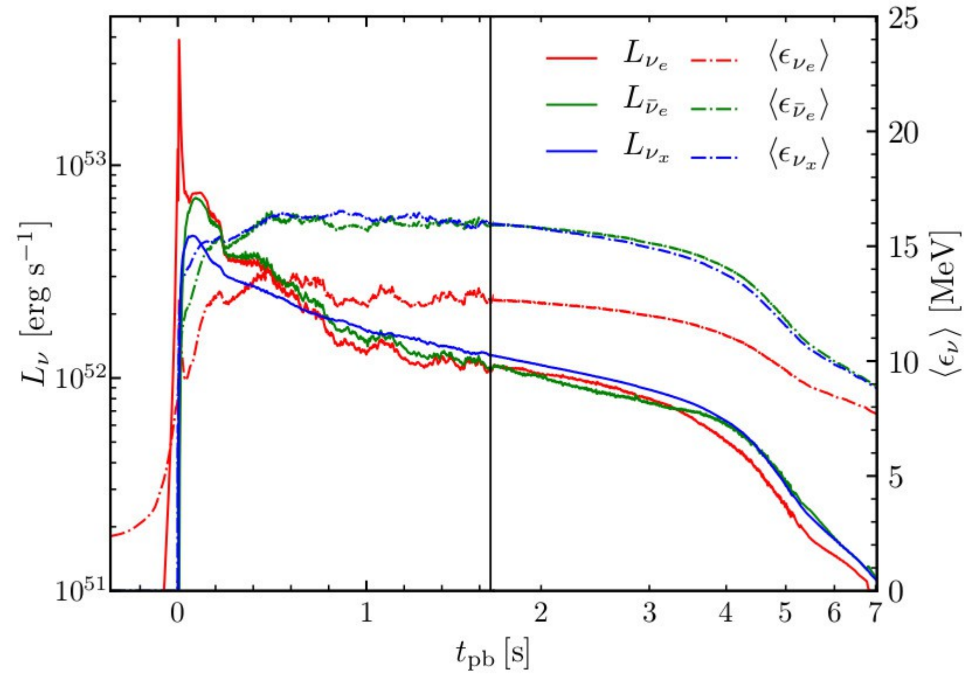

R. Bollig et al., ApJ 915 (2021) 28

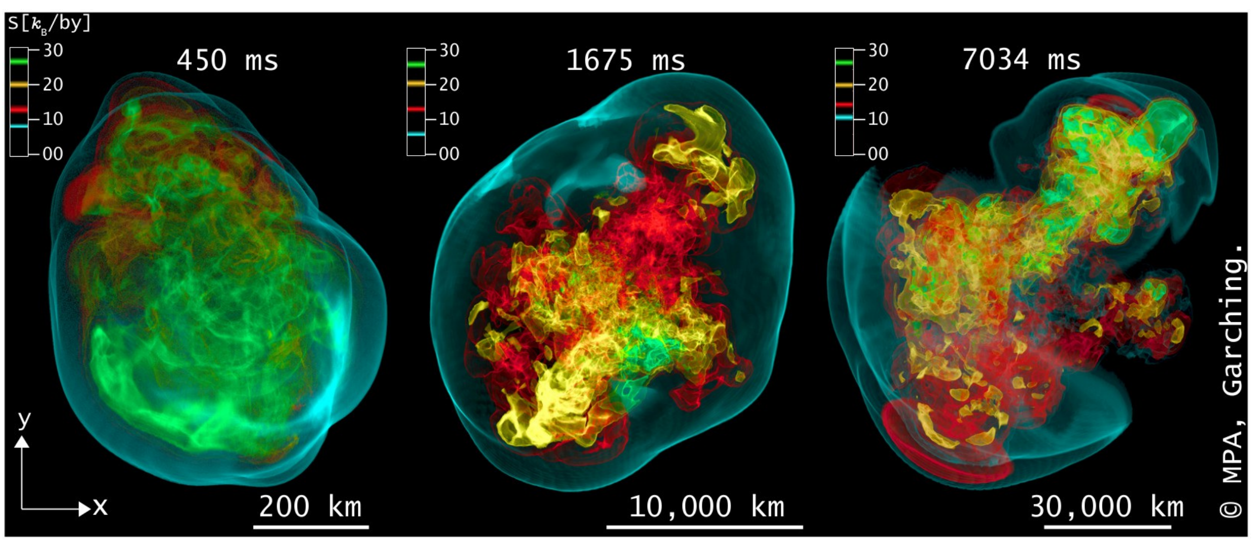

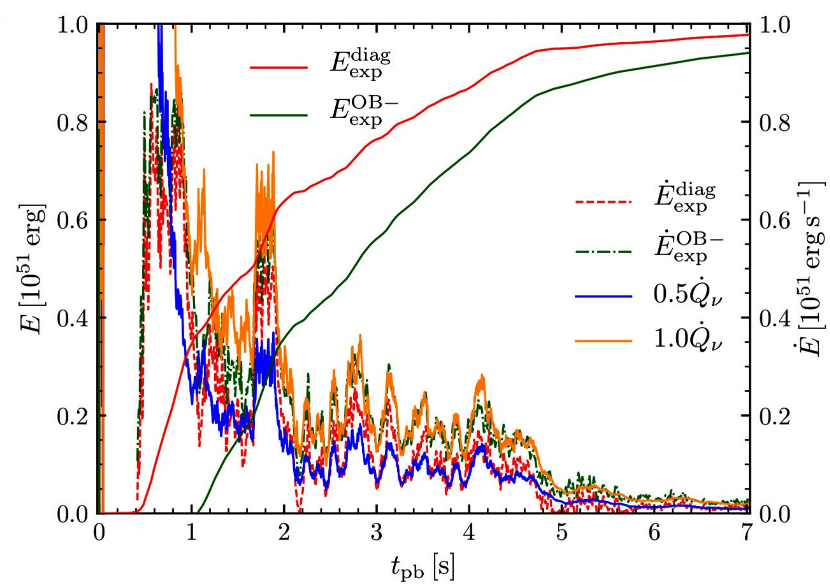

3D Explosion of ~19 M_{sun} Star after Neon-oxygen-shell Merger

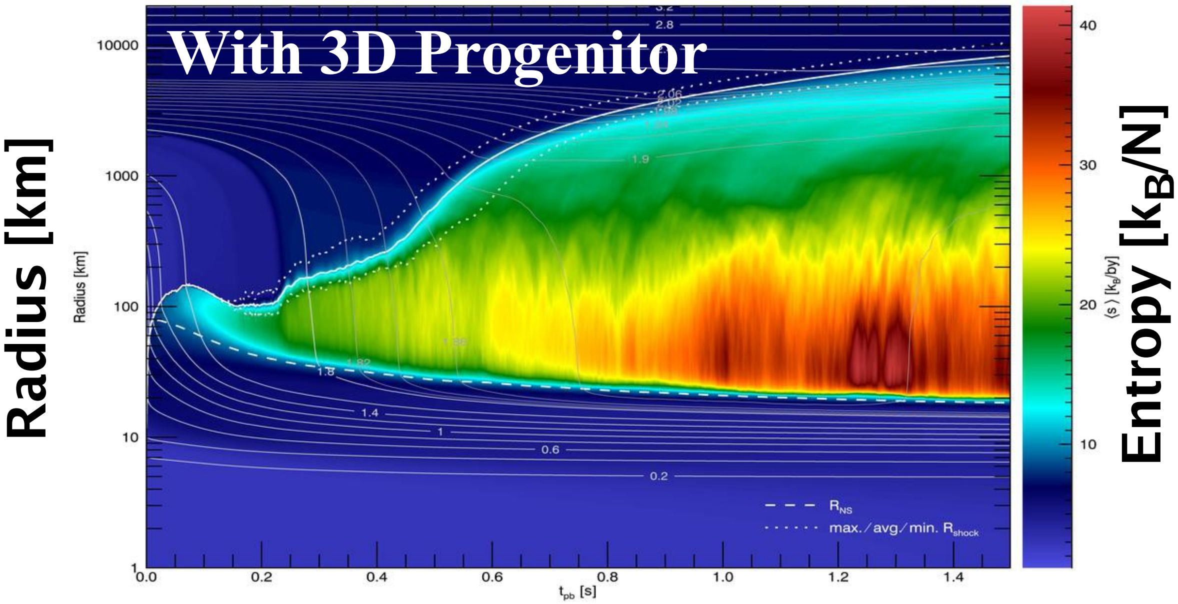

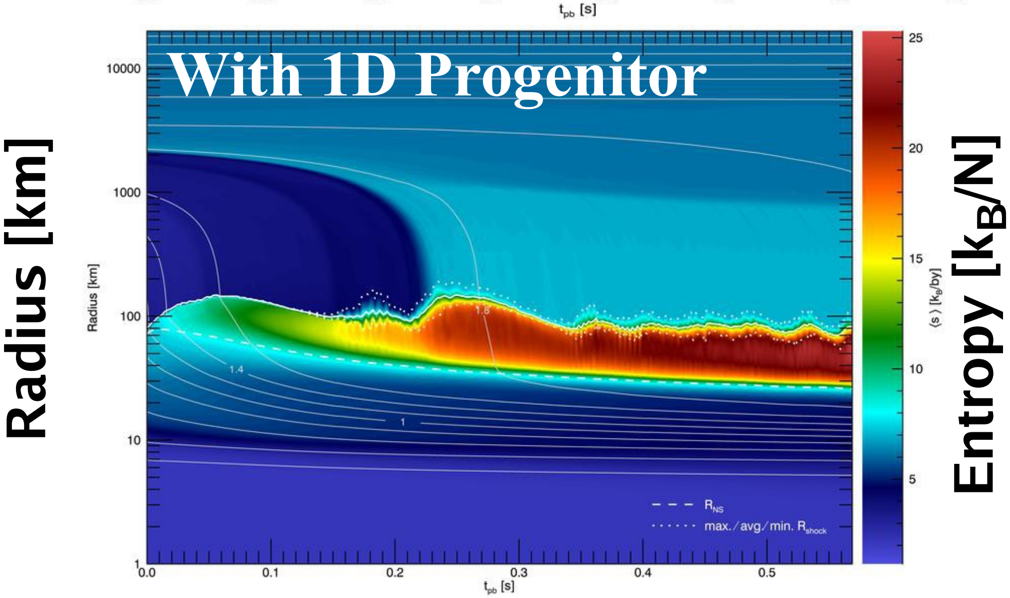

Post-bounce Time [sec]

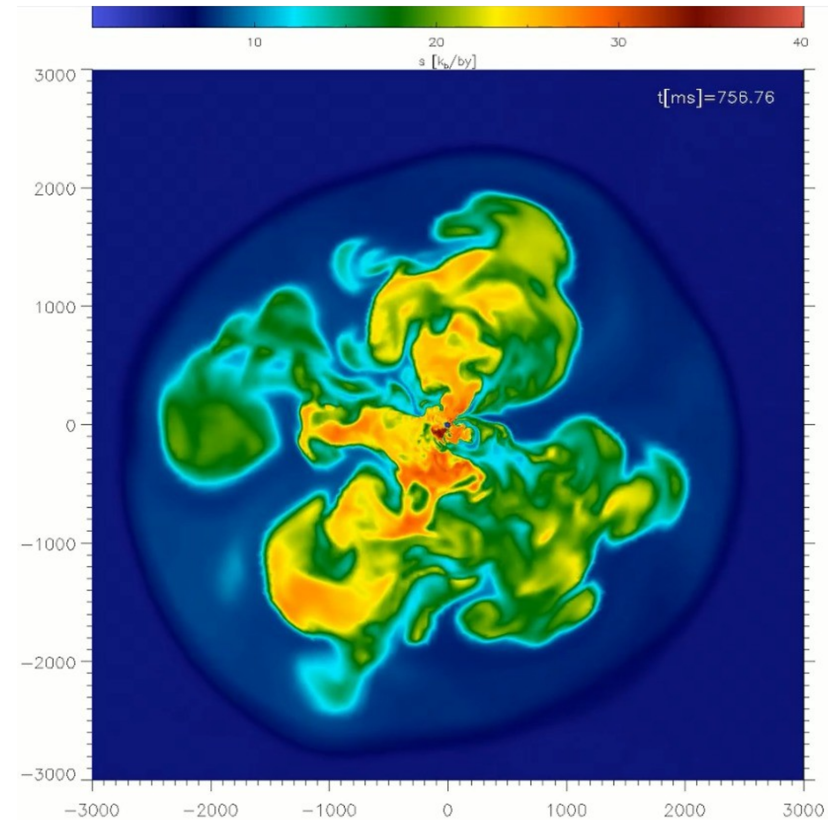

Pre-collapse perturbations in convectively burning O-shell aid explosion because they stir strong postshock convection.

R. Bollig et al., ApJ 915 (2021) 28

Evolution of 3D CCSN Explosions Towards Energy Saturation

Daniel Kresse (MPA),
PhD/PostDoc

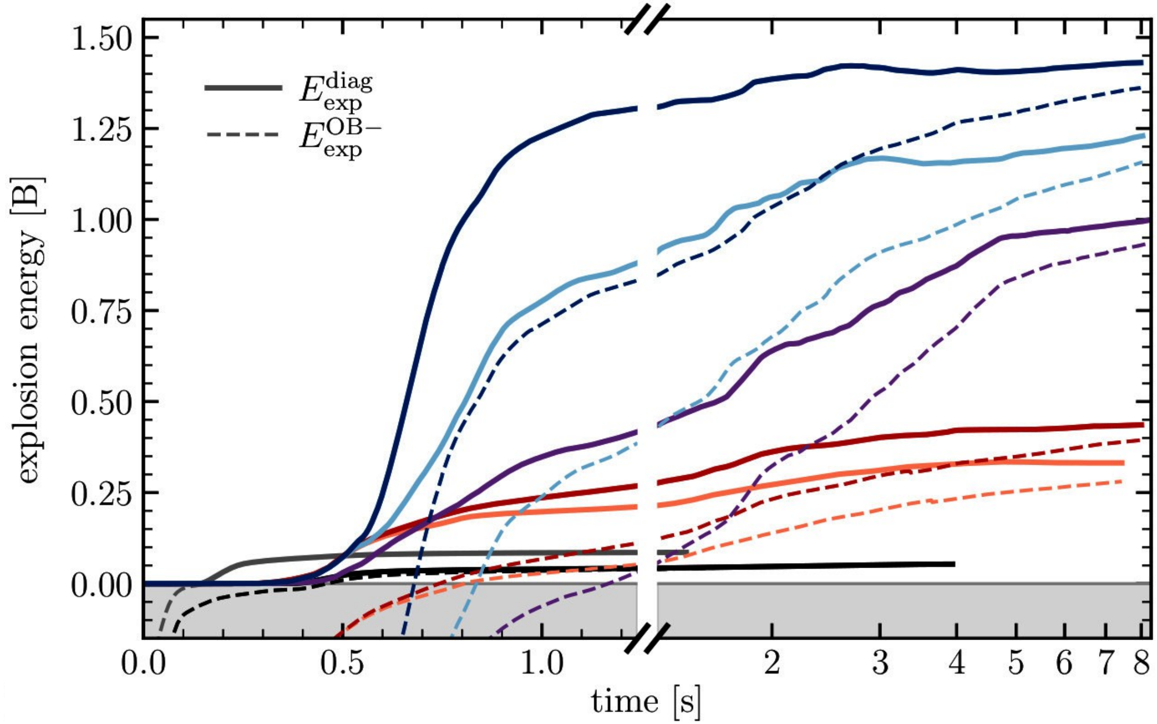

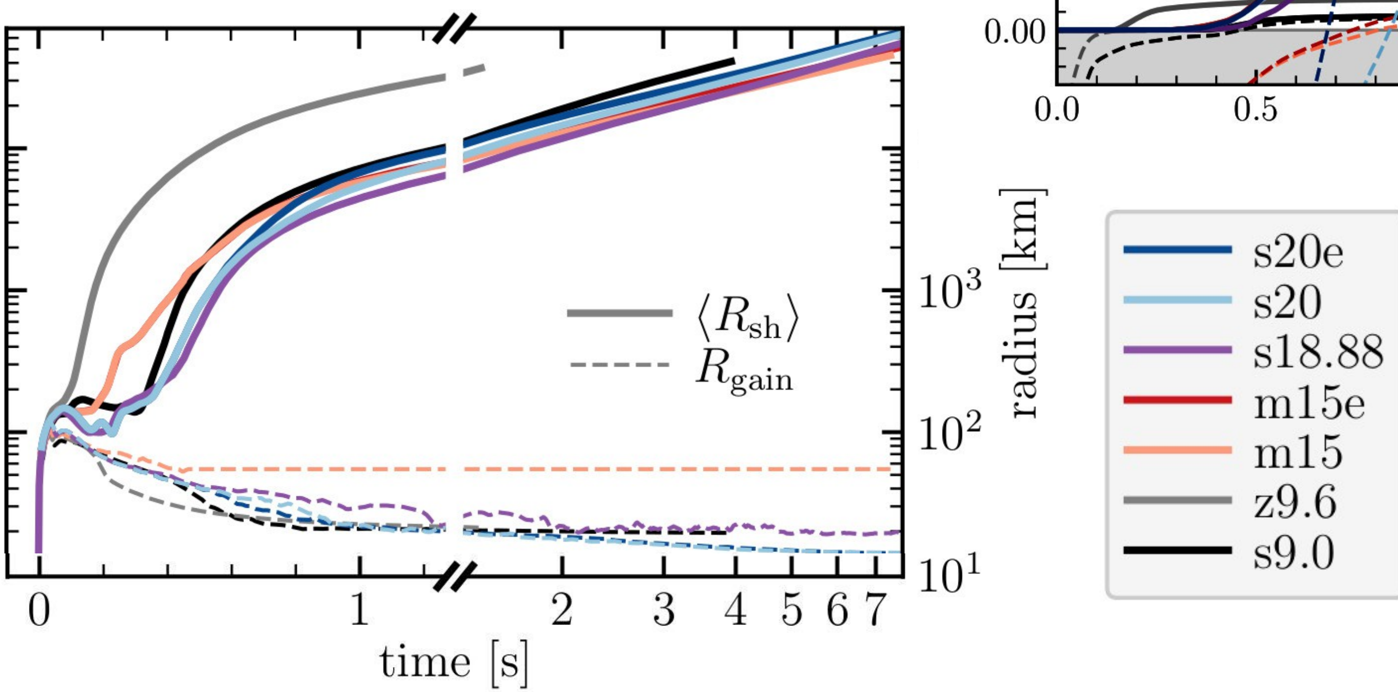

(D. Kresse, PhD Thesis, TUM, 2023)

3D Core-Collapse SN Explosion Models

Garching/QUB/Monash: 9.0, 9.6, 15, 18, ~19, 20, BH cases: 40, 75 M_{sun}

Monash/QUB: 9.6, 11.8, 12, 12.5, he2.8, he3.0, he3.5 M_{sun}, BH cases

Oak Ridge/NCSU: 9.6, 15 M_{sun}

Fukuoka/Tokyo: Large model grid ------> see Kei Kotake's talk

Caltech/LSU/Perimeter: 15, 20, 27, 40 M_{sun}

Princeton/Berkeley: 9–40 M_{sun}, large model grid -----> Adam Burrows' talk

MSU/Stockholm: 20 M_{sun}, ...

Modeling inputs and results differ in various aspects.
3D code comparison is missing but desirable!

3D Core-Collapse SN Explosion Models

About half a dozen groups are active in 3D CCSN modeling:

Garching, Monash/QUB, Oak Ridge, Fukuoka/Tokyo, Caltech, Princeton/Berkeley, MSU/Stockholm

3D simulations differ in many aspects of numerics, physics inputs, and, qualitatively and quantitatively, in their outcomes.

3D code comparison is missing and highly desirable.

Nakamura, Matsumoto, KK+ in prep (3D-MHD)

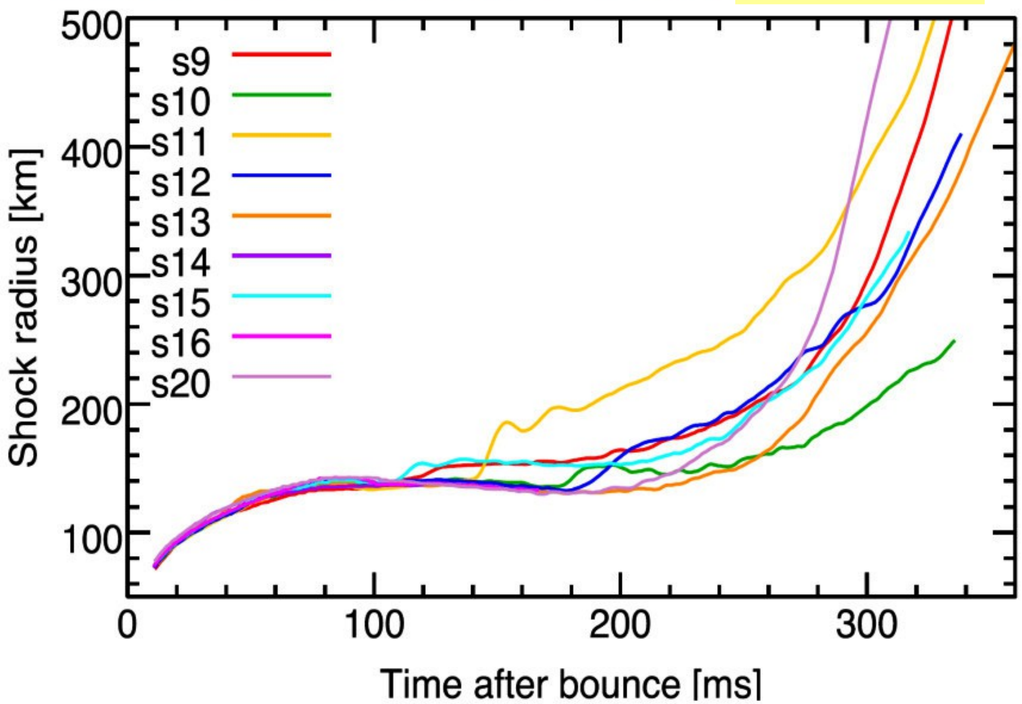

c.f.) Burrows+20 (3D-non MHD)

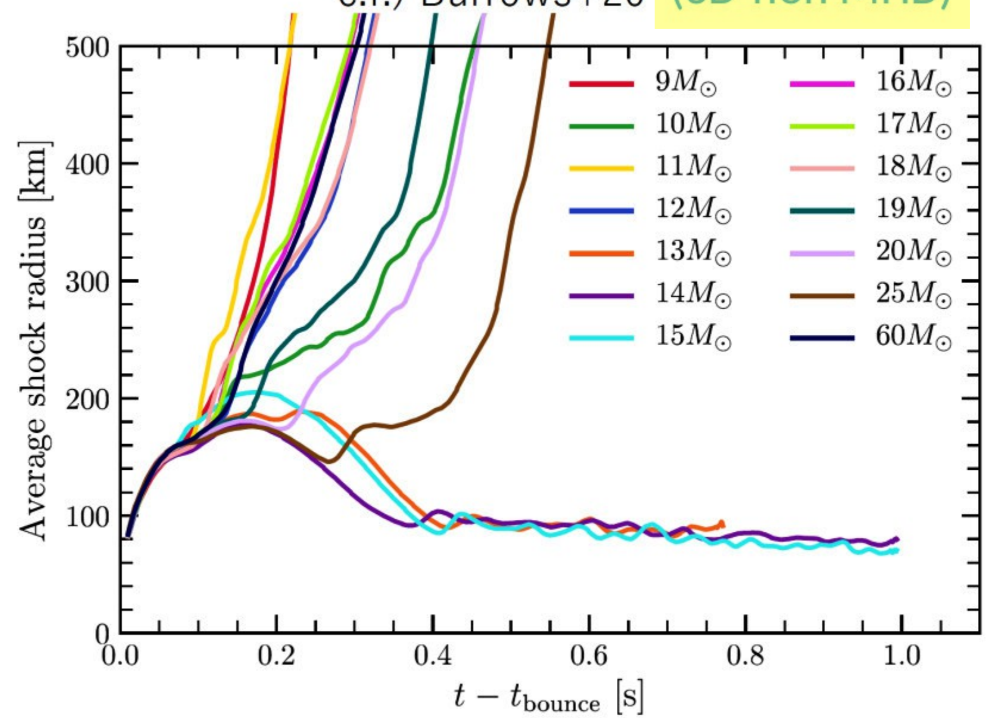

(Plots from Kei Kotake's talk at MPA on March 29, 2023)

Onset of Explosion Depends on Nuclear Equation of State

Robert Bollig
(MPA), Ex-PostDoc

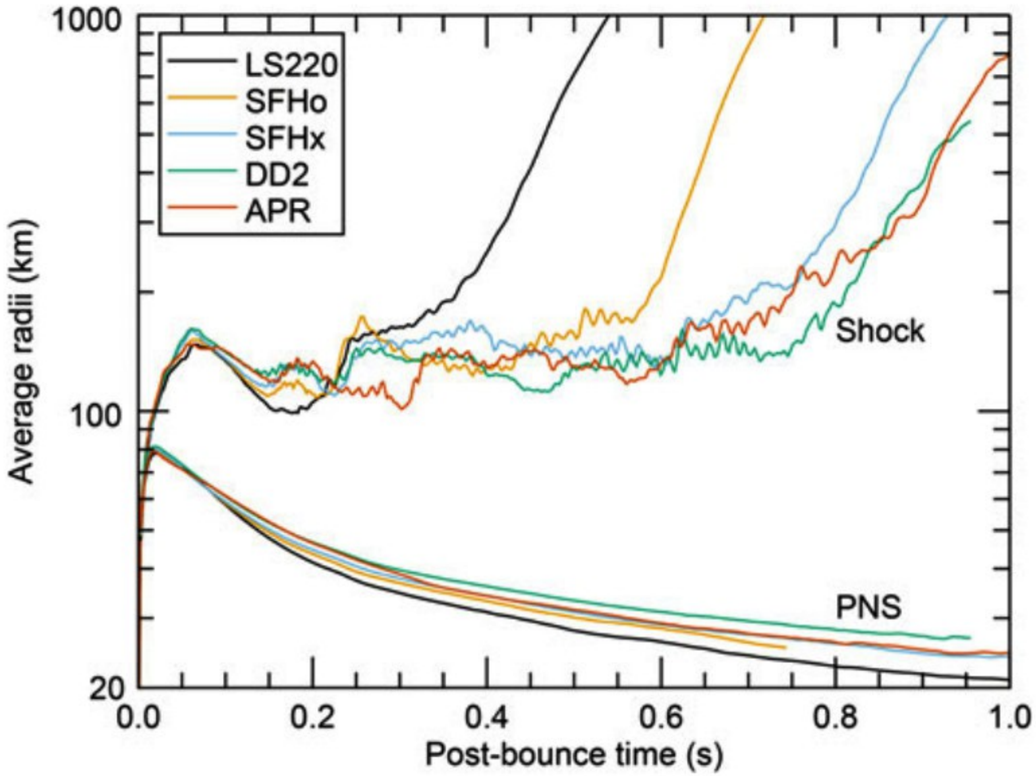

Fig. 11 Shock radii and PNS radii (spherically averaged) in 3D simulations of CCSN explosions of a 19 $M_\odot$ progenitor for different nuclear EoSs widely used in SN simulations: LS220 of Lattimer and Swesty (1991), SFHo, SFHx of Steiner et al. (2013) and Hempel and Schaffner-Bielich (2010), DD2 of Typel et al. (2010) and Hempel et al. (2012), and APR of Schneider et al. (2019a). In all cases, successful explosions were obtained in 3D core-collapse simulations started from 3D progenitor conditions (Yadav et al. 2020; Bollig et al. 2021), but there is a clear correlation between the onset of the explosion and the contraction of the PNS. The faster the PNS contracts, the earlier the explosion sets in. This signals the dominant relevance of the PNS radius evolution over other EoS dependent effects. (Figure courtesy of Robert Bollig)

HTJ & Bauswein, Handbook of Nuclear Physics (Springer-Nature, 2023); **Figure coutesy of Robert Bollig**

Onset of Explosion Depends on (Fast) Neutrino Flavor Oscillations

General overview SN ν oscillations: Jim Kneller's talk of 05/29!

Jakob Ehring (MPP/MPA), PhD

Here: Fast pair-wise conversion of heavy-lepton neutrinos and antineutrinos with their higher mean energies to electron neutrinos and antineutrinos can boost the neutrino heating =====> leads to earlier explosion.

[NFC = no flavor conversion]

(Ehring, Abbar, HTJ, Raffelt, Tamborra, arXiv:2305.11207 & PRD 107 (2023) 103034)

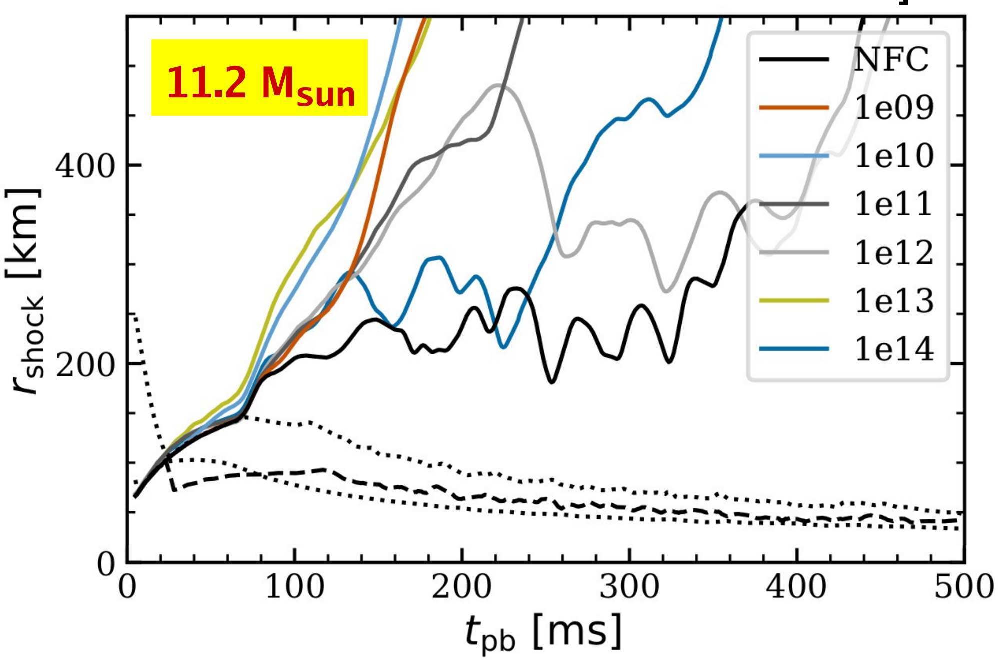

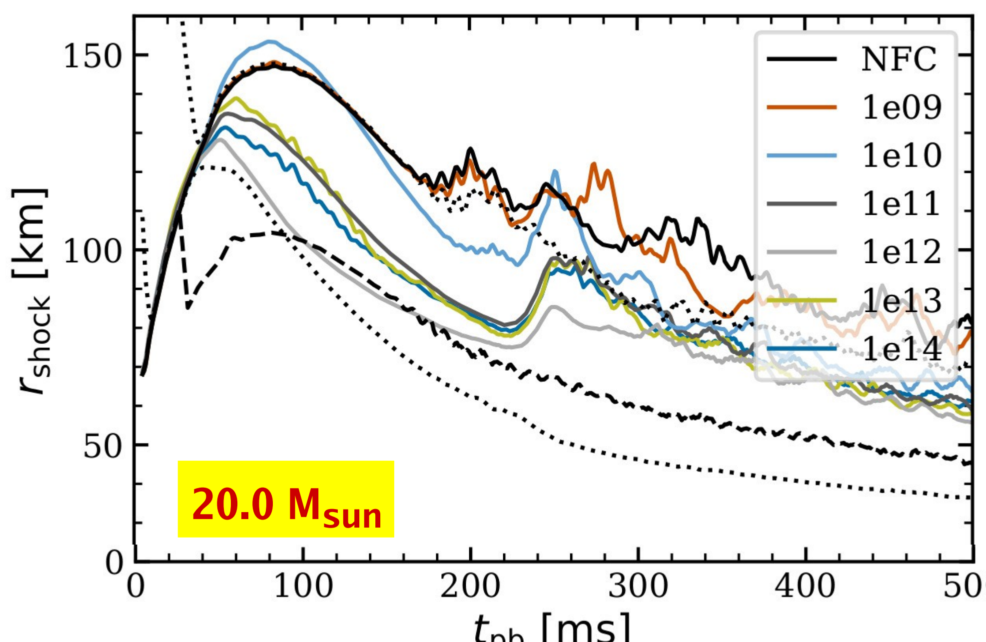

Neutrino-driven Explosion Models

vs.

Observations

Observational consequences

Direct and indirect evidence for neutrino heating and hydrodynamic instabilities at the onset of stellar explosions:

- Neutrino signals (characteristic time dependencies)
- Gravitational-wave signals
- Neutron star kicks
- Asymmetric mass ejection & large-scale radial mixing in supernovae (elm. light curve shape, spectral features)
- Detailed comparison to young supernova remnants (e.g., Crab, Cas A, SN 1987A)
- Progenitor – explosion – remnant connection
- Nucleosynthesis

Observational consequences

Direct and indirect evidence for neutrino heating and hydrodynamic instabilities at the onset of stellar explosions:

- Neutrino signals (characteristic time dependencies)
- Gravitational-wave signals
- Neutron star kicks
- Asymmetric mass ejection & large-scale radial mixing in supernovae (elm. light curve shape, spectral features)
- Detailed comparison to young supernova remnants (e.g., Crab, Cas A, SN 1987A)
- Progenitor – explosion – remnant connection
- Nucleosynthesis

Neutron Star Recoil in 3D Explosion Models

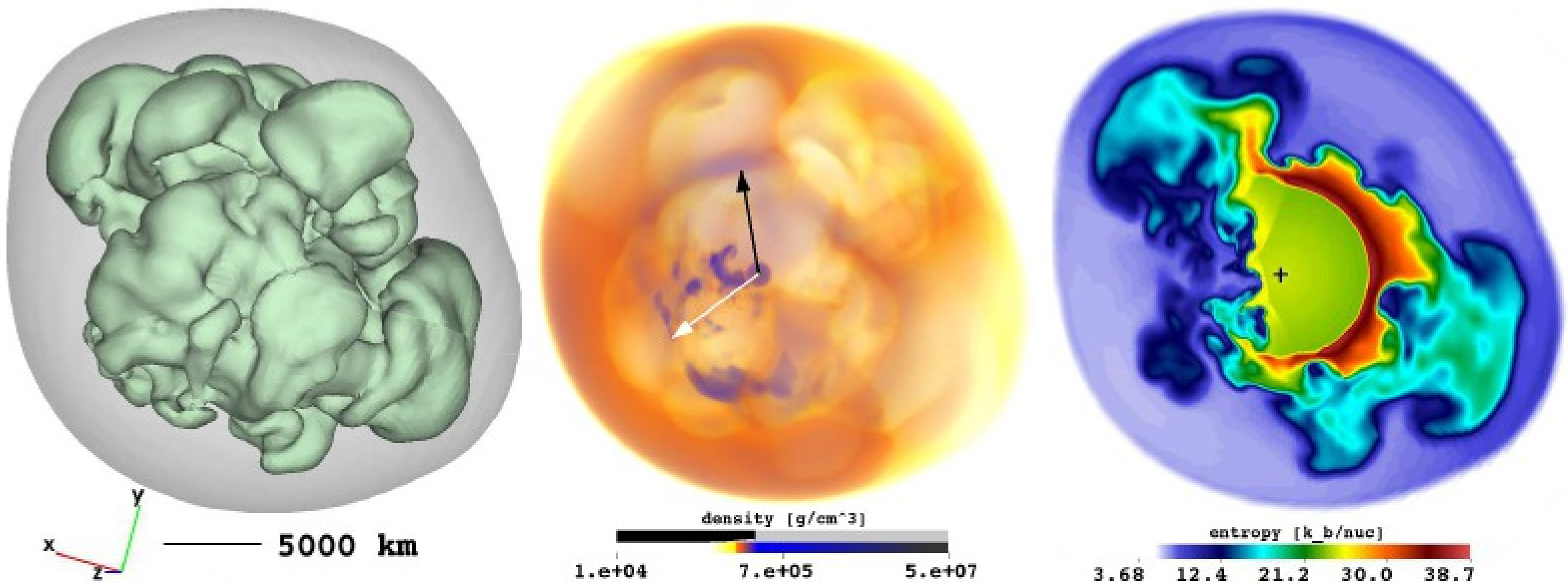

W15-2
@ 1.3 s

"Gravitational tug-boat" mechanism

$$v_{\rm NS} = 211\,{\rm km\,s^{-1}} \left(\frac{f_{\rm kin}}{\epsilon_5\,\beta_\nu}\right)^{1/2} \left(\frac{\alpha_{\rm ej}}{0.1}\right) \times \\ \times \left(\frac{E_{\rm exp}}{10^{51}\,{\rm erg}}\right) \left(\frac{M_{\rm NS}}{1.5\,M_\odot}\right)^{-1}$$

Wongwathanarat, Janka, Müller,
ApJL 725, 106 (2010); A&A 552, 126 (2013);
Scheck et al., PRL 92, 011103 (2004), A&A 457, 963 (2006);
Janka, ApJ 837, 84 (2017)

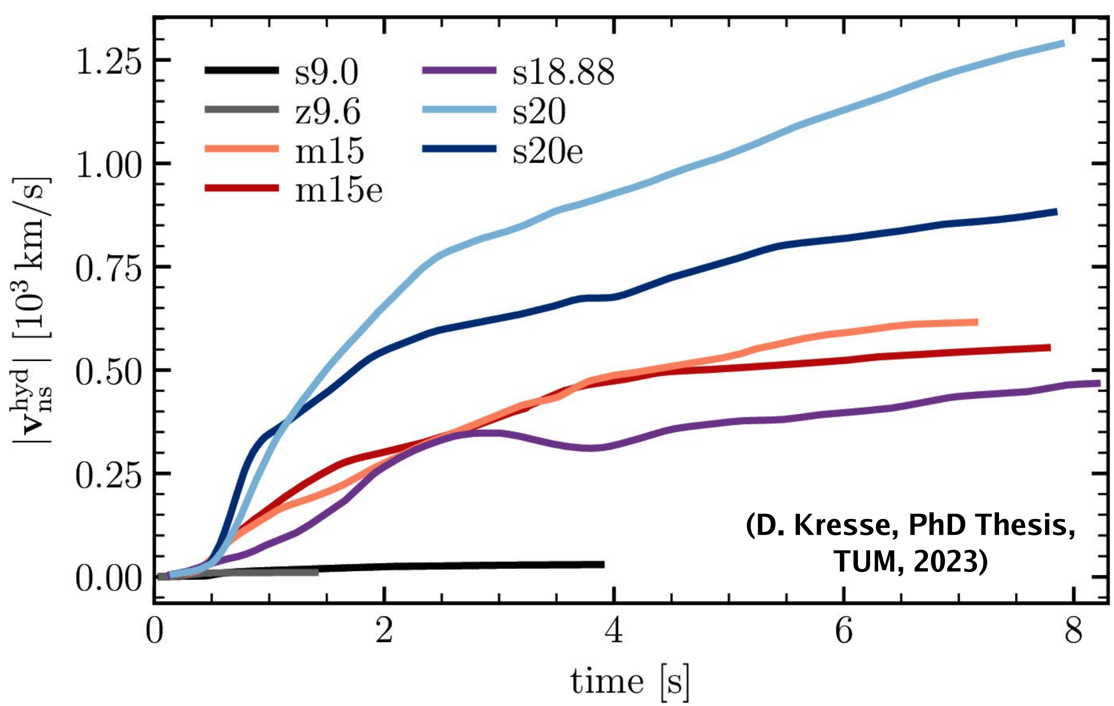

Asymmetric Ejection of Radioactive Nuclei and IME from Ne to Fe-group

Wongwathanarat, Janka, Müller, A&A 552 (2013) A126

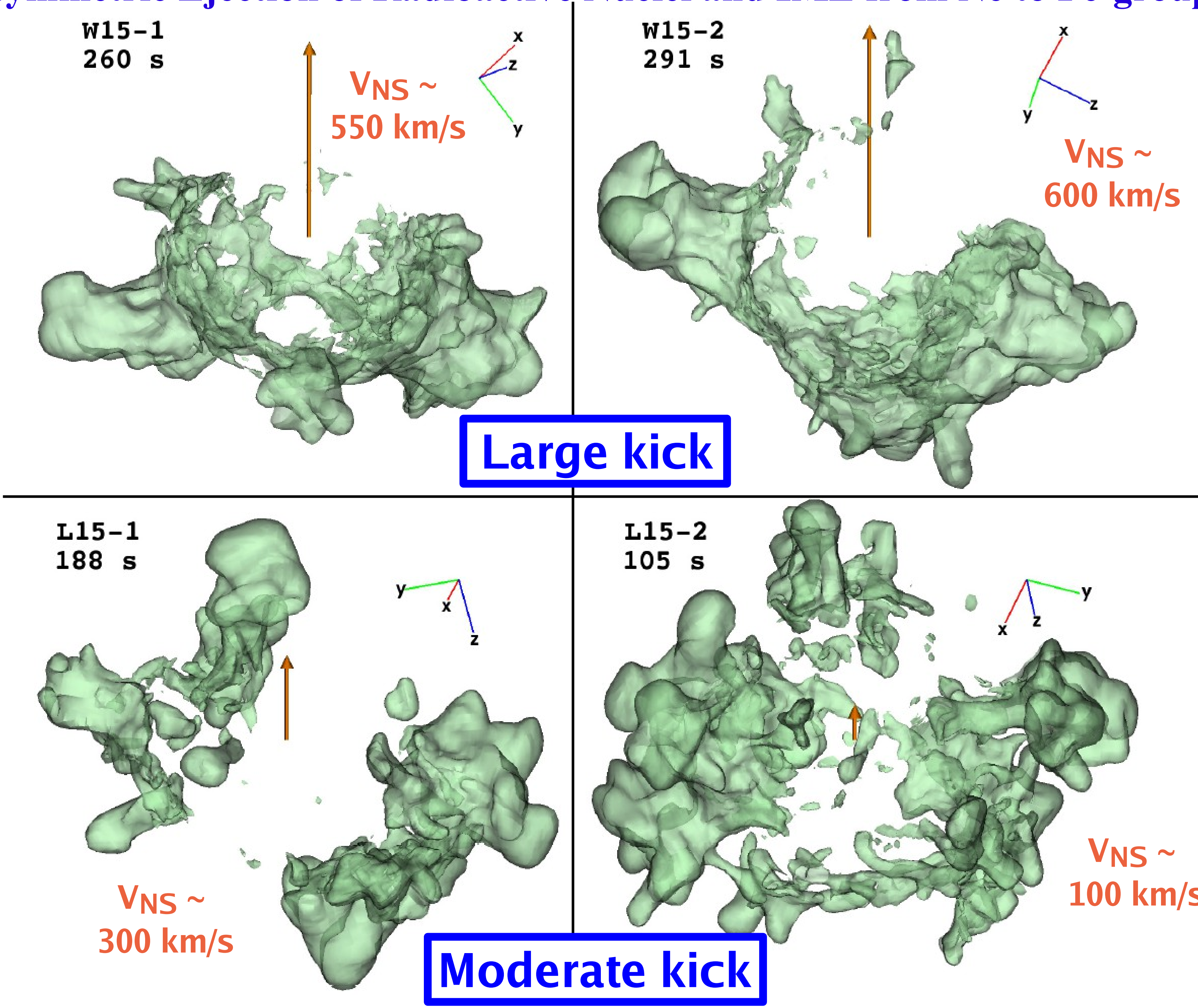

Neutron Star Kicks and Young SN Remnants

Analysis of spatial distribution of IMEs (from Ne to Fe-group) in young, nearby SNRs with known NS kick velocities.

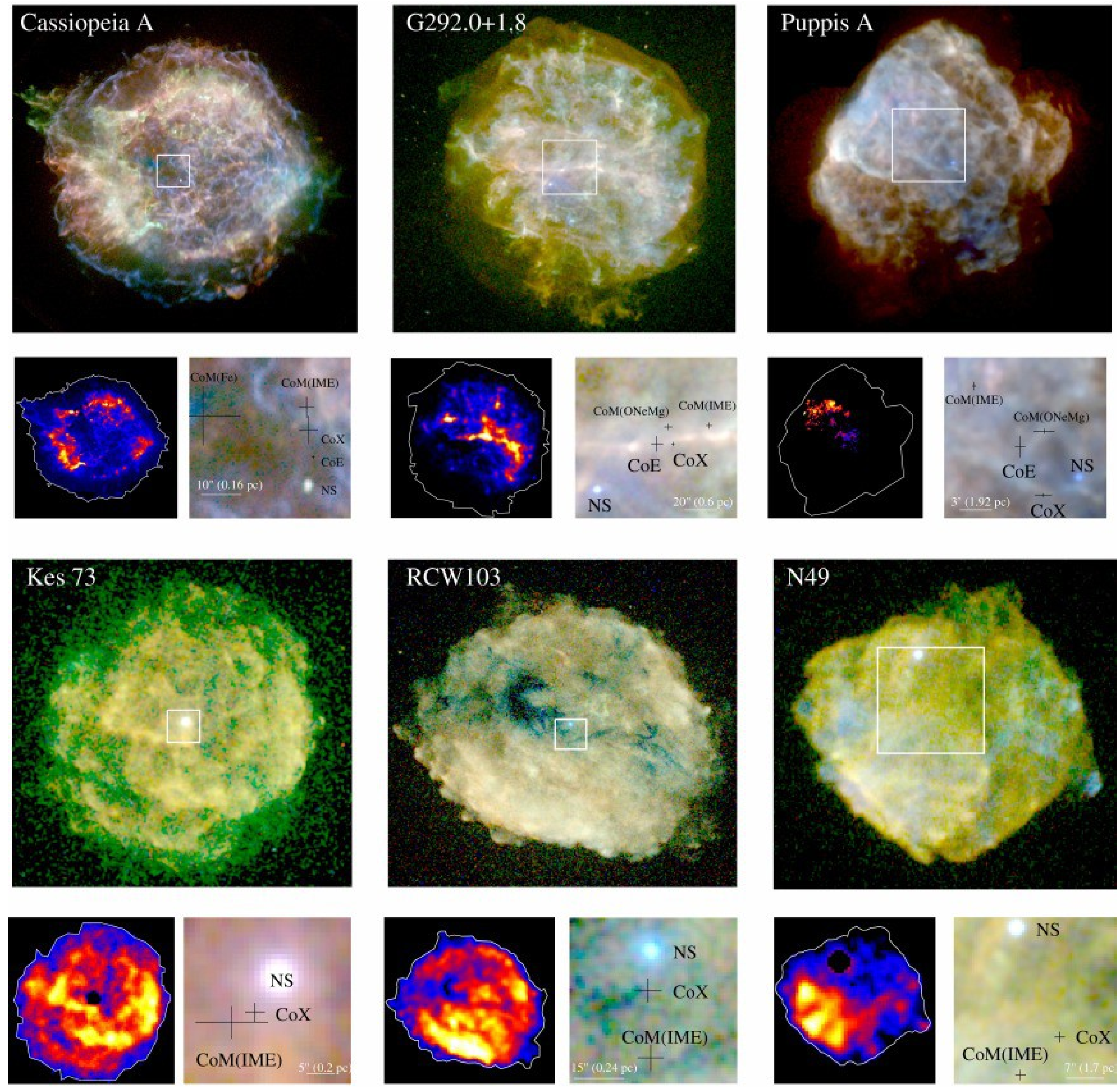

S. Katsuda, Morii, THJ, et al., ApJ 856 (2018) 18;

see also:
Holland-Ashford, et al., ApJ 844 (2017) 84;
Bear & Soker, ApJ 855 (2018) 82

Neutron Star Kicks and Young SN Remnants

Analysis of spatial distribution of IMEs (from Ne to Fe-group) in young, nearby SNRs with known NS kick velocities.

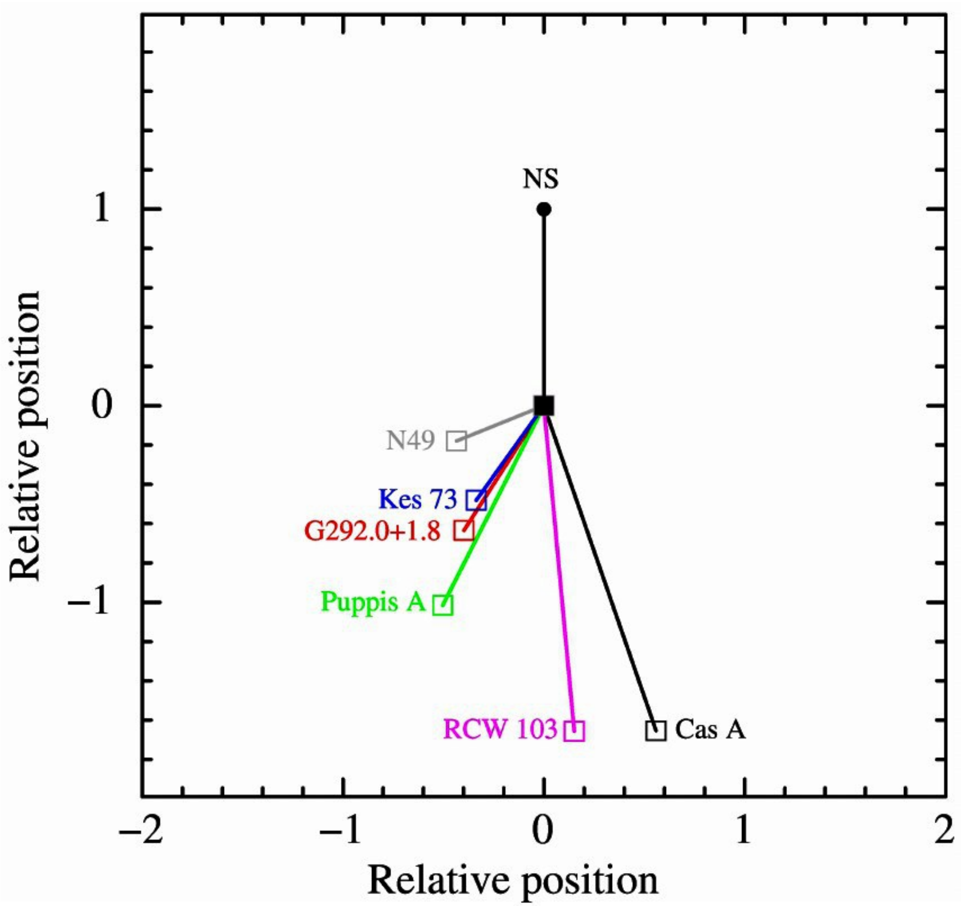

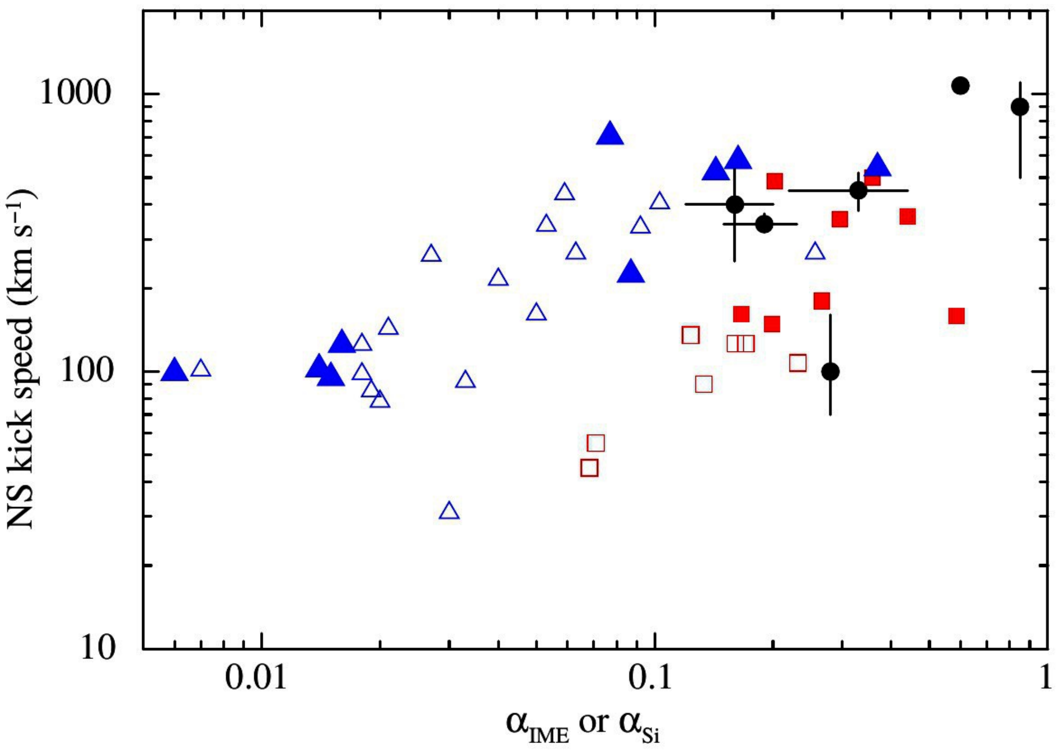

Katsuda, Morii, THJ, et al. ApJ 856 (2018) 18

Observational consequences

Direct and indirect evidence for neutrino heating and hydrodynamic instabilities at the onset of stellar explosions:

- Neutrino signals (characteristic time dependencies)
- Gravitational-wave signals
- Neutron star kicks
- Asymmetric mass ejection & large-scale radial mixing in supernovae (elm. light curve shape, spectral features)
- Detailed comparison to young supernova remnants (e.g., Crab, Cas A, SN 1987A)
- Progenitor – explosion – remnant connection
- Nucleosynthesis

3D asymmetries from the onset of the explosion determine asymmetry of the SN ejecta and SN remnant.

Modeling of the explosion has to be performed in 3D consistently from pre-collapse stage to SNR phase !

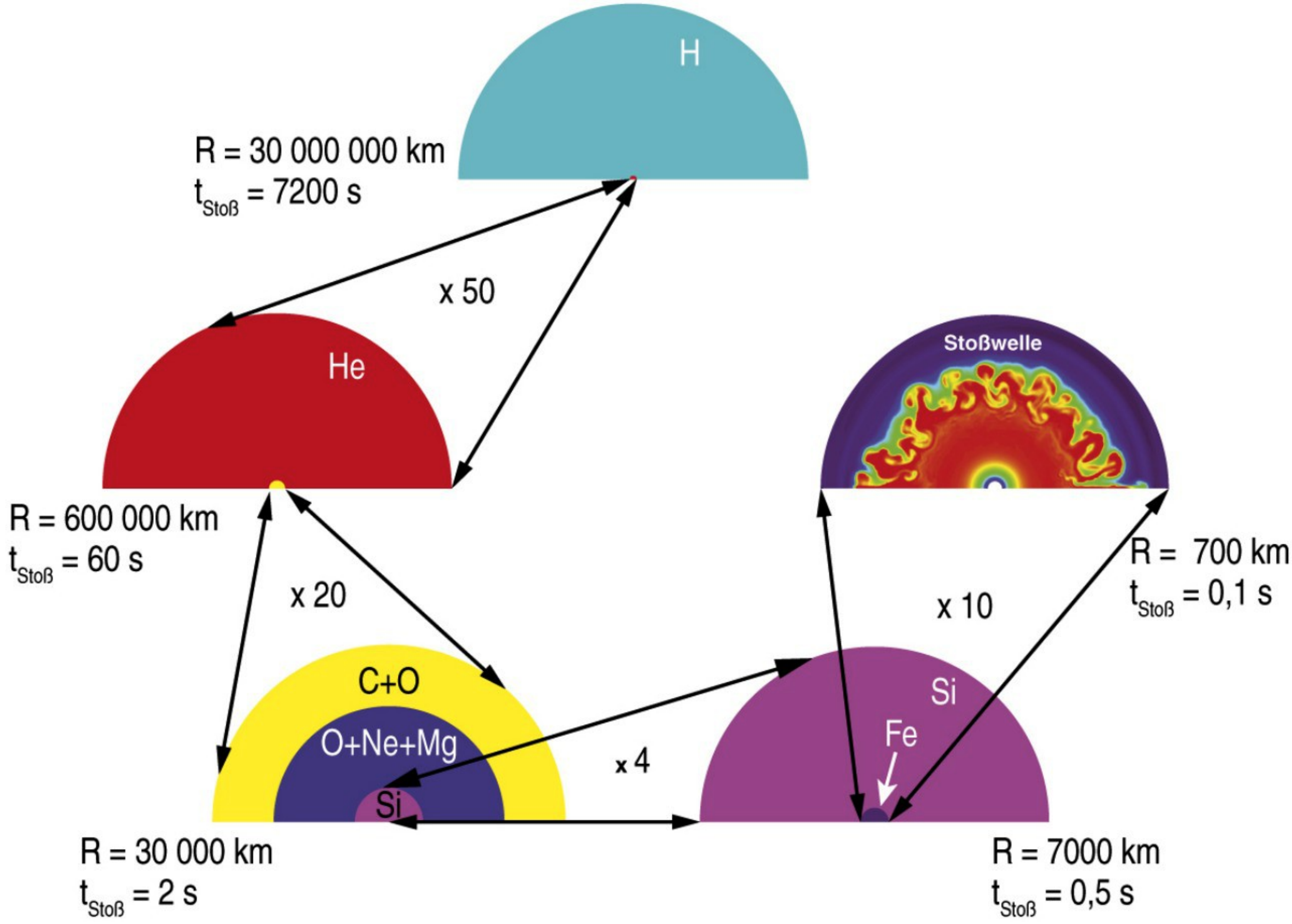

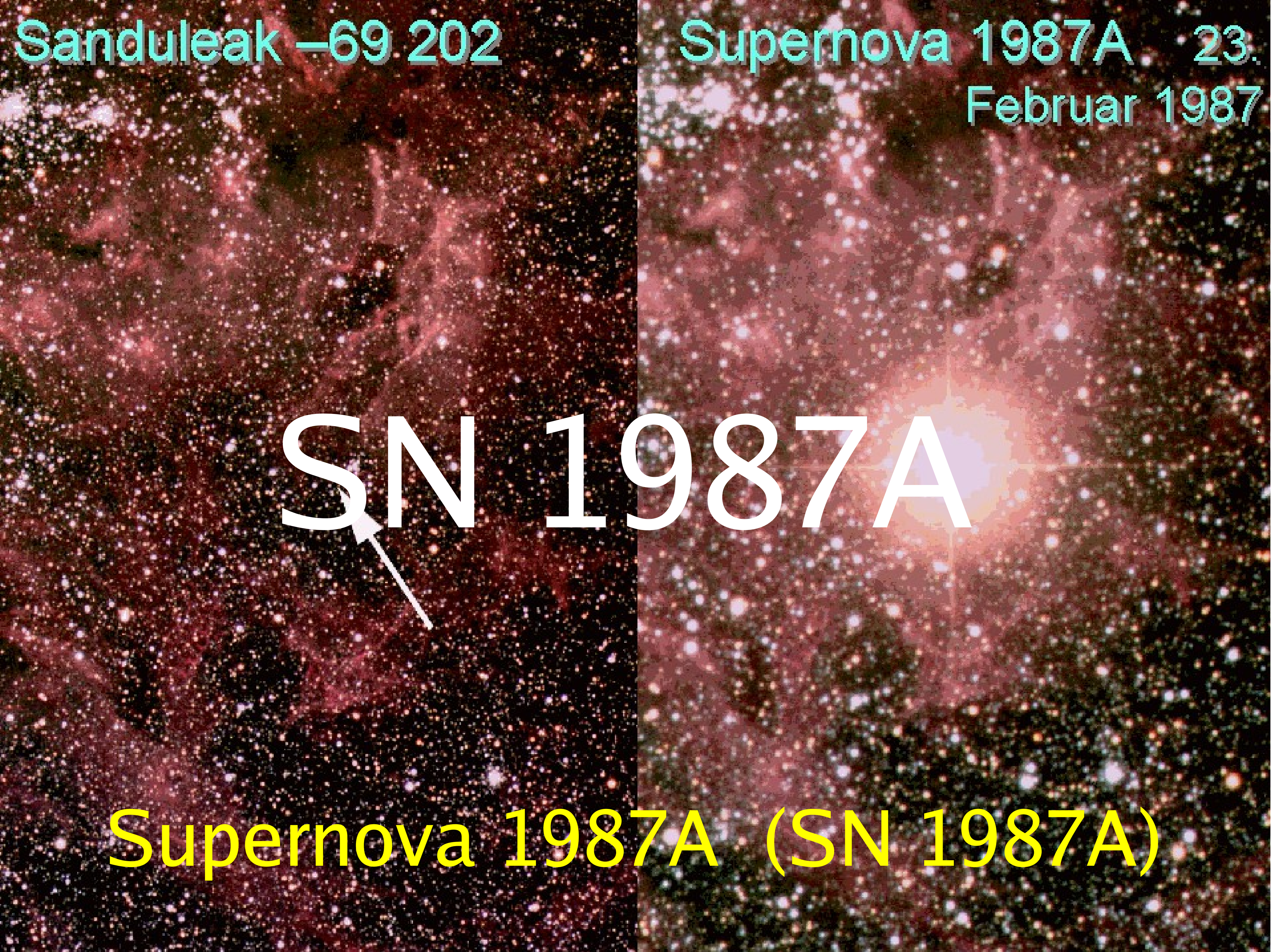
Sanduleak –69 202
Supernova 1987A 23. Februar 1987
SN 1987A
Supernova 1987A (SN 1987A)

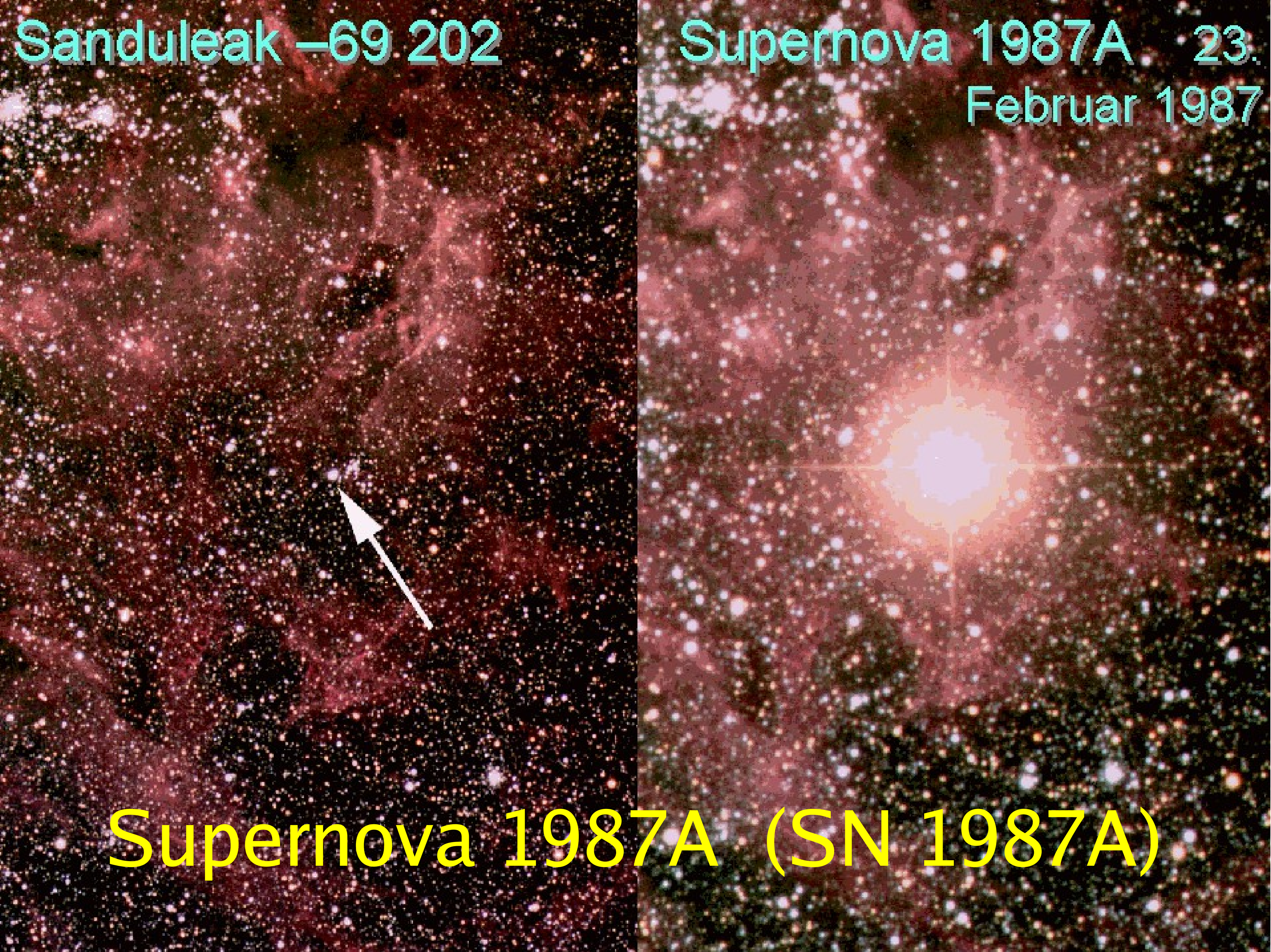

Supernova 1987A (SN 1987A)

Supernova 1987A aging

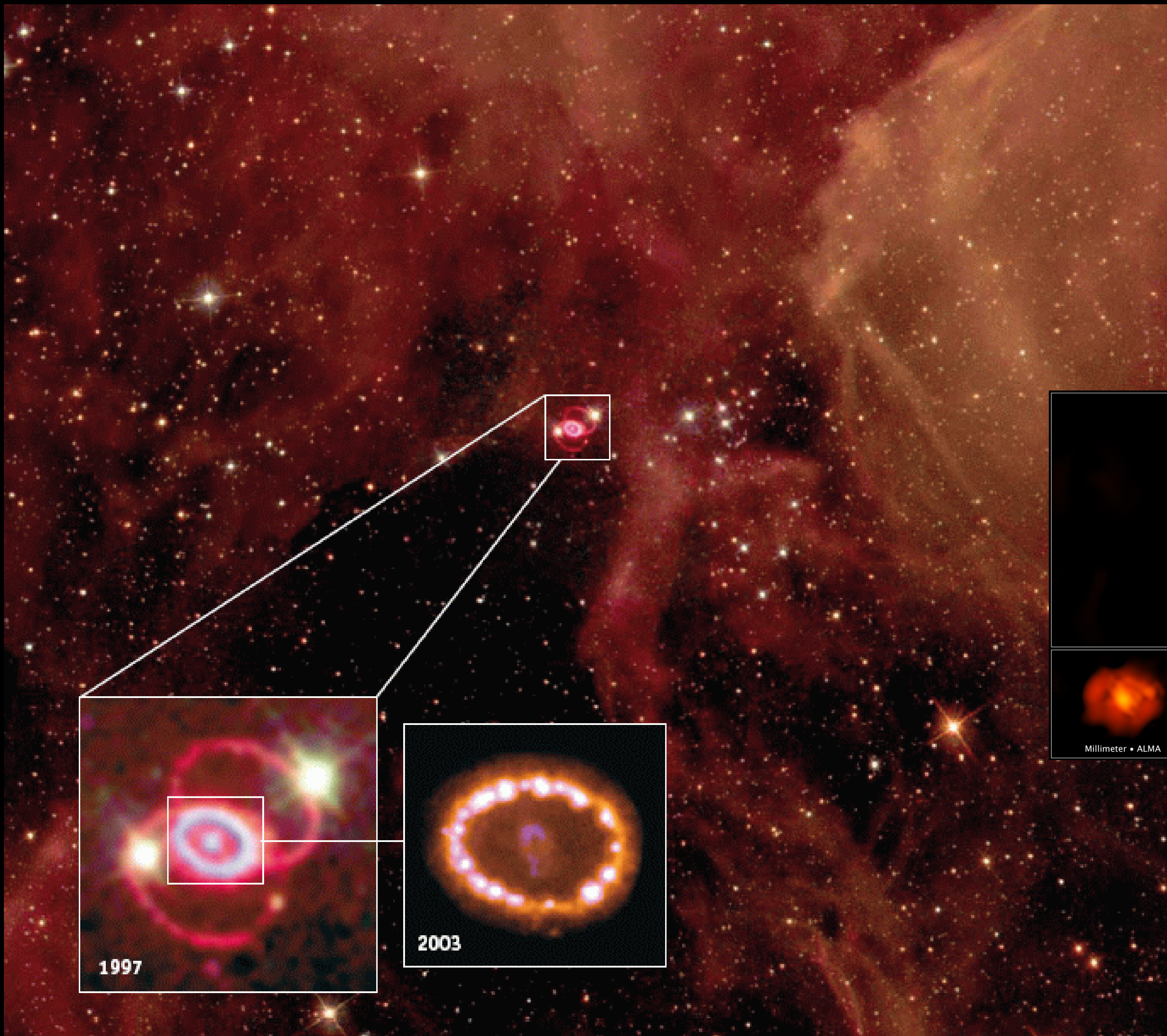

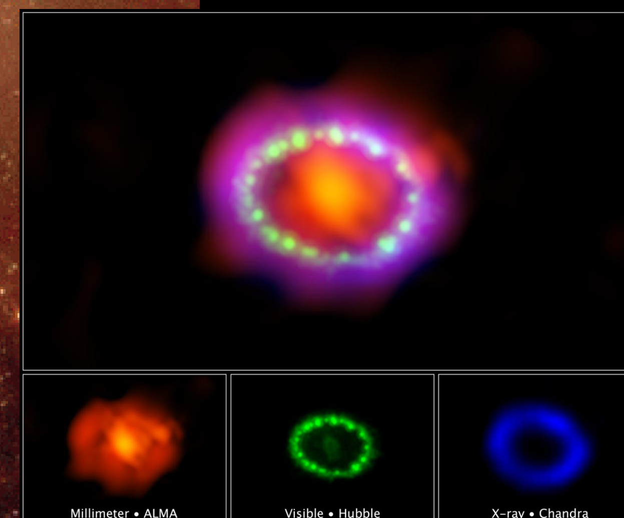

ALMA: radio, red
Hubble: visible, green
Chandra: X-ray, blue

3D SN from Binary Model

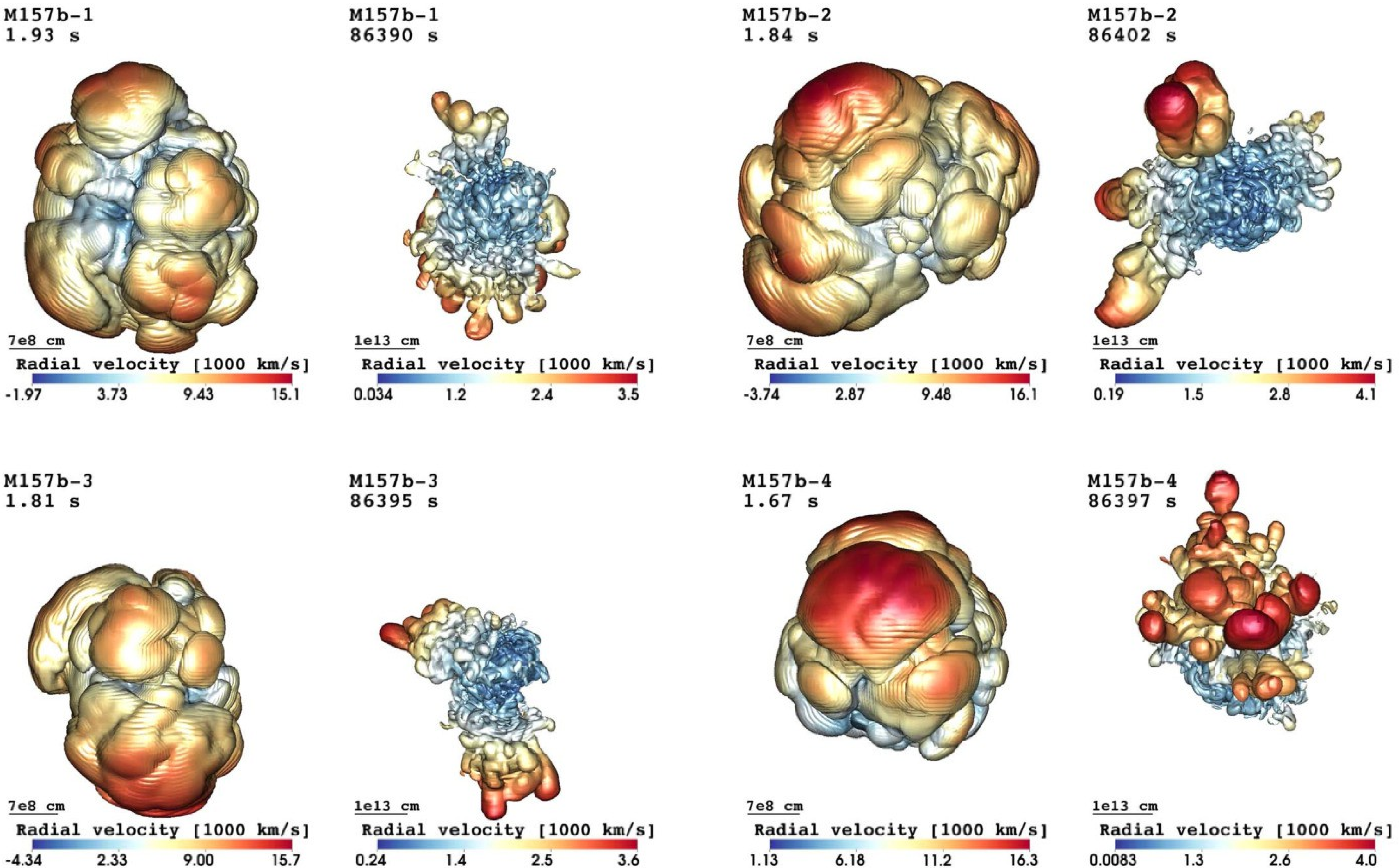

Figure 9. Morphology of radioactive ^{56}Ni-rich ejecta in models M15-7b-1, M15-7b-2, M15-7b-3, and M15-7b-4. See caption of Figure 5 for details.

Utrobin et al., ApJ 914 (2021) 4

Single-star Models for SN1987A: Bolometric Light Curves from 3D Explosions

Hertzsprung-Russell Diagram for SN 1987A Progenitors.

Single Star Scenario

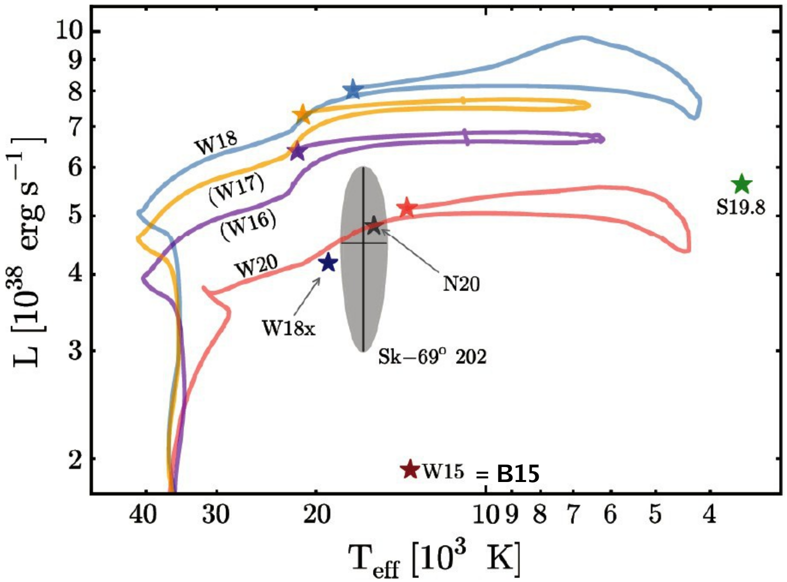

Sukhbold et al. (2016)

Utrobin et al., A&A 624 (2019) A116

Bolometric Light Curves

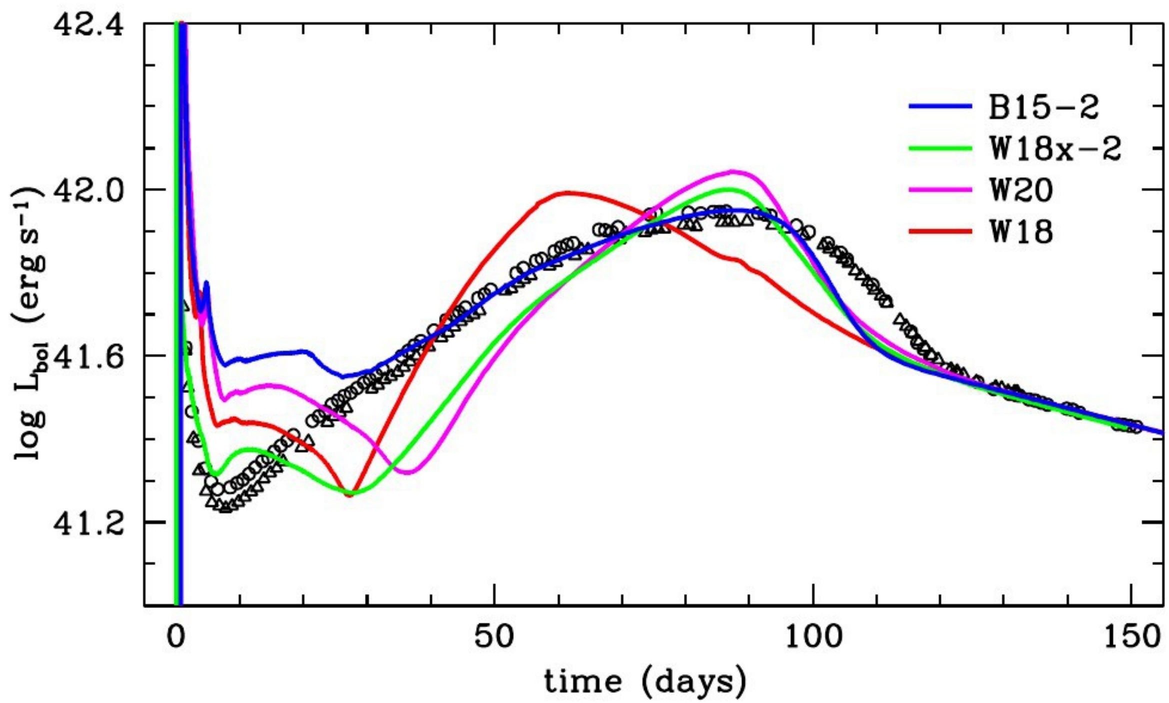

The total ^{56}Ni mass is scaled to fit the observed luminosity in the radioactive tail.

Self-consistent 3D simulations of explosions by neutrino heating do not produce sufficient outward mixing of Ni and inward mixing of H in most progenitors.

Binary-star Models for SN1987A:
Bolometric Light Curves from 3D Explosions

Hertzsprung-Russell Diagram for SN 1987A Progenitors

Binary Merger Scenario

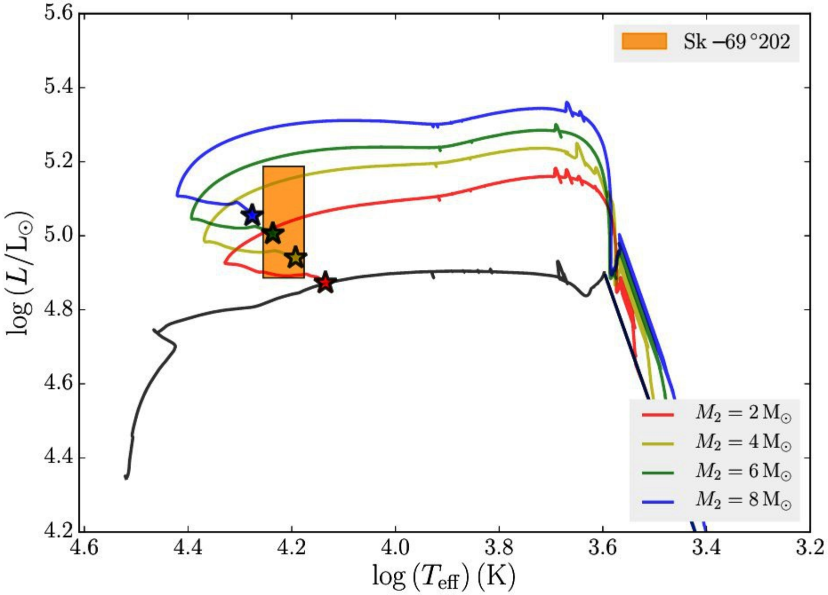

$M_1 = 16\,M_\odot$ Menon & Heger (2017)

Menon & Heger (2017);
Binary merger progenitors, following an original suggestion by Podsiadlowski and coworkers (1990ff)

Utrobin et al., ApJ 914 (2021) 4

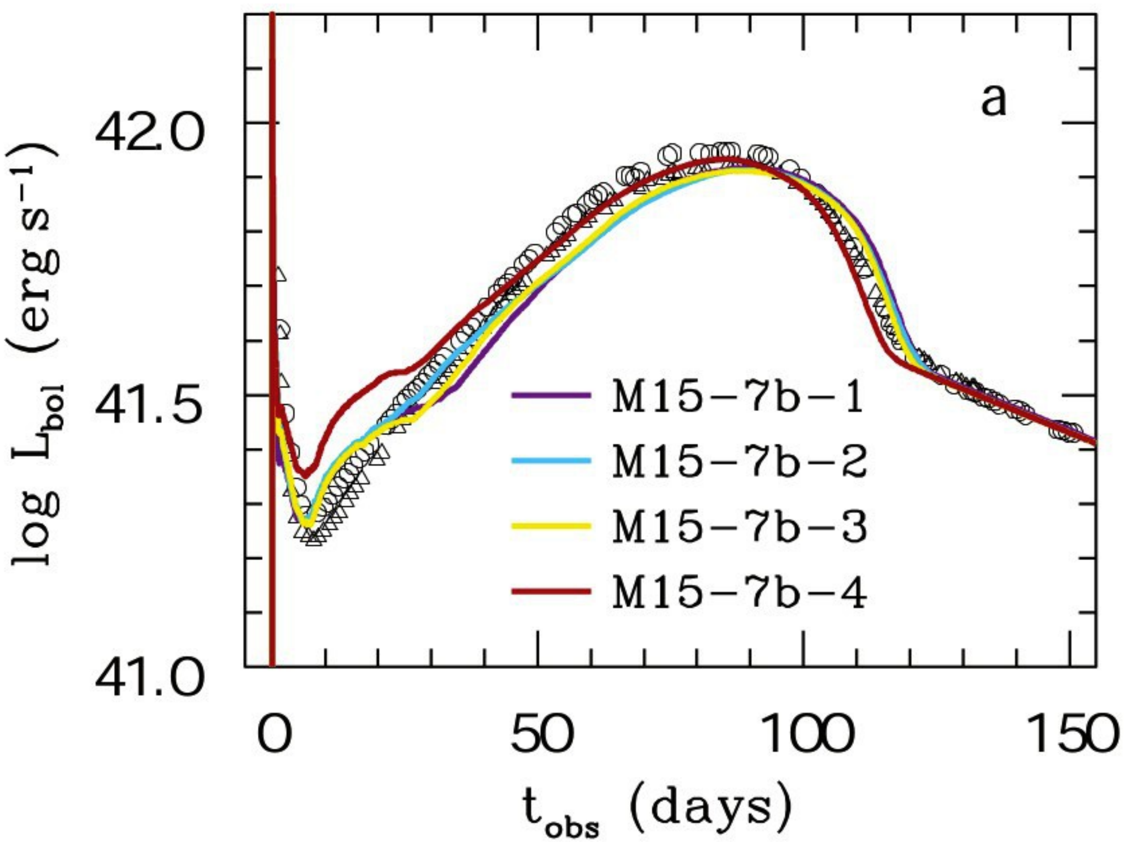

Comparison of Single and Binary Stars:

Radial Mixing and Rayleigh-Taylor Growth Factors

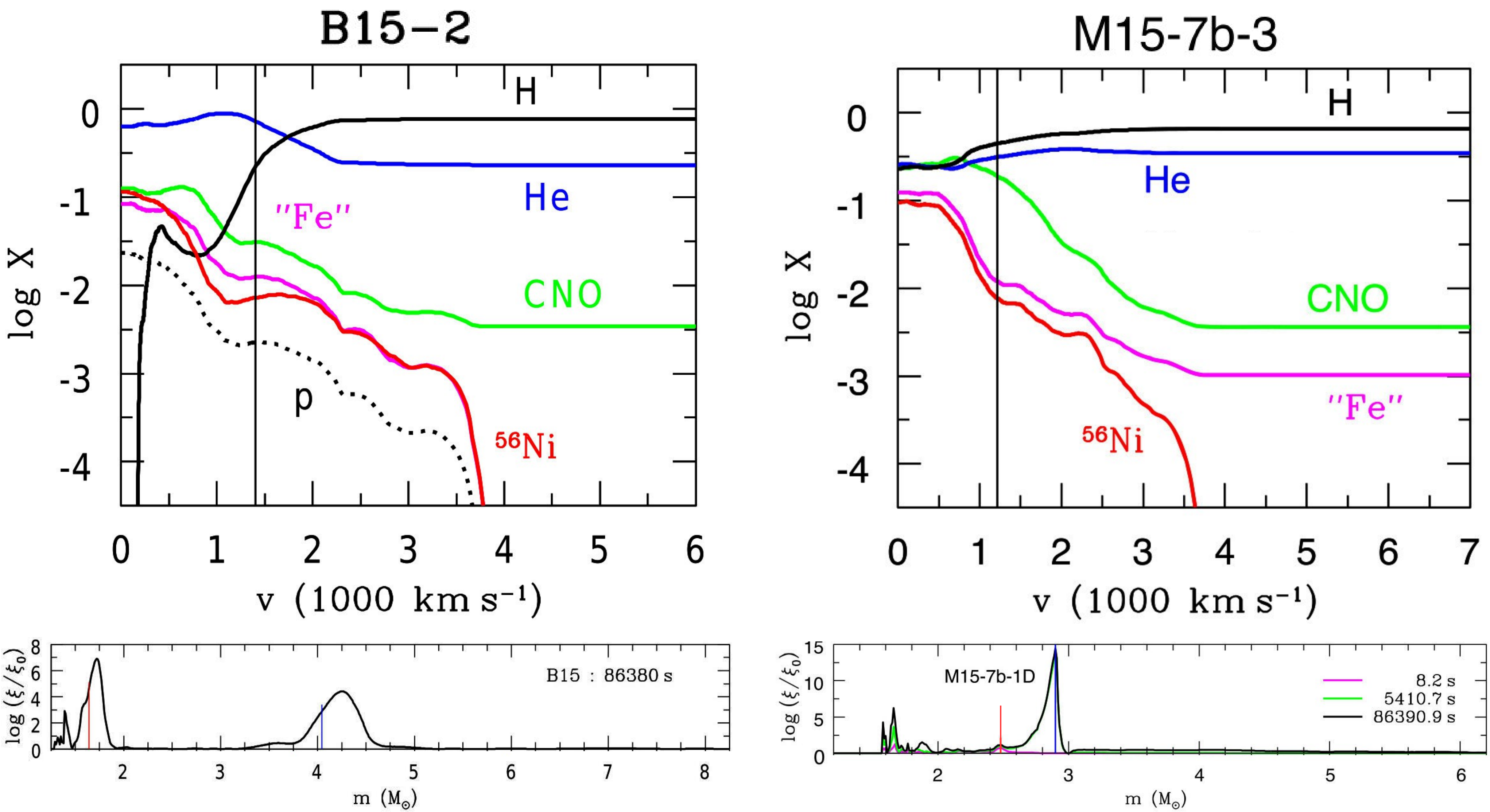

Binary-star vs. Single-star Models for SN1987A:

Table 6. Comparative analysis of single-star and binary-merger models

Observational constraint	Single-star	Binary-merger
	B15-2 / W18x-2	M15-7b-3 / M15-8b-1
1. location of Sanduleak $-69°202$ in the HRD	− / +	+ / +
2. production of ^{56}Ni in 3D simulations	+ / +	+ / +
3. maximum velocity of the bulk of ^{56}Ni	+ / −	+ / −
4. minimum velocity of hydrogen matter	+ / +	+ / +
5. mass of hydrogen with $v < 2000\,\mathrm{km\,s^{-1}}$	− / −	+ / +
6. dome shape of the light curve	+ / −	+ / +
7. global shape of the light curve	− / −	+ / −
8. evolution of the photospheric velocity	+ / −	+ / −
9. oxygen mass in the SN ejecta	− / −	+ / +
10. 3D shape of the ^{56}Ni ejecta	− / +	+ / −
11. X-ray and gamma-ray emission	+ /	+ / −
12. gamma-ray decay lines	+ / −	− / −
Total score	7 : 12 / 4 : 11	11 : 12 / 6 : 12

Utrobin et al., ApJ 914 (2021) 4

Binary-star vs. Single-star Models
for SN1987A:

Table 6. Comparative analysis of single-star and binary-merger models

Observational constraint	Single-star	Binary-merger
	B15-2 / W18x-2	M15-7b-3 / M15-8b-1
1. location of Sanduleak −69°202 in the HRD	− / +	+ / +
2. production of ^{56}Ni in 3D simulations	+ / +	+ / +
3. maximum velocity of the bulk of ^{56}Ni	+ / −	+ / −
4. minimum velocity of hydrogen matter	+ / +	+ / +
5. mass of hydrogen with $v < 2000\,\mathrm{km\,s^{-1}}$	− / −	+ / +
6. dome shape of the light curve	+ / −	+ / +
7. global shape of the light curve	− / −	+ / −
8. evolution of the photospheric velocity	+ / −	+ / −
9. oxygen mass in the SN ejecta	− / −	+ / +
10. 3D shape of the ^{56}Ni ejecta	− / +	+ / −
11. X-ray and gamma-ray emission	+ /	+ / −
12. gamma-ray decay lines	+ / −	− / −
Total score	7 : 12 / 4 : 11	11 : 12 / 6 : 12

Utrobin et al., ApJ 914 (2021) 4

3D Geometry of SN1987A: Observations vs. Models

Molecular CO 2-1 and SiO 5-4 emission observed by ALMA

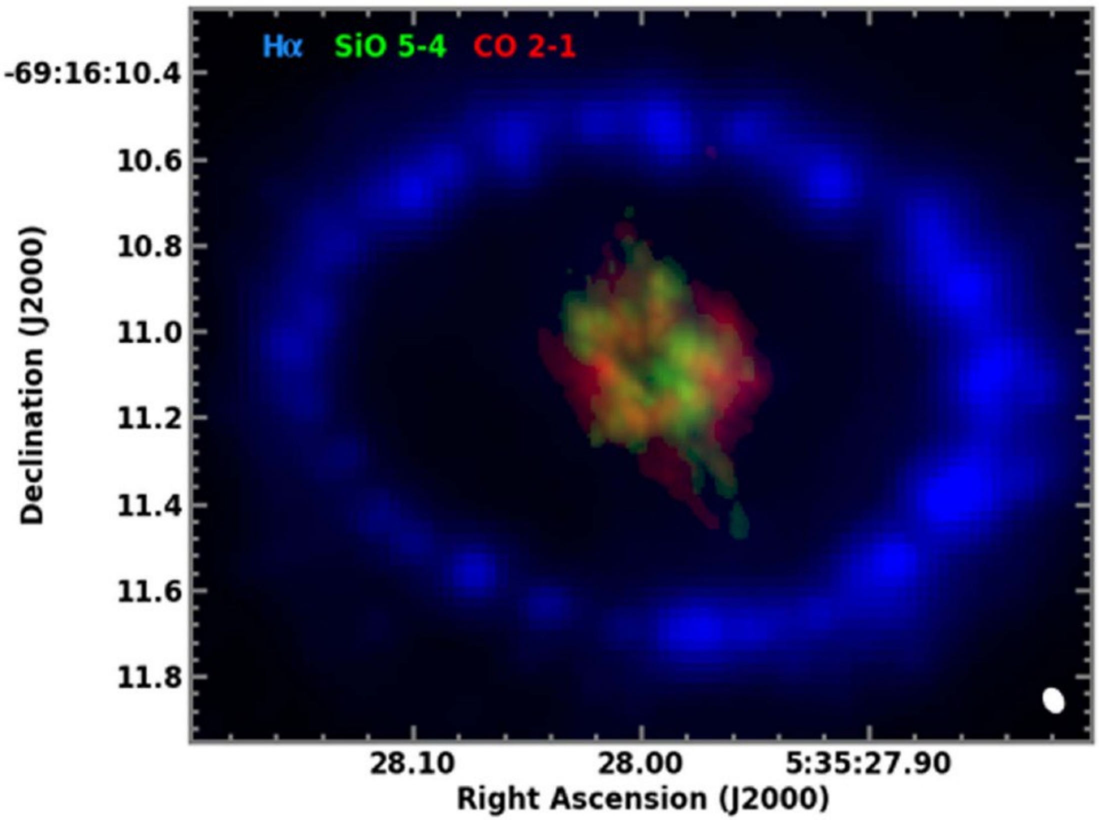

Abellán et al., ApJL 842 (2017) L24

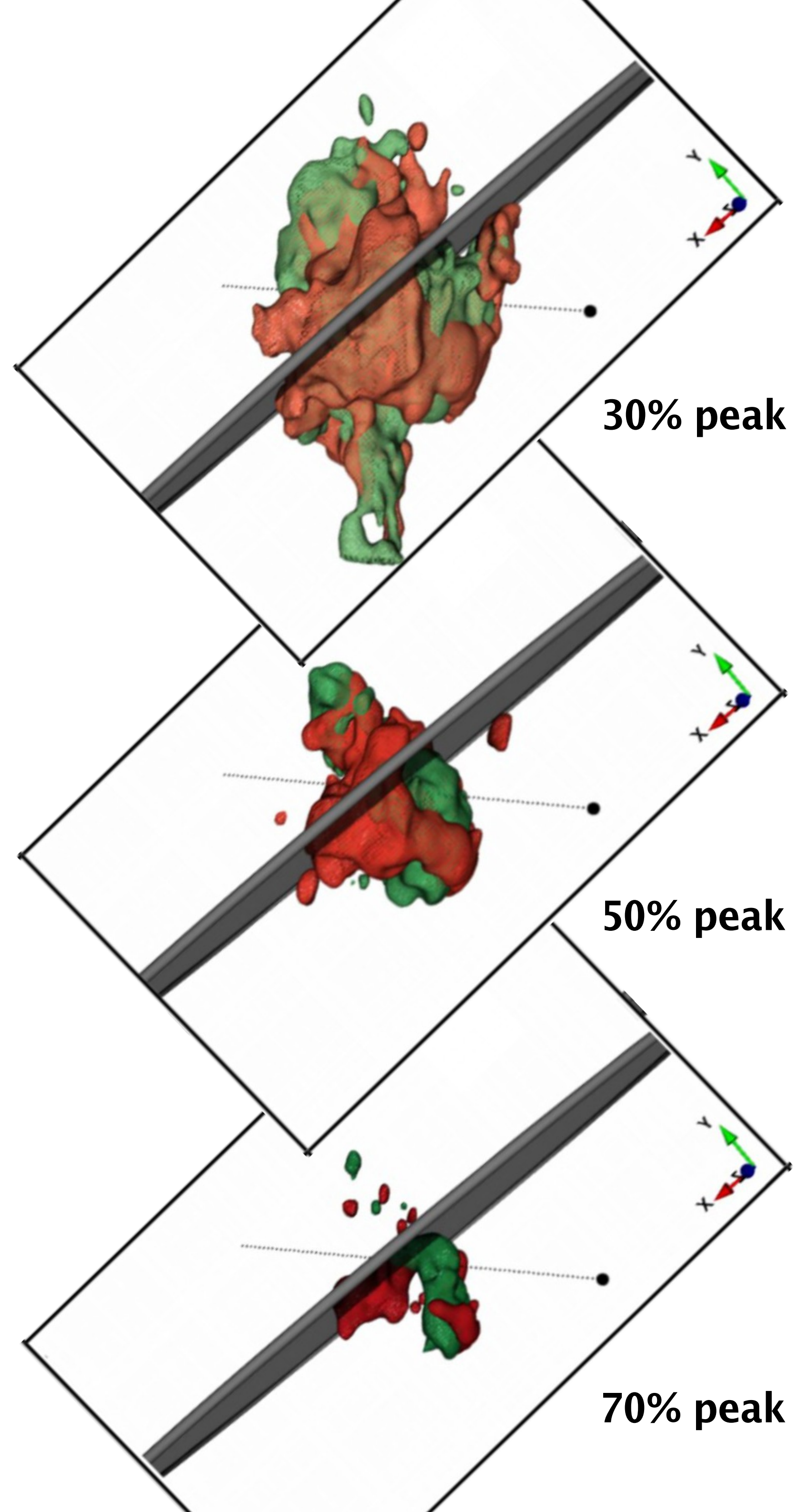

30% peak

50% peak

70% peak

3D Geometry of SN1987A: Observations vs. Models

Molecular CO 2-1 and SiO 5-4 emission observed by ALMA

Abellán et al., ApJL 842 (2017) L24

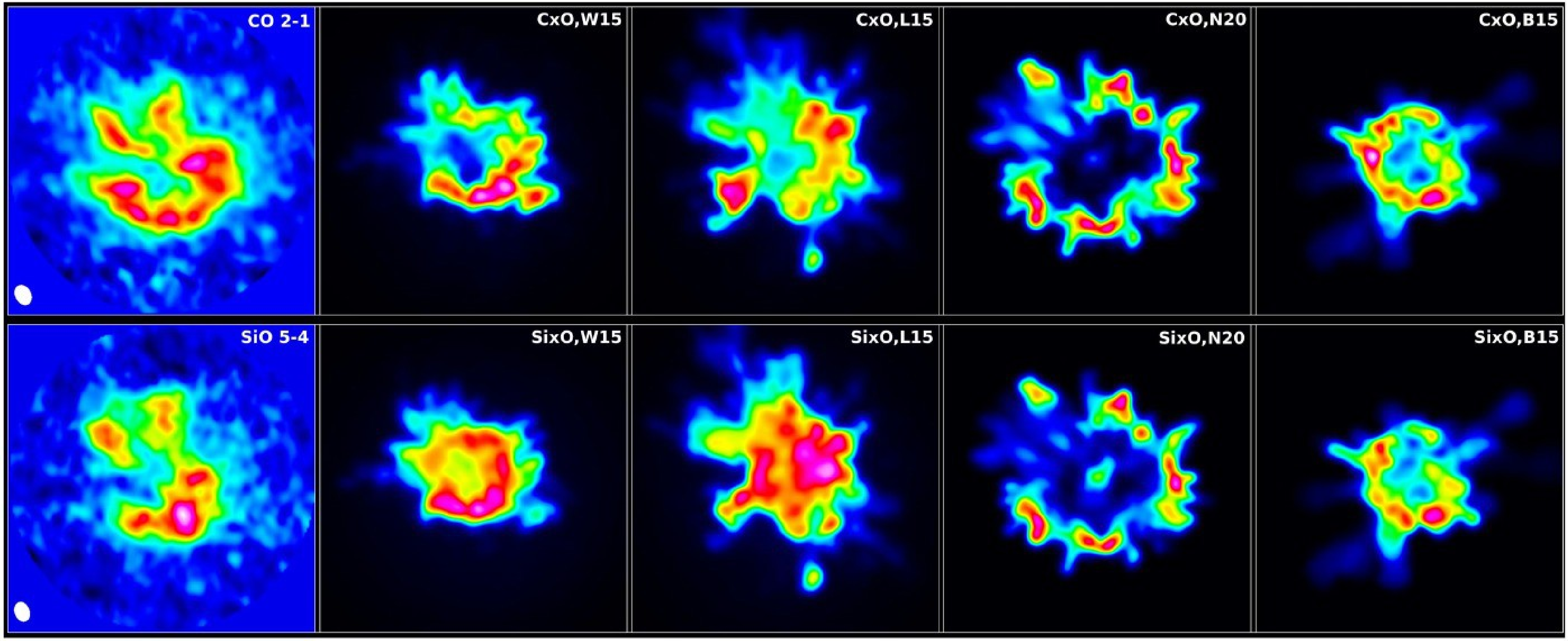

W15 L15 N20 B15

3D Geometry of SN1987A: Observations vs. Models

Molecular CO 2-1 and SiO 5-4 emission observed by ALMA

Abellán et al., ApJL 842 (2017) L24

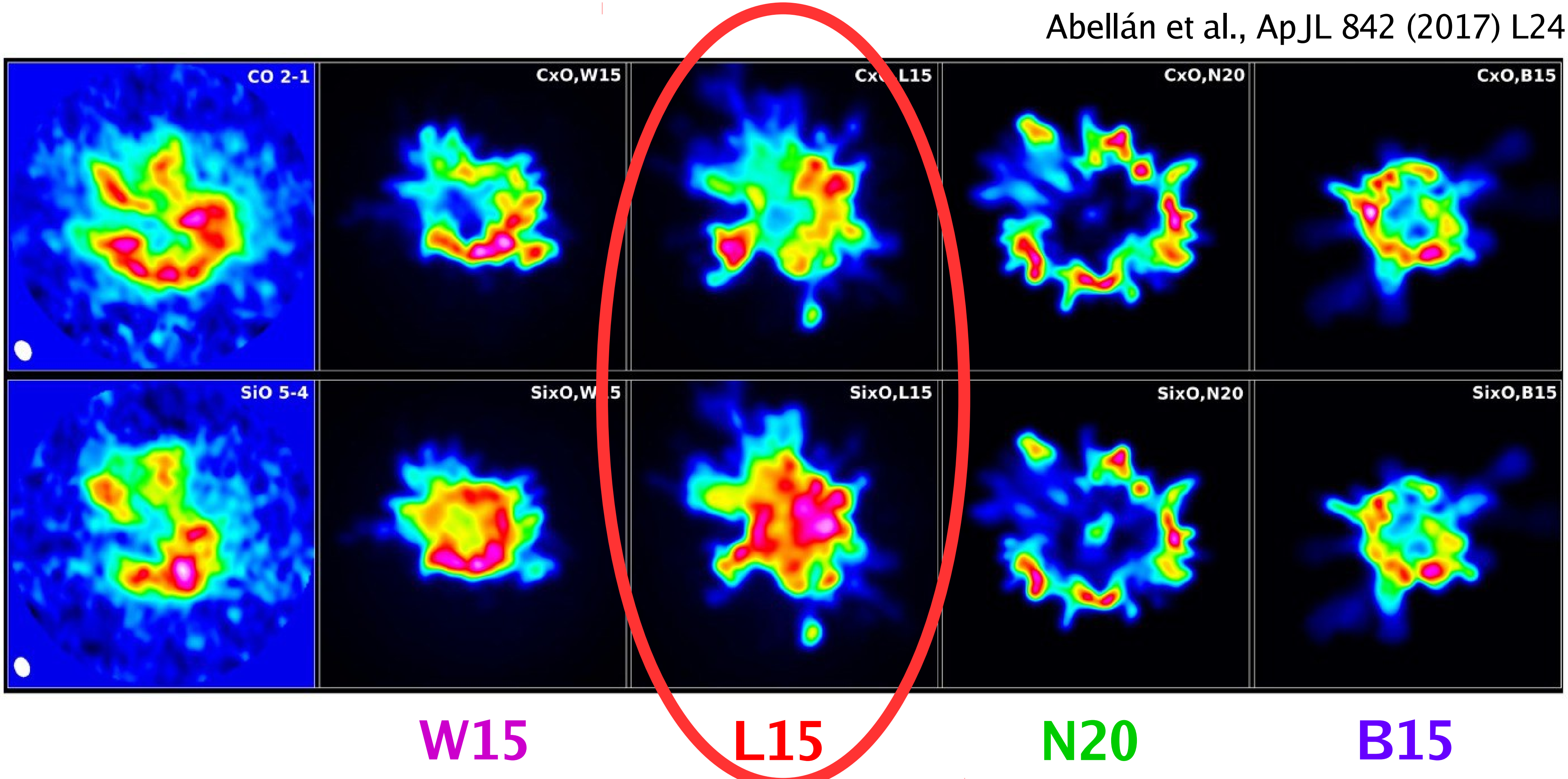

3D Geometry of SN1987A: Observations vs. Models

3D isosurfaces of iron and silicon ([FeII]+[SiI])

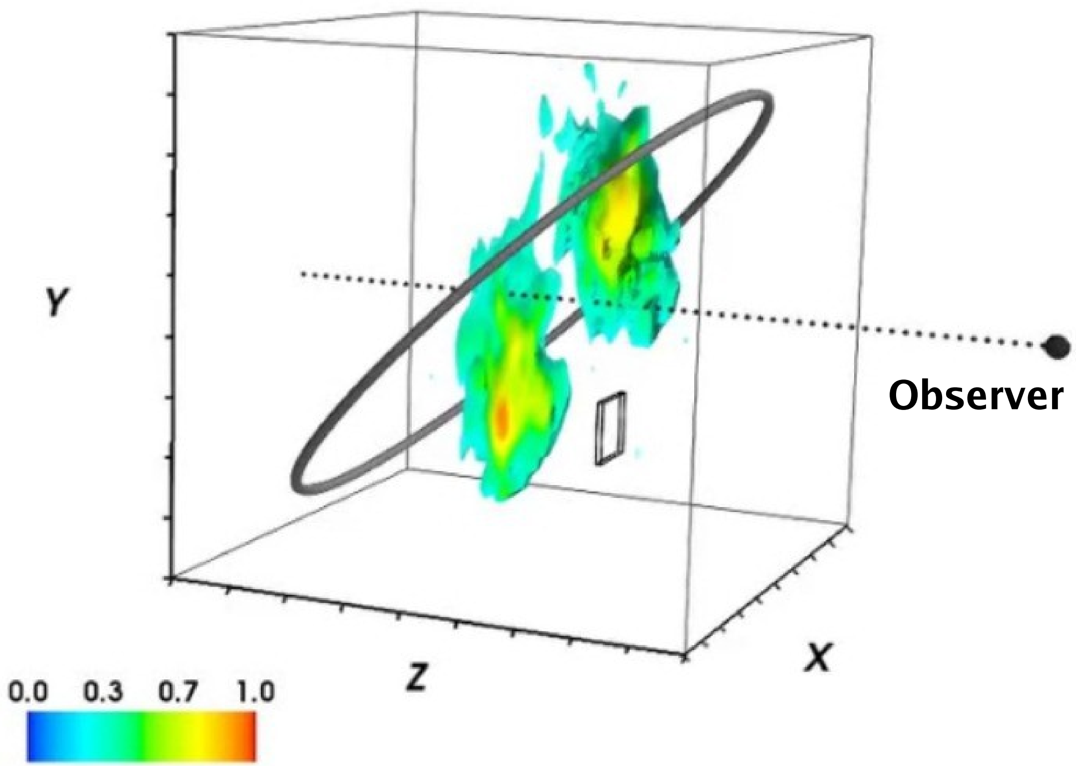

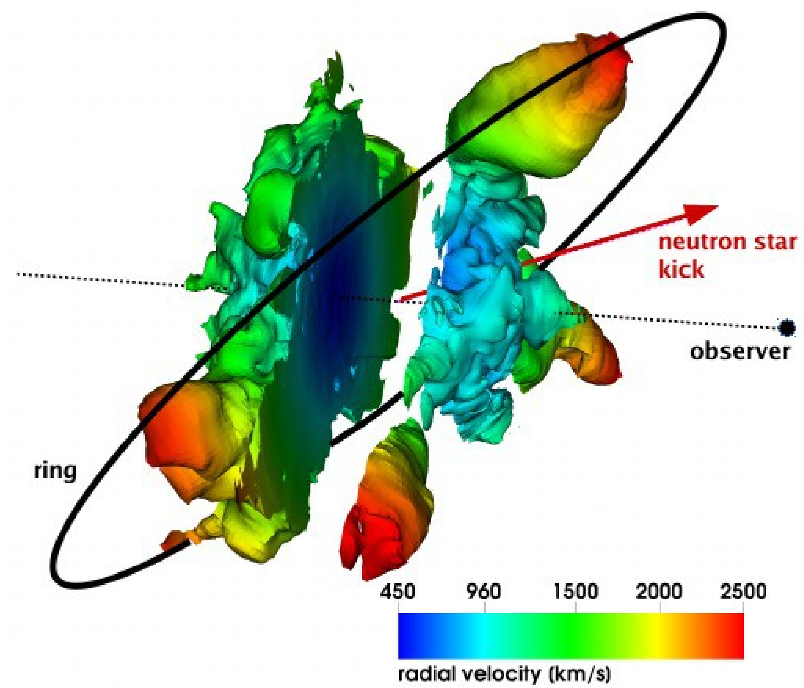

HST & VLT obs. (Larsson et al., ApJ 833 (2016) 147)

3D model L15 (Janka et al., arXiv:1705.01159)

SN 1987A: Gamma Lines of ^{44}Ti & ^{56}Co

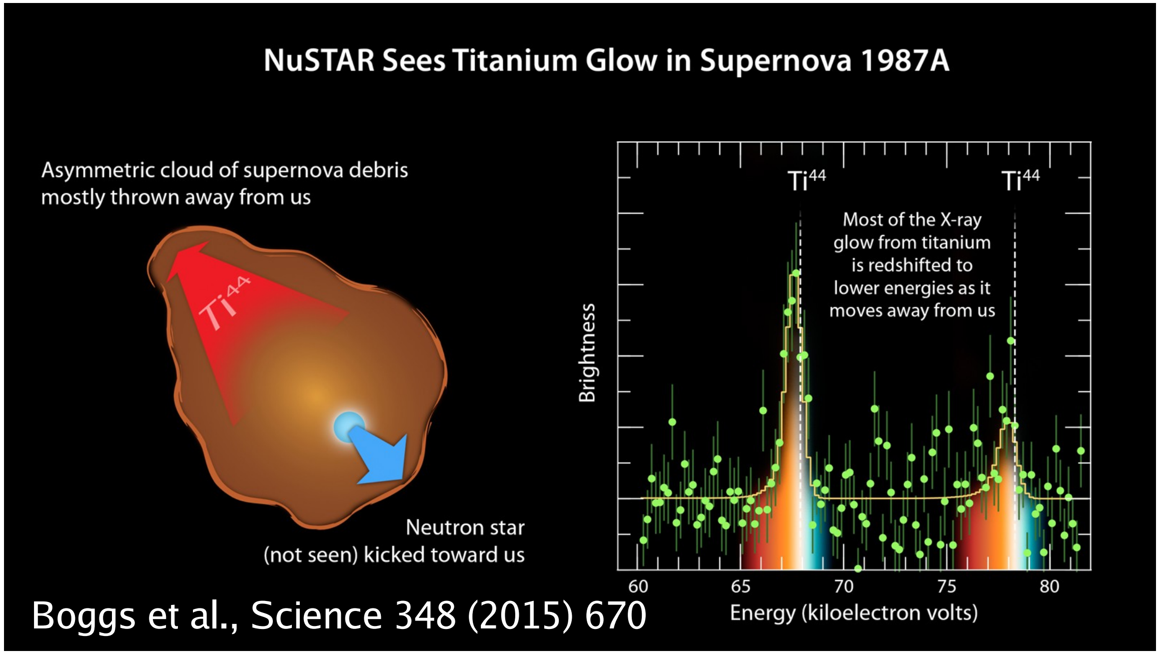

Boggs et al. (2015):
Redshifted ^{44}Ti lines suggest that NS in SN 1987A is likely to have fairly high kick towards us.

Jerkstrand et al., MNRAS 494 (2020) 2471

v_{ns} ~100 km/s: Incompatible

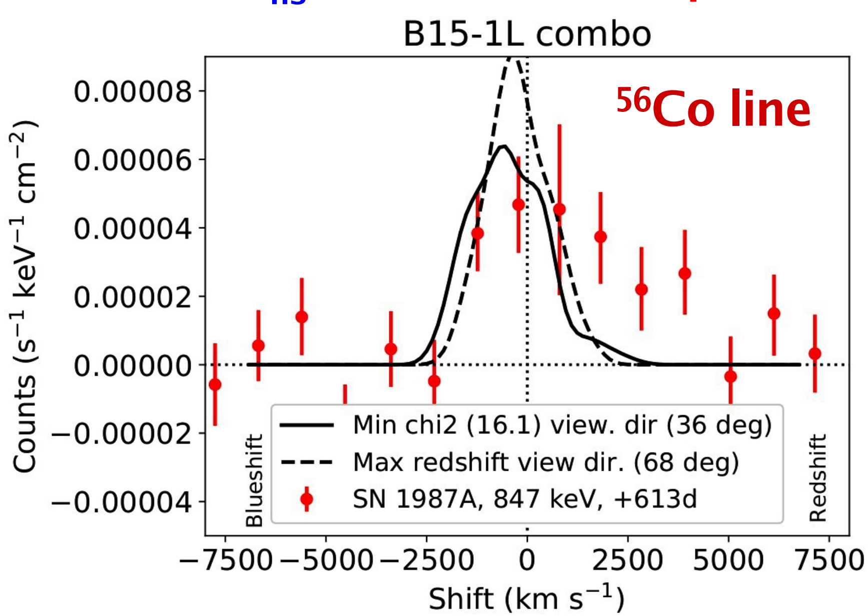

v_{ns} ~300 km/s: Better fit!

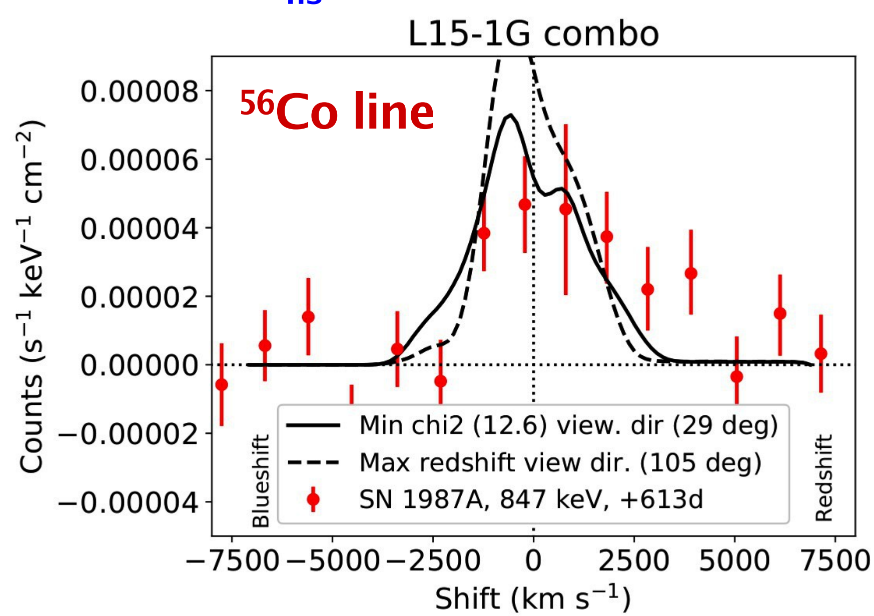

A Compact Object in SN1987A?

High angular resolution ALMA images of dust and molecules in the ejecta of SN 1987A

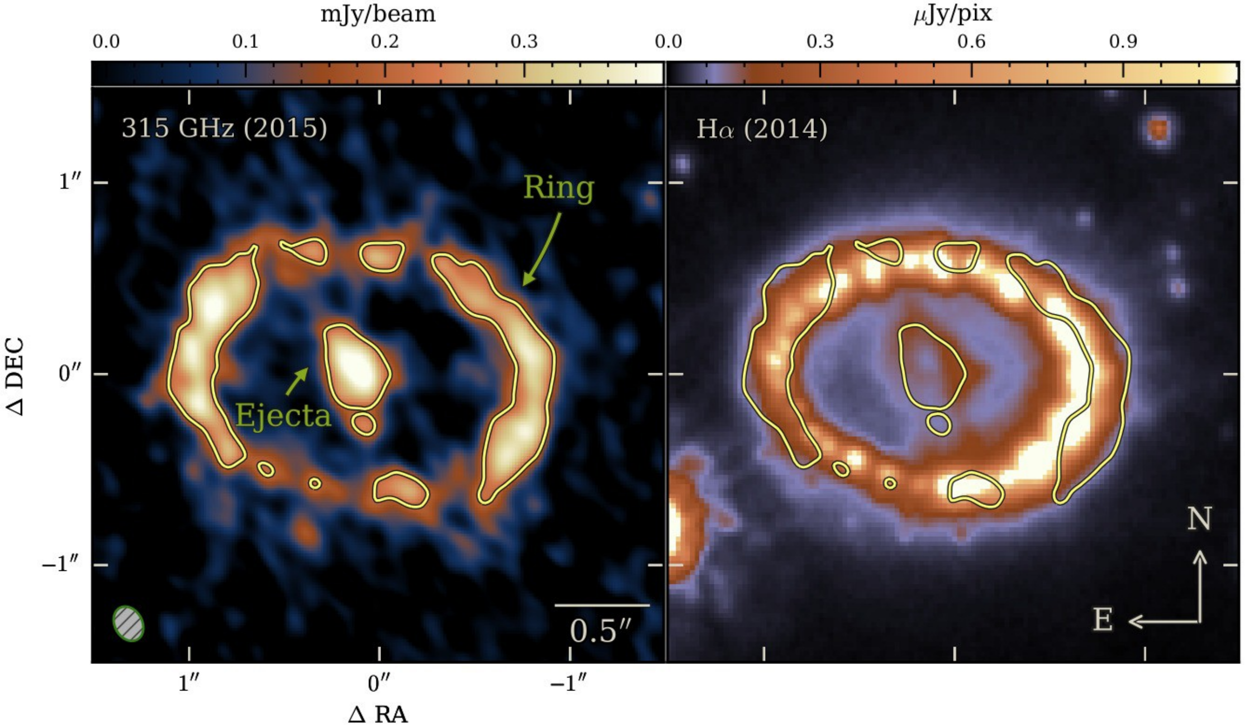

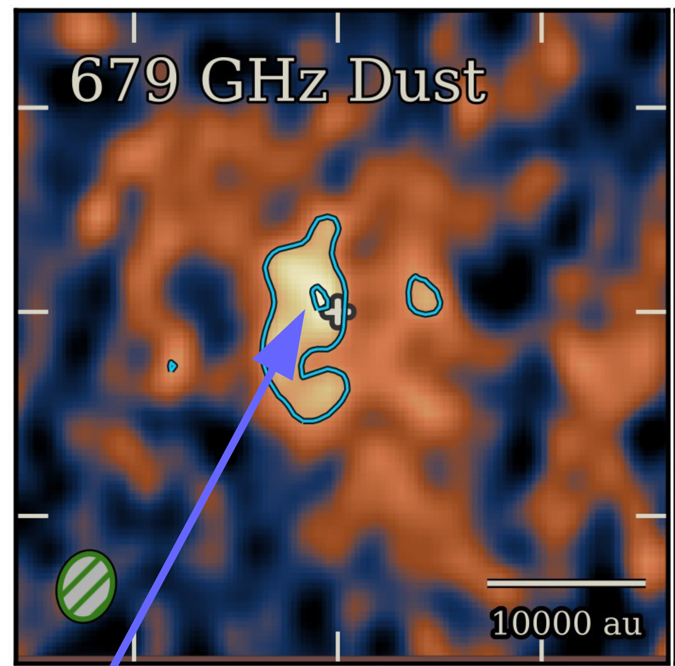

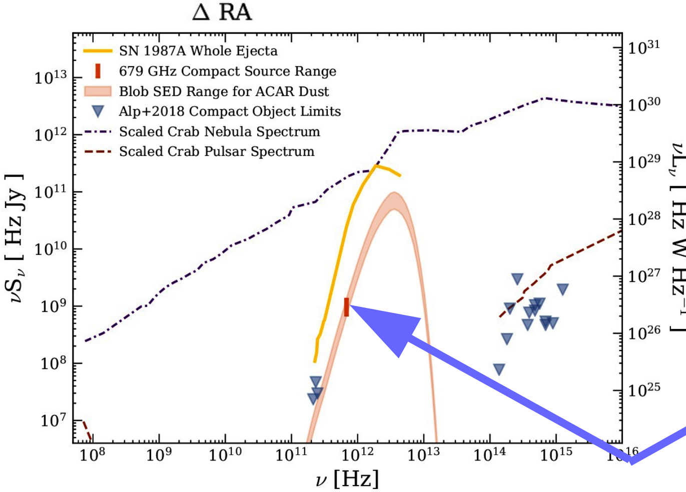

5-sigma hot "blob" north-east of ejecta center:

Compact source would be compatible with recent limits by Alp et al. (ApJ 864 (2018) 174).

Luminosity can be explained by energy input from a thermally cooling NS (or, less likely, accretion by BH)

(Cigan et al., ApJ 886 (2019) 51; Page et al., ApJ 898 (2020) 125)

A Compact Object in SN1987A?

High angular resolution ALMA images of dust and molecules in the ejecta of SN 1987A: Thermally cooling neutron star or PWN?

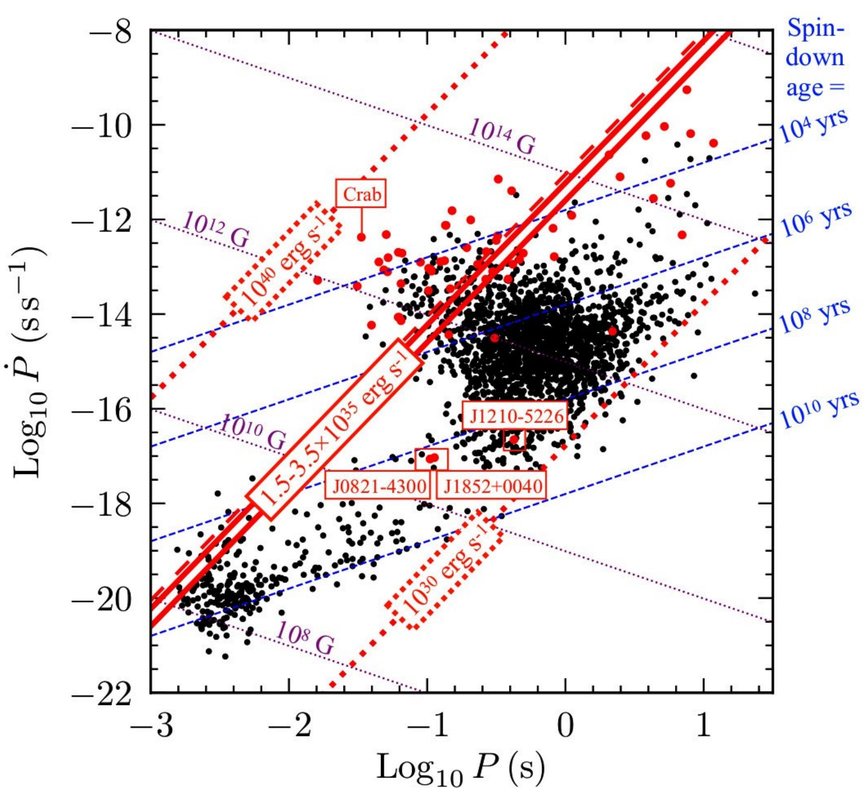

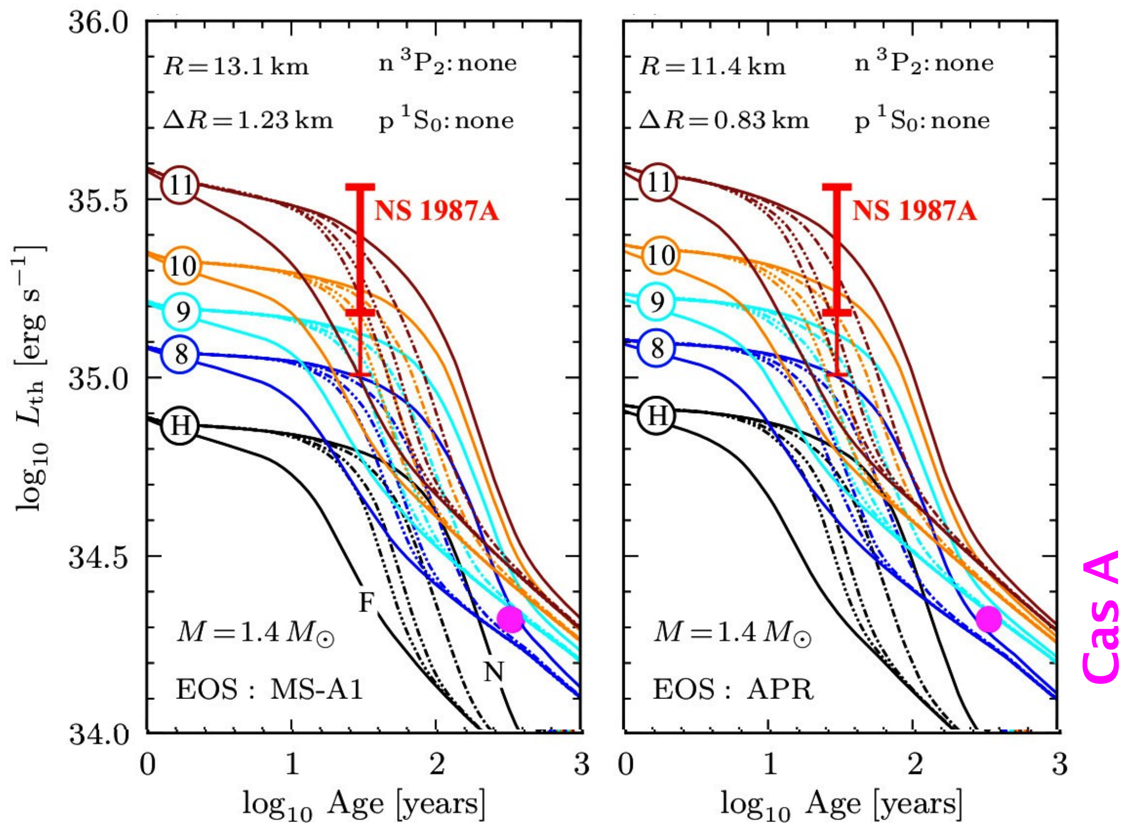

Luminosity can be explained by energy input from a thermally cooling NS (or, less likely, accretion by BH)

(Page et al., ApJ 898 (2020) 125)

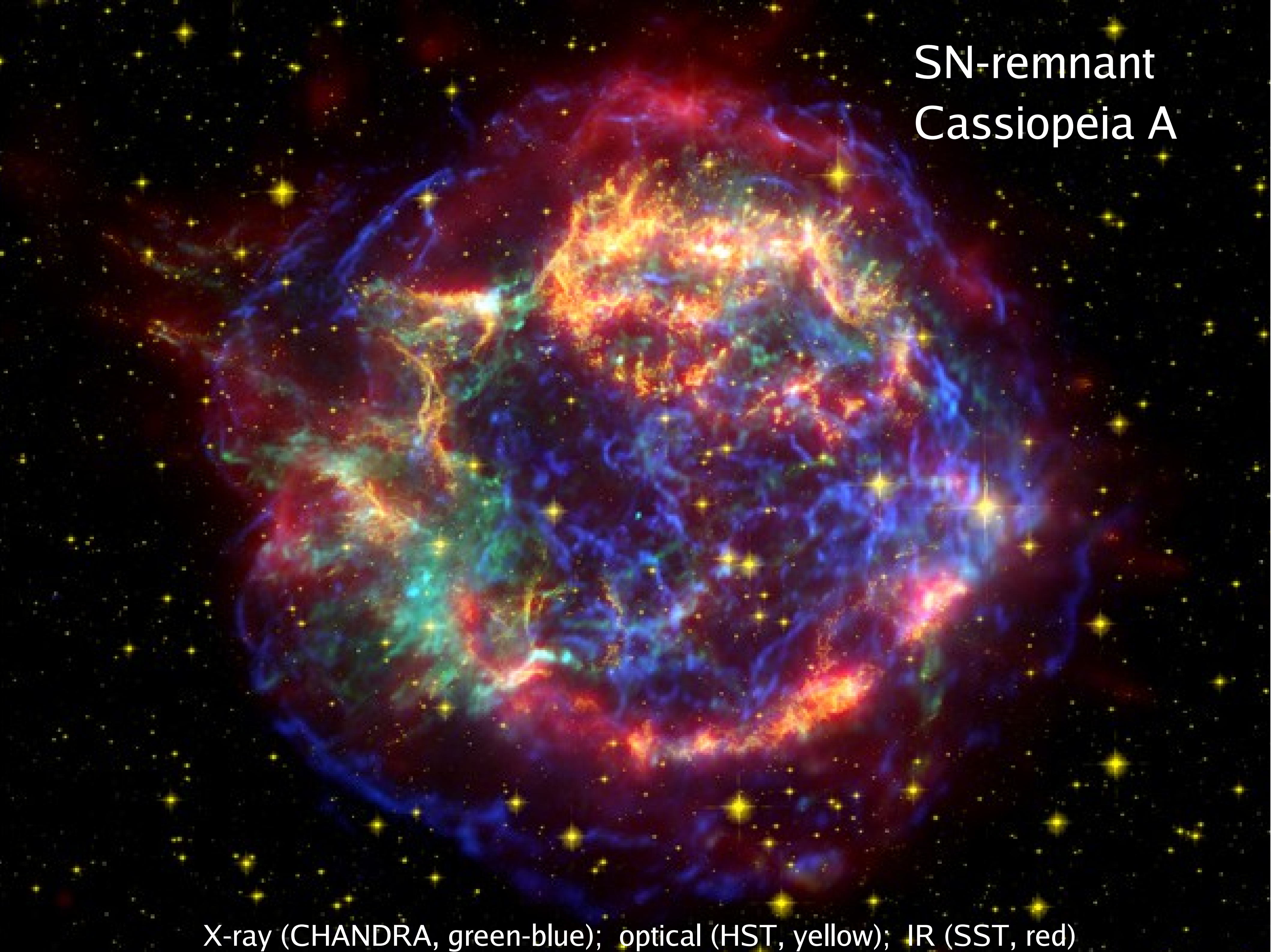

X-ray (CHANDRA, green-blue); optical (HST, yellow); IR (SST, red)

Intermediate-mass-element Asymmetries in CAS A Remnant

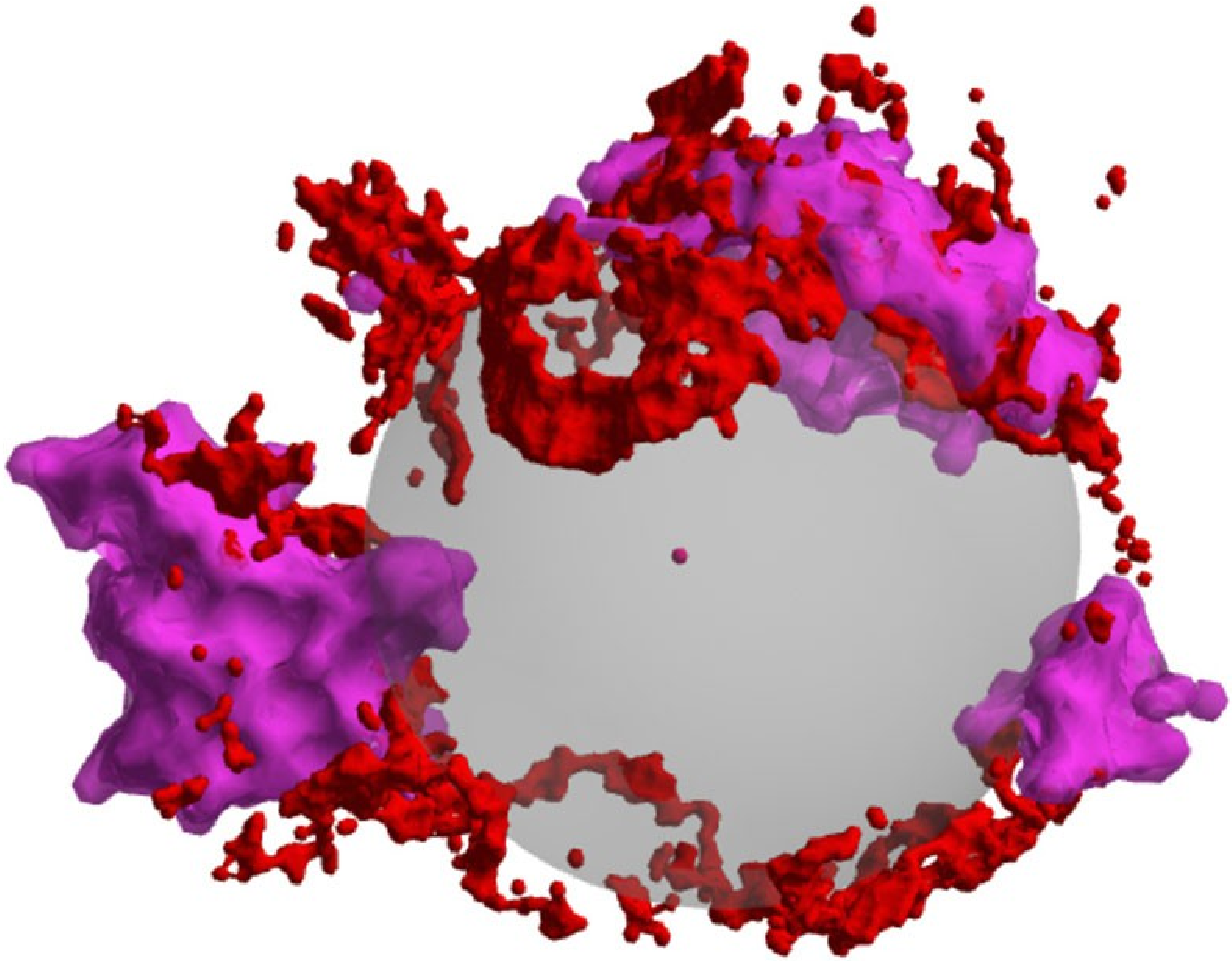

Red: Ar, Ne, and O (optical)
Purple: Iron (X-ray)

Image: Robert Fesen and Dan Milisavljevic, using iron data from DeLaney et al. (2010)

Chemical Asymmetries in CAS A Remnant

Iron in Cas A is visible in three big "fingers" in the remnant shell that is heated by reverse shock from circumstellar medium interaction.

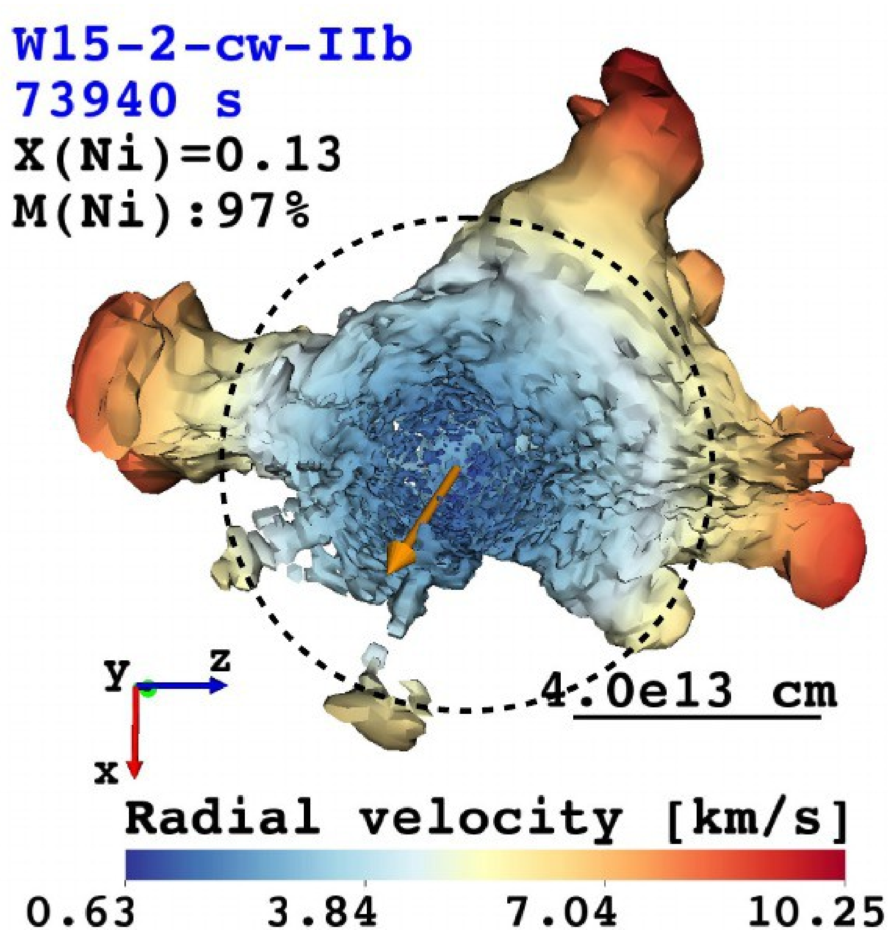

Hot, shocked iron (observed)

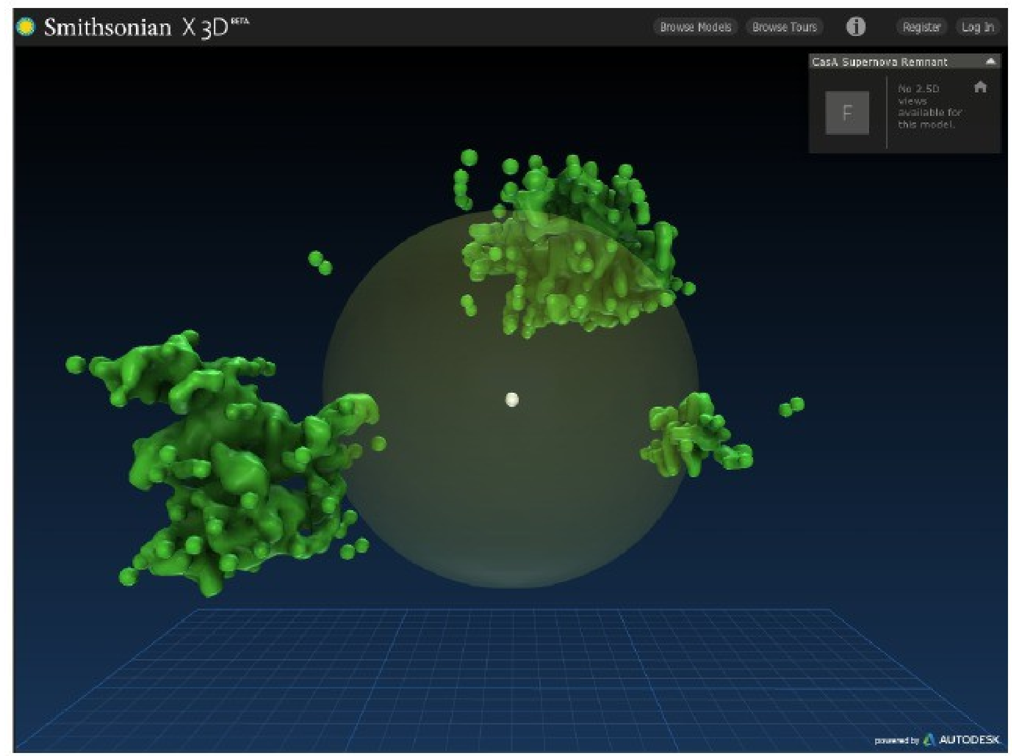

Wongwathanarat et al., ApJ 842 (2017) 13

^{44}Ti Asymmetry in the CAS A Remnant

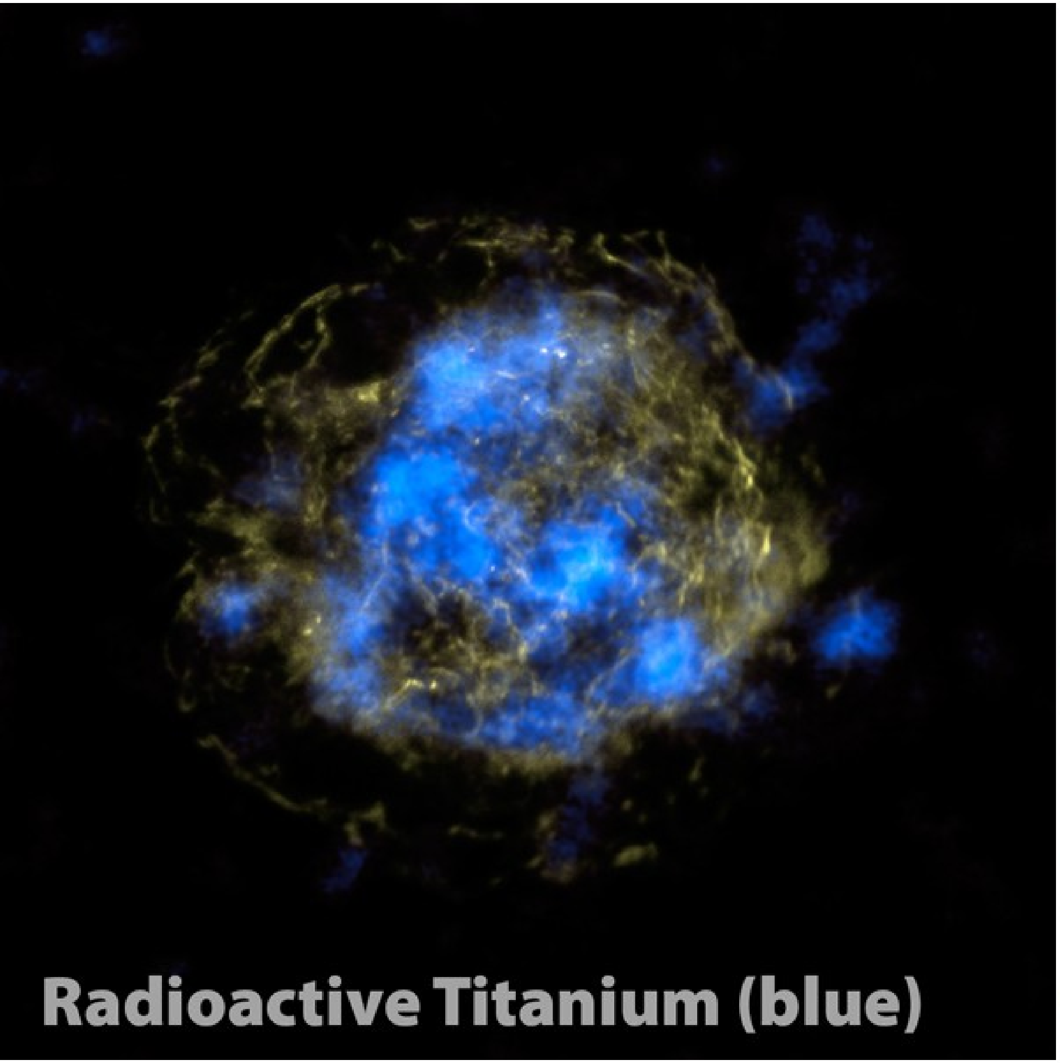

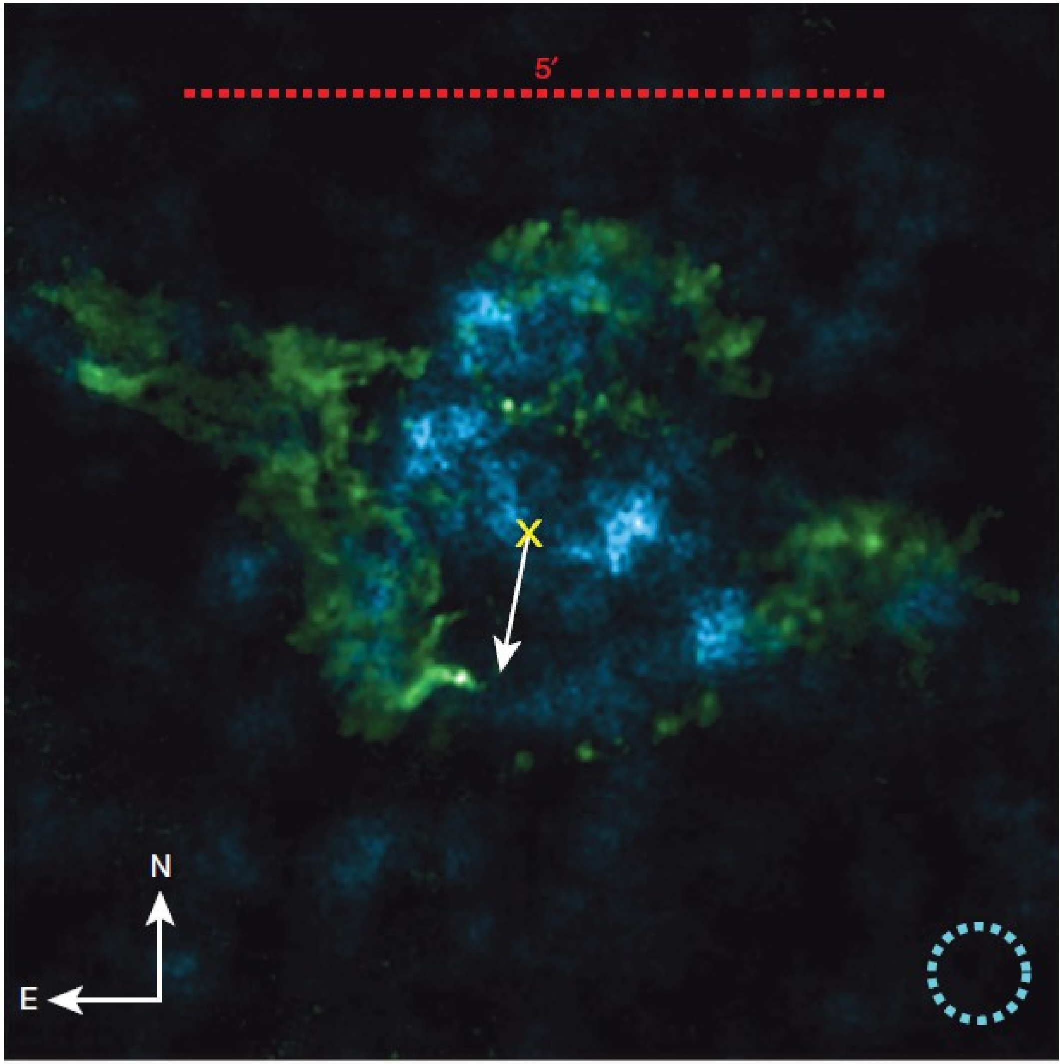

Grefenstette et al., Nature 506 (2014) 340

NuSTAR observations

Neutron Star Recoil and Nickel & 44Ti Distribution

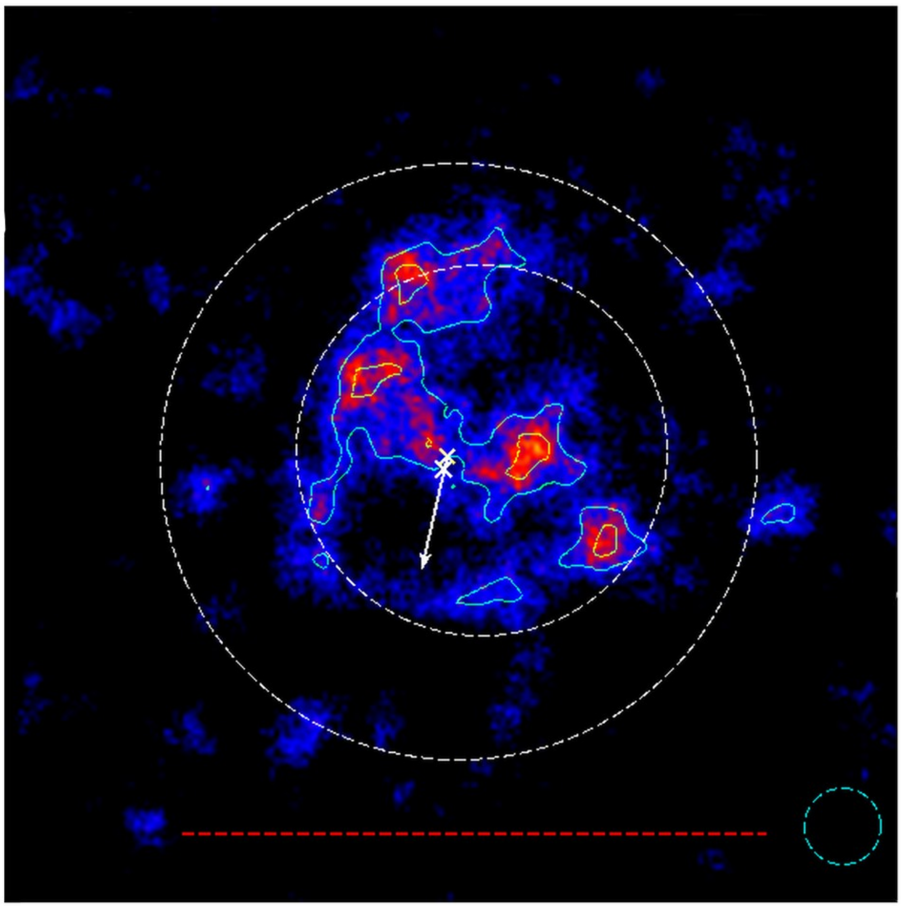

Grefenstette et al., Nature 506 (2014) 340

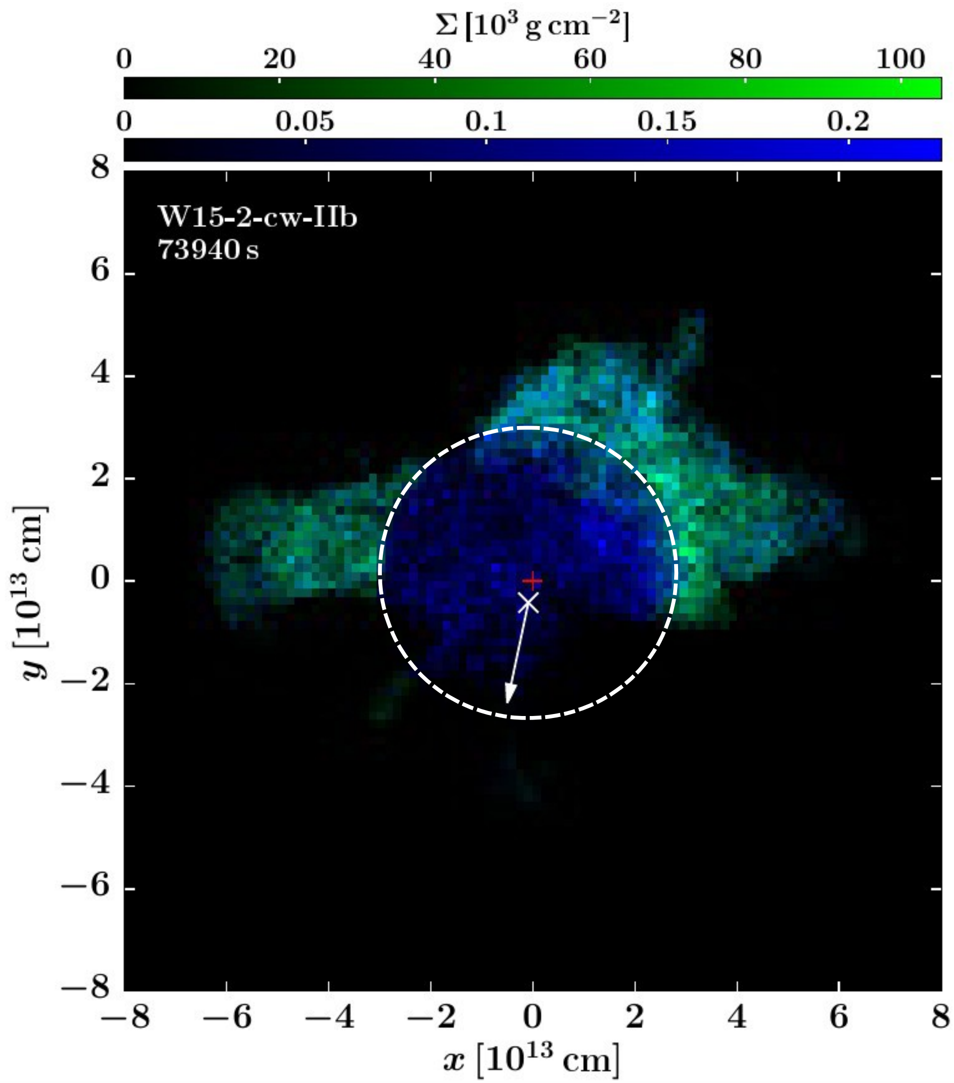

Wongwathanarat et al., ApJ 842 (2017) 13

Cas A: Gamma-Ray Line Profiles of ^{44}Ti

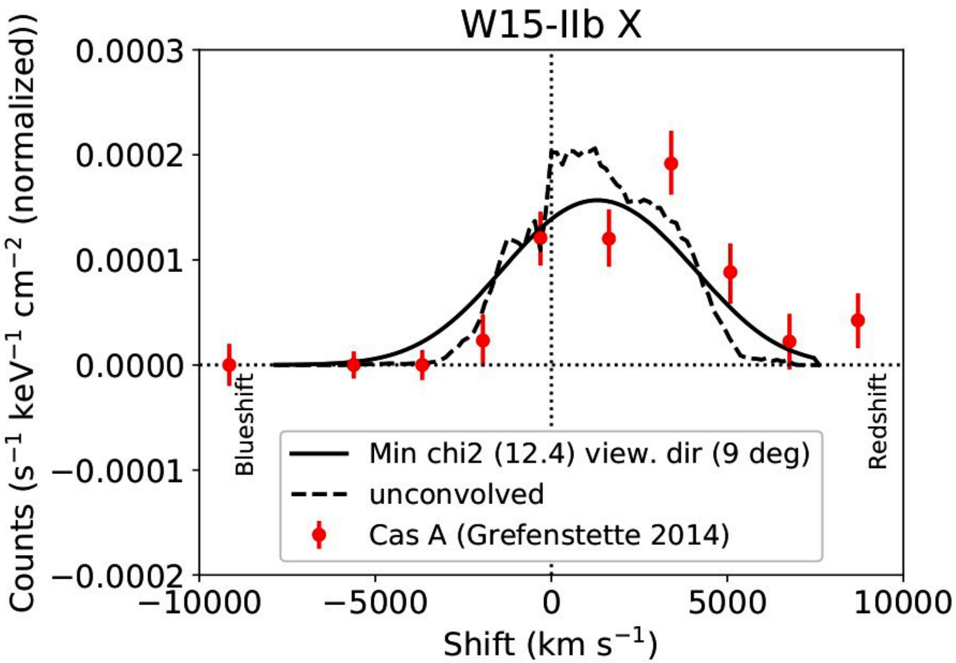

Line centroid of ^{44}Ti decay line strongly redshifted

NS in Cas A has high kick (~500–700 km/s) with small inclination angle (within <40–5 0 degrees) to line of sight.

Consistent with 3D analysis of 44Ti distribution by Grefenstette et al. (2017).

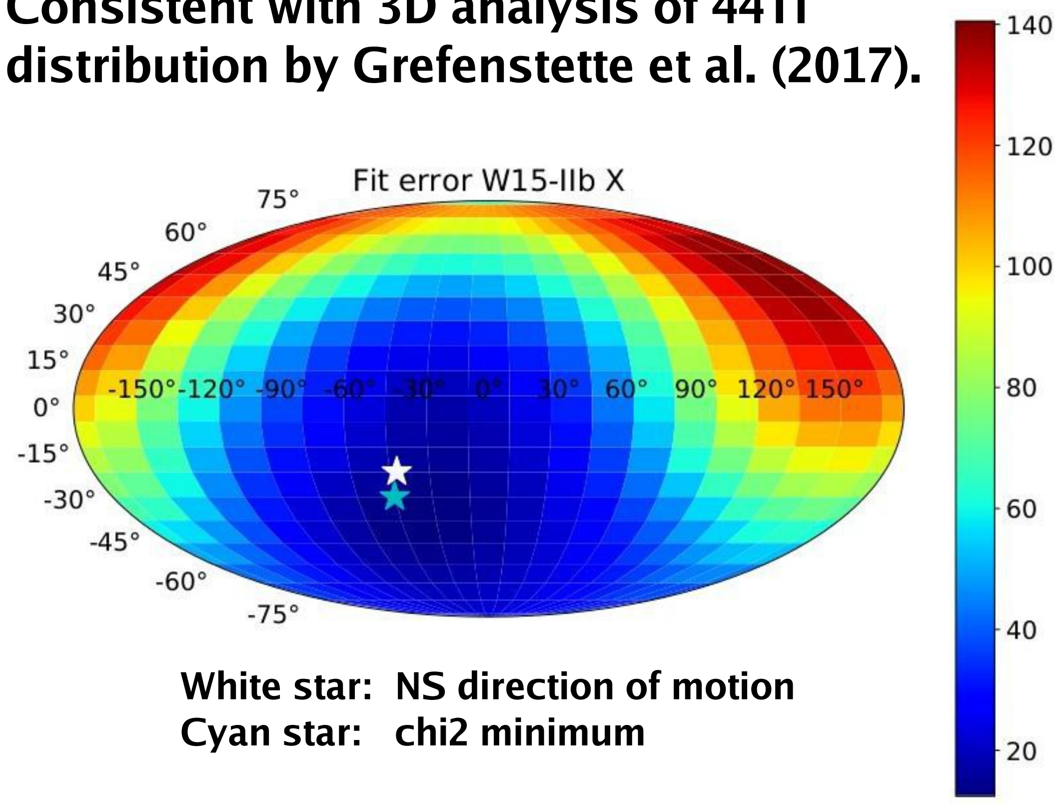

White star: NS direction of motion
Cyan star: chi2 minimum

Jerkstrand et al., MNRAS 494 (2020) 2471

Observed 3D ^{44}Ti Distribution in CAS A

CAS A "Thick Disk"

Grefenstette et al., ApJ 834 (2017) 19

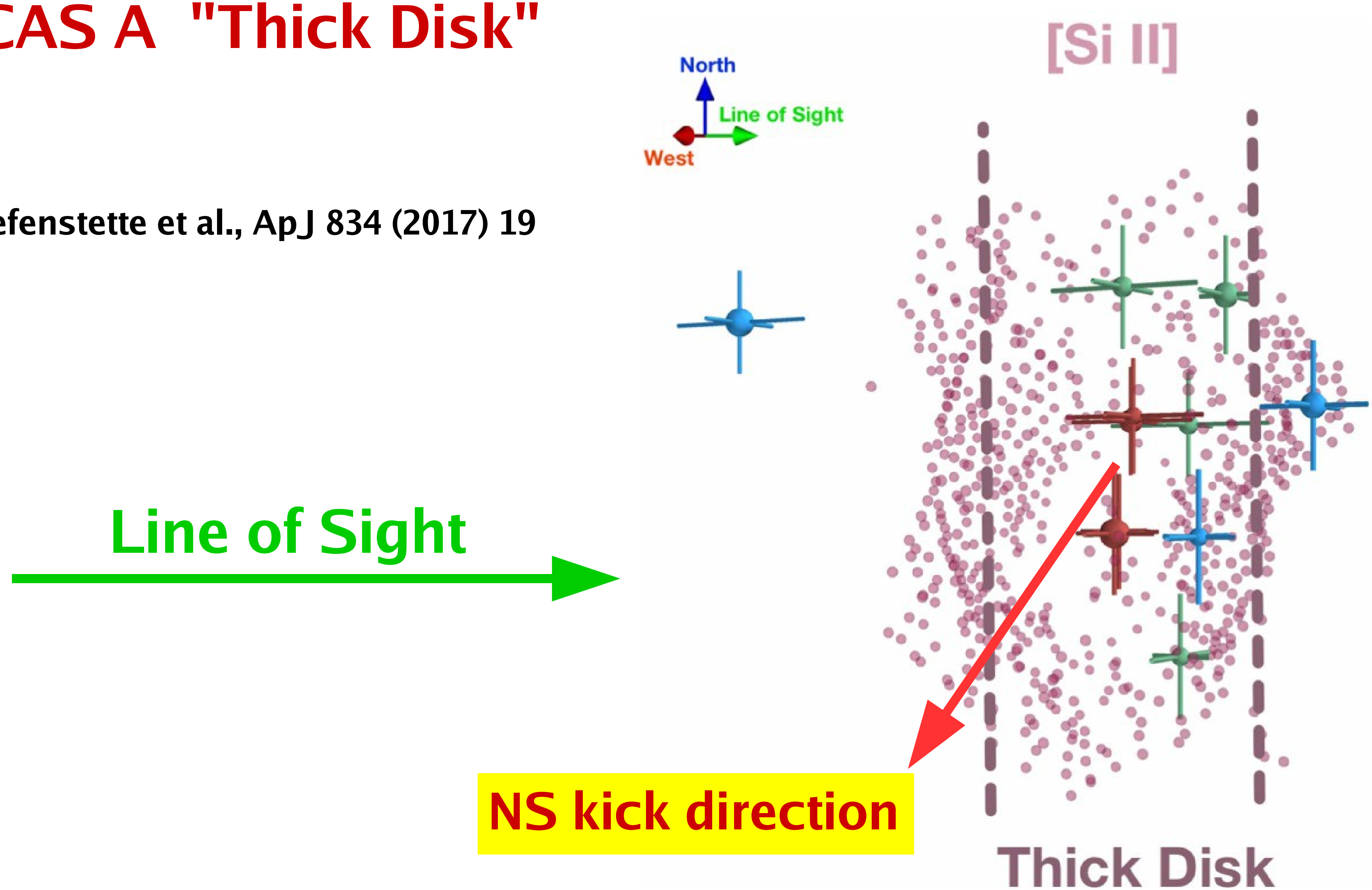

Figure 12. The 3D distribution of the observed ^{44}Ti ejecta compared with the IR [Si II] emission observed by *Spitzer* (DeLaney et al. 2010). The ^{44}Ti ejecta

Thick Disk Structure of CAS A Model

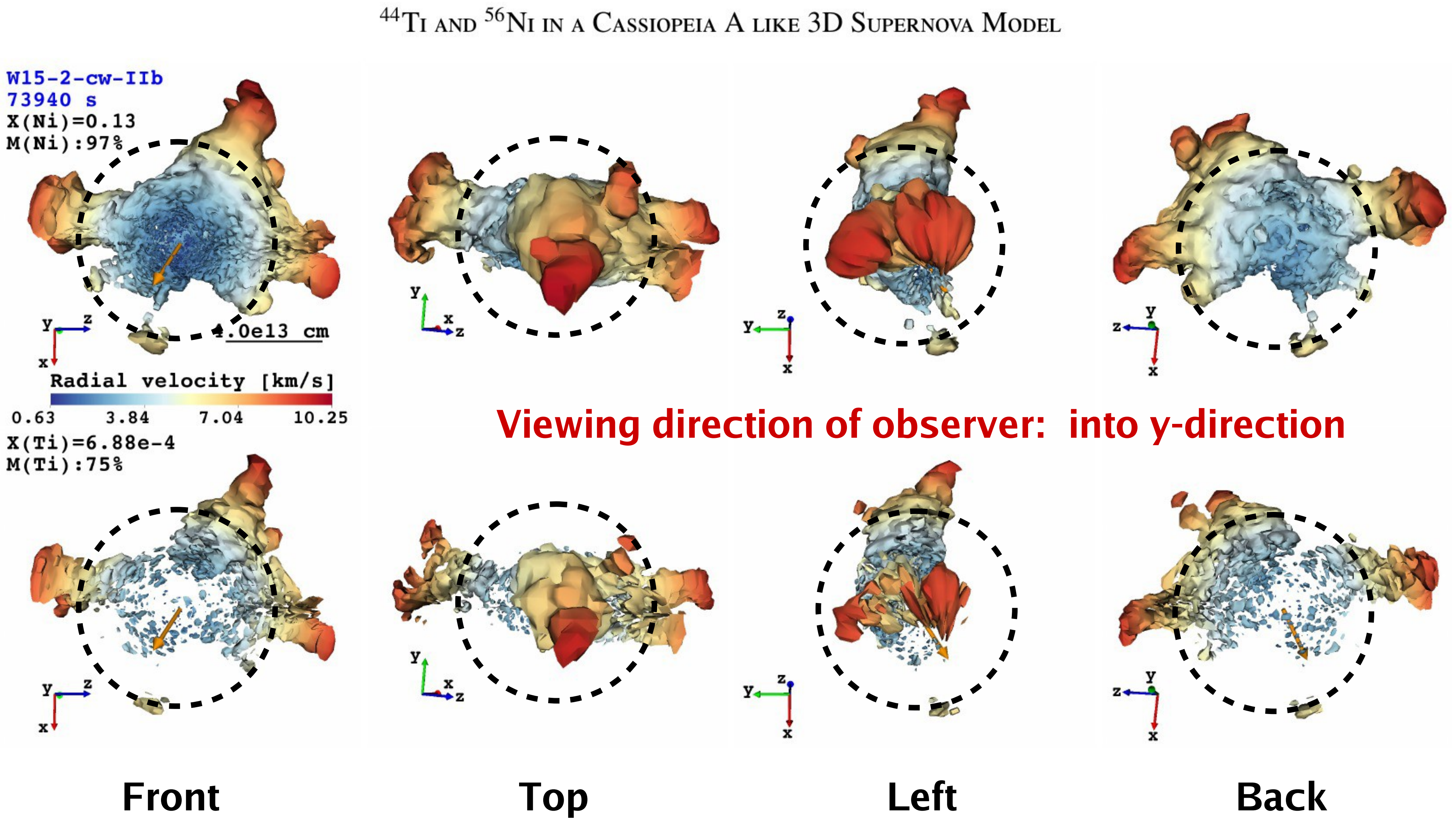

Wongwathanarat et al., ApJ 842 (2017) 13

Evolution of 3D Supernova Model of CAS A into the Remnant Stage

Morphology of the remnant and distribution of chemical elements is affected by Rayleigh-Taylor instabilities growing between forward shock and reverse shock

CAS A evolution until ~1600 years

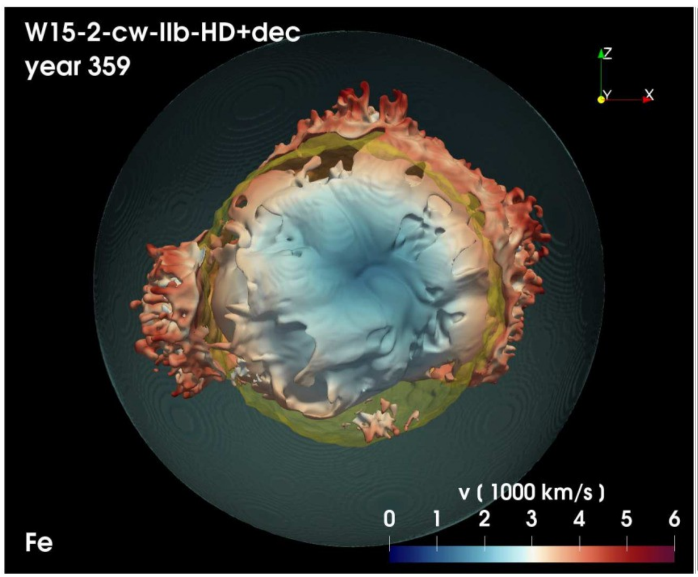

Isosurface of Fe for 5% of Fe peak density; radial velocity color coded

CAS A at ~360 years

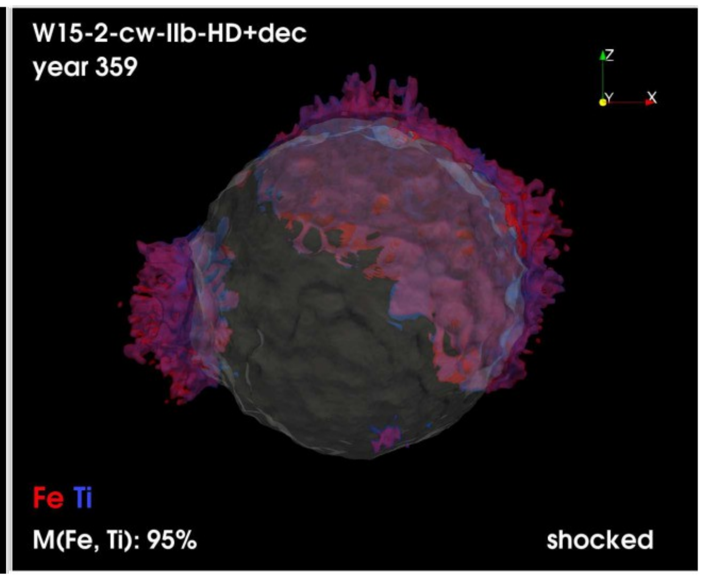

red: shocked Fe
blue: shocked Ti

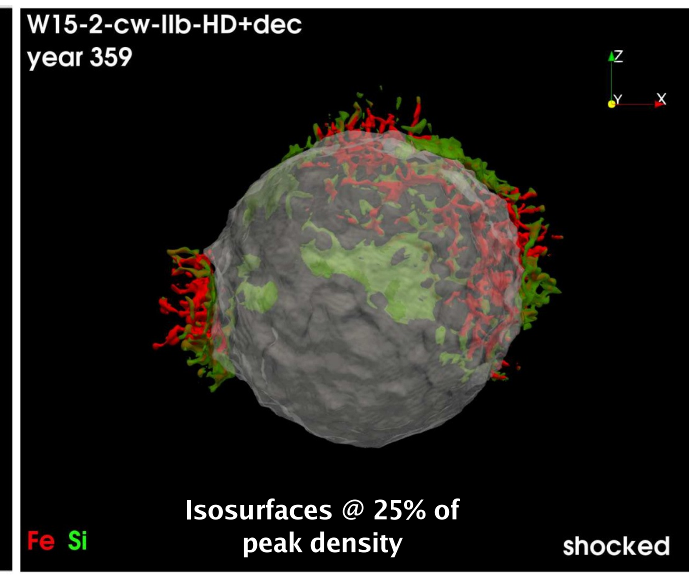

red: shocked Fe
green: shocked Si

Orlando, Wongwathanarat, HTJ, et al.,
A&A 645 (2021) 645

Evolution of 3D Supernova Model of CAS A into the Remnant Stage

EM = Emission Measure
kT_e = electron temperature
$n_e t$ = ionization age

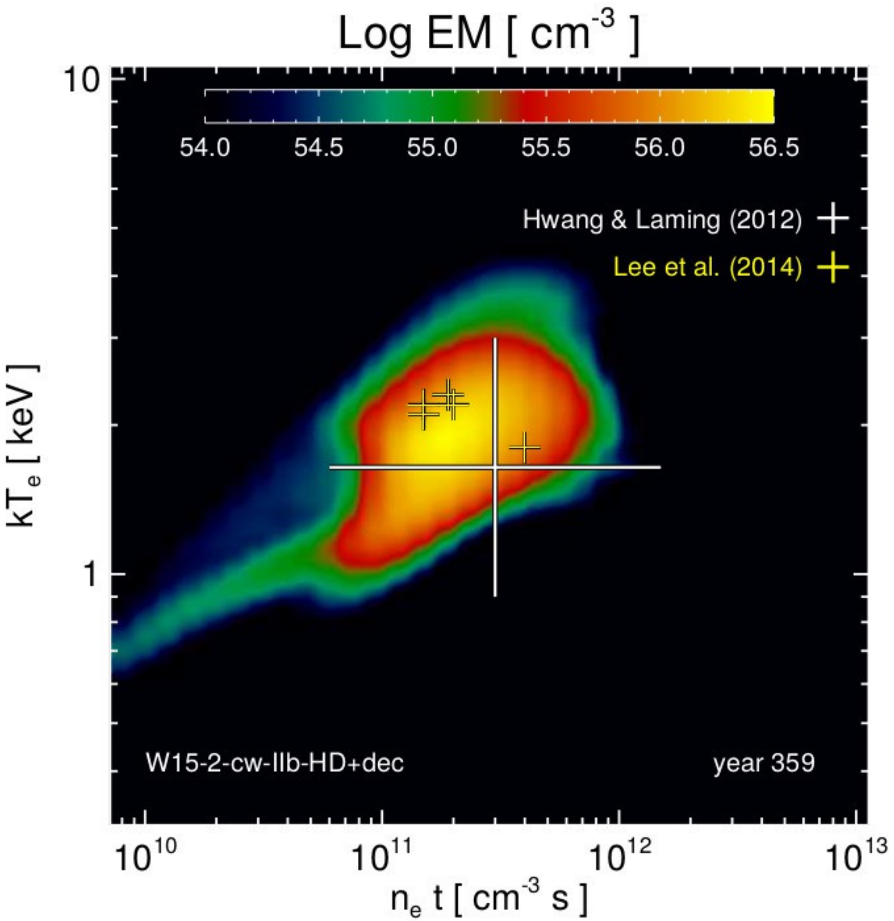

CAS A at 360 years

Fig. 18: Distribution of emission measure vs. electron temperature (kT_e) and ionization age ($n_e t$) at the epoch of Cas A derived from model W15-2-cw-IIb-HD+dec compared with the results of *Chandra* X-ray observations. The large white cross marks the ranges of kT_e and $n_e t$ derived from an X-ray survey of ejecta in Cas A (Hwang & Laming 2012); the small yellow crosses mark the values inferred from the analysis of regions dominated by thermal emission of shocked ambient gas (Lee et al. 2014).

Orlando, Wongwathanarat, HTJ, et al., A&A 645 (2021) 645

Cas A "Jets" ?

Sulfur, silicon rich knots, moving with speeds up to ~15,000 km/s

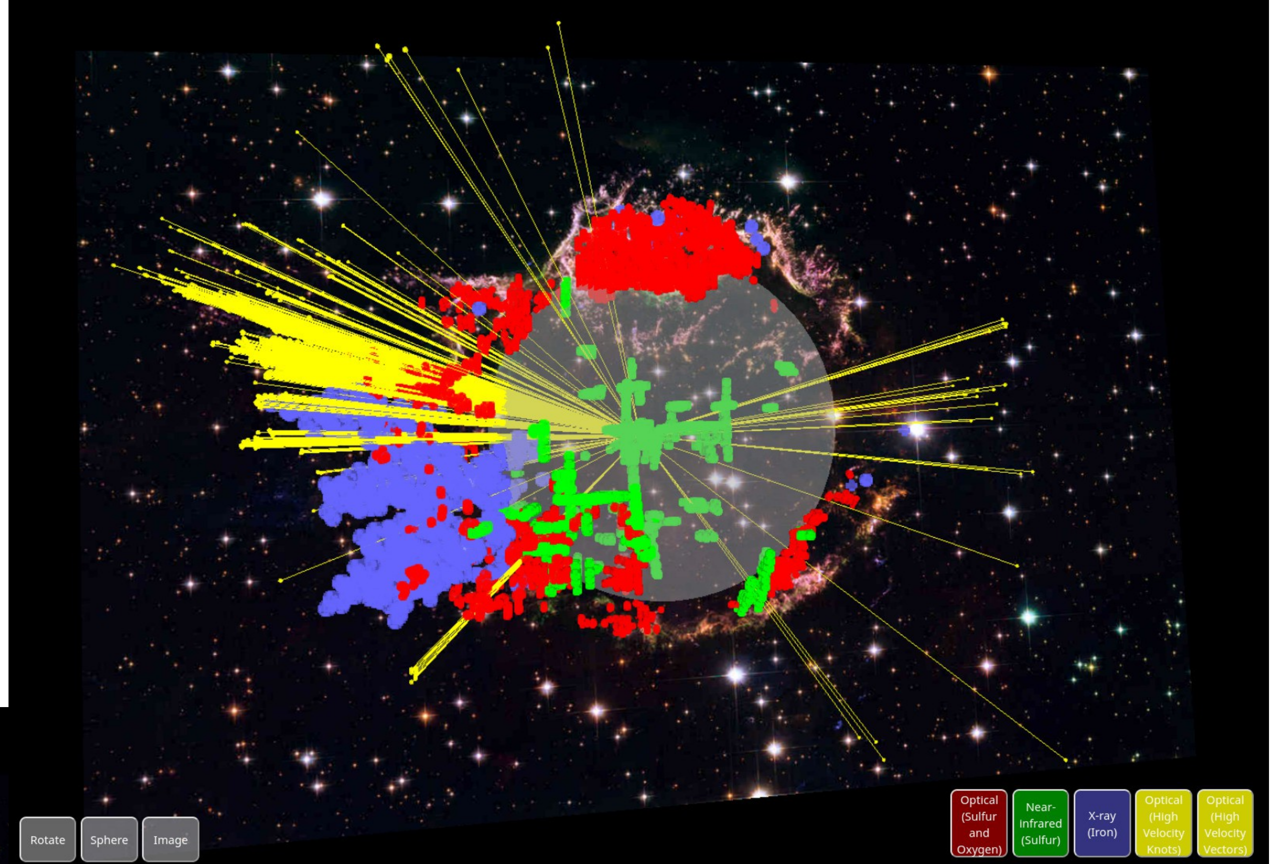

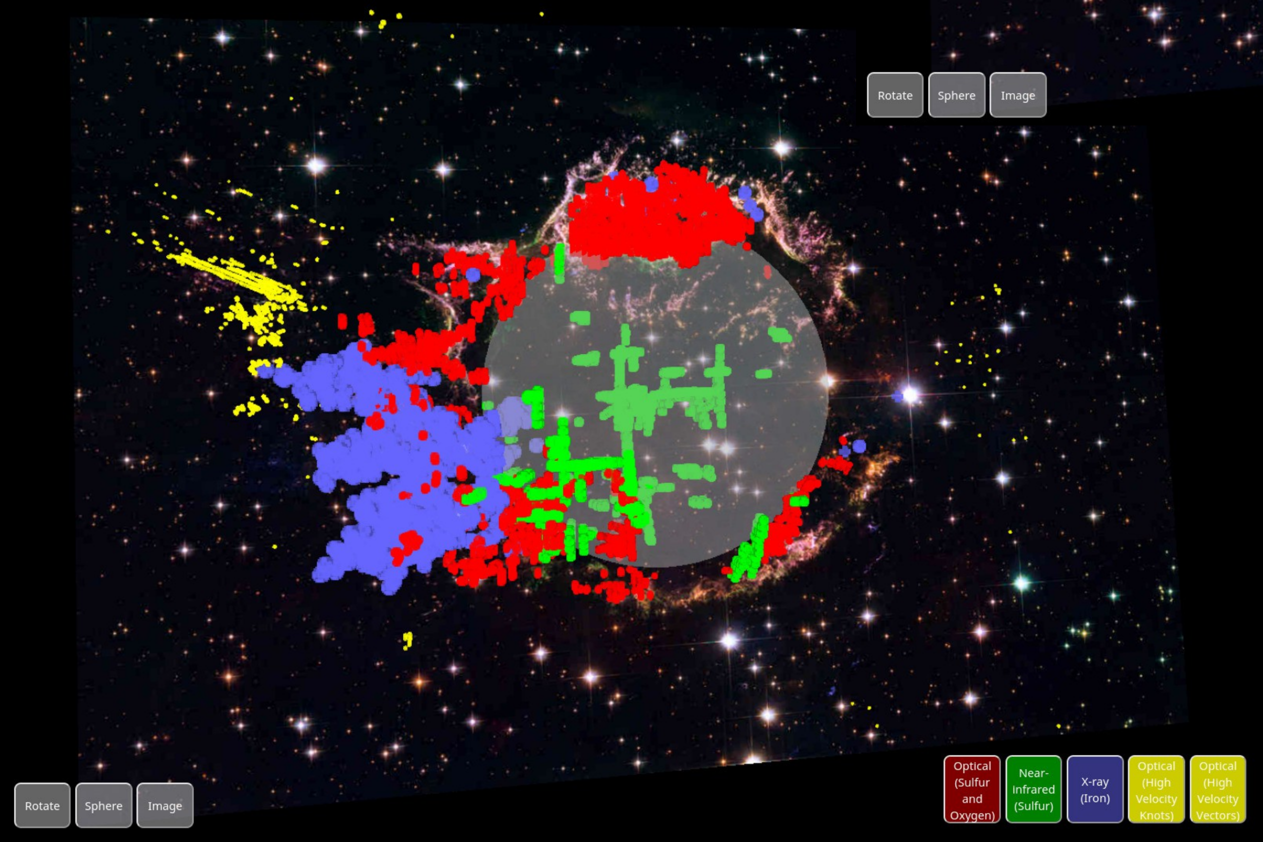

Danny Milisavljevic, Purdue Univ.
https://www.physics.purdue.edu/kaboom/casa-webapp/model.html

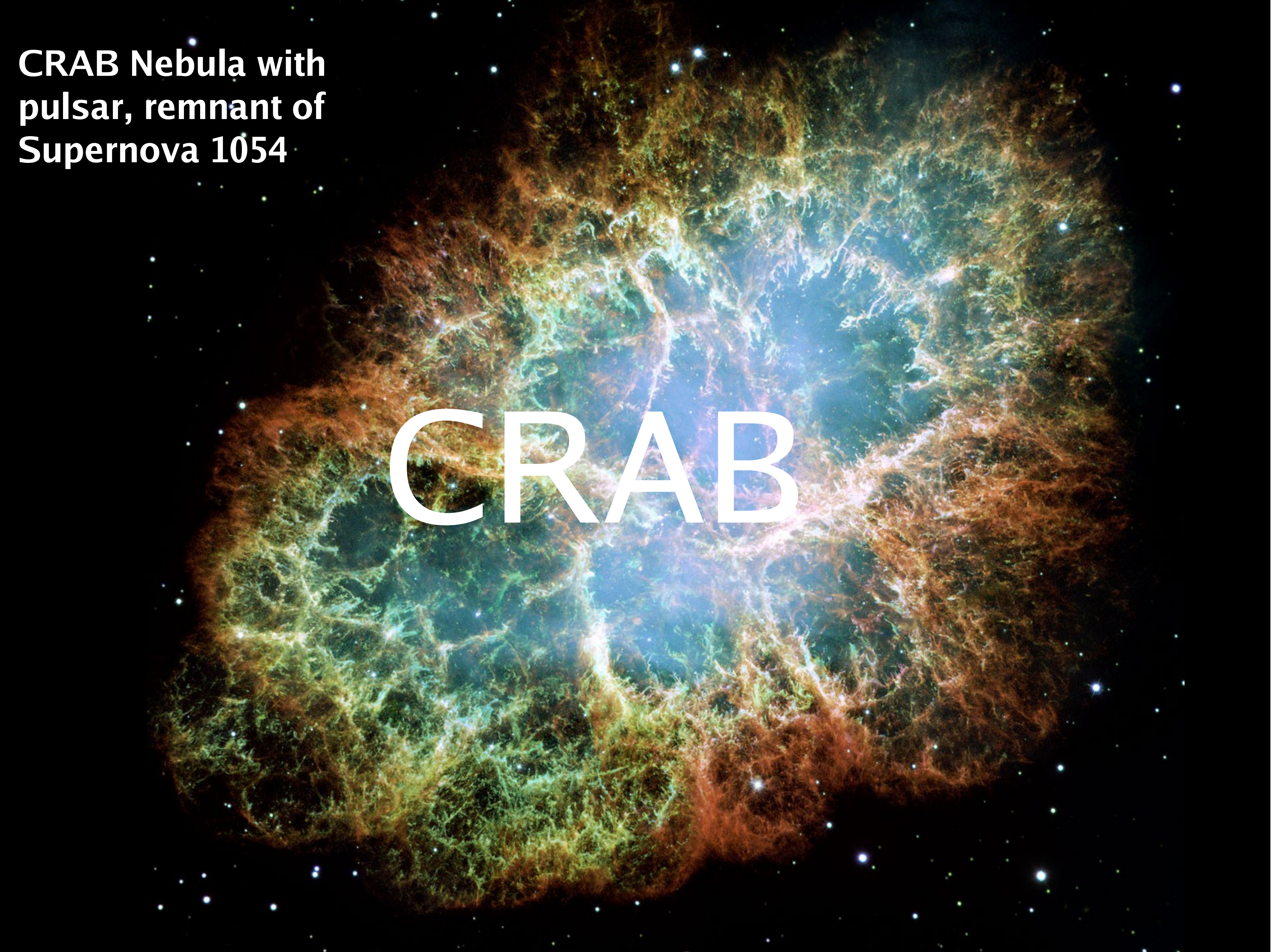
CRAB Nebula with
pulsar, remnant of
Supernova 1054
CRAB

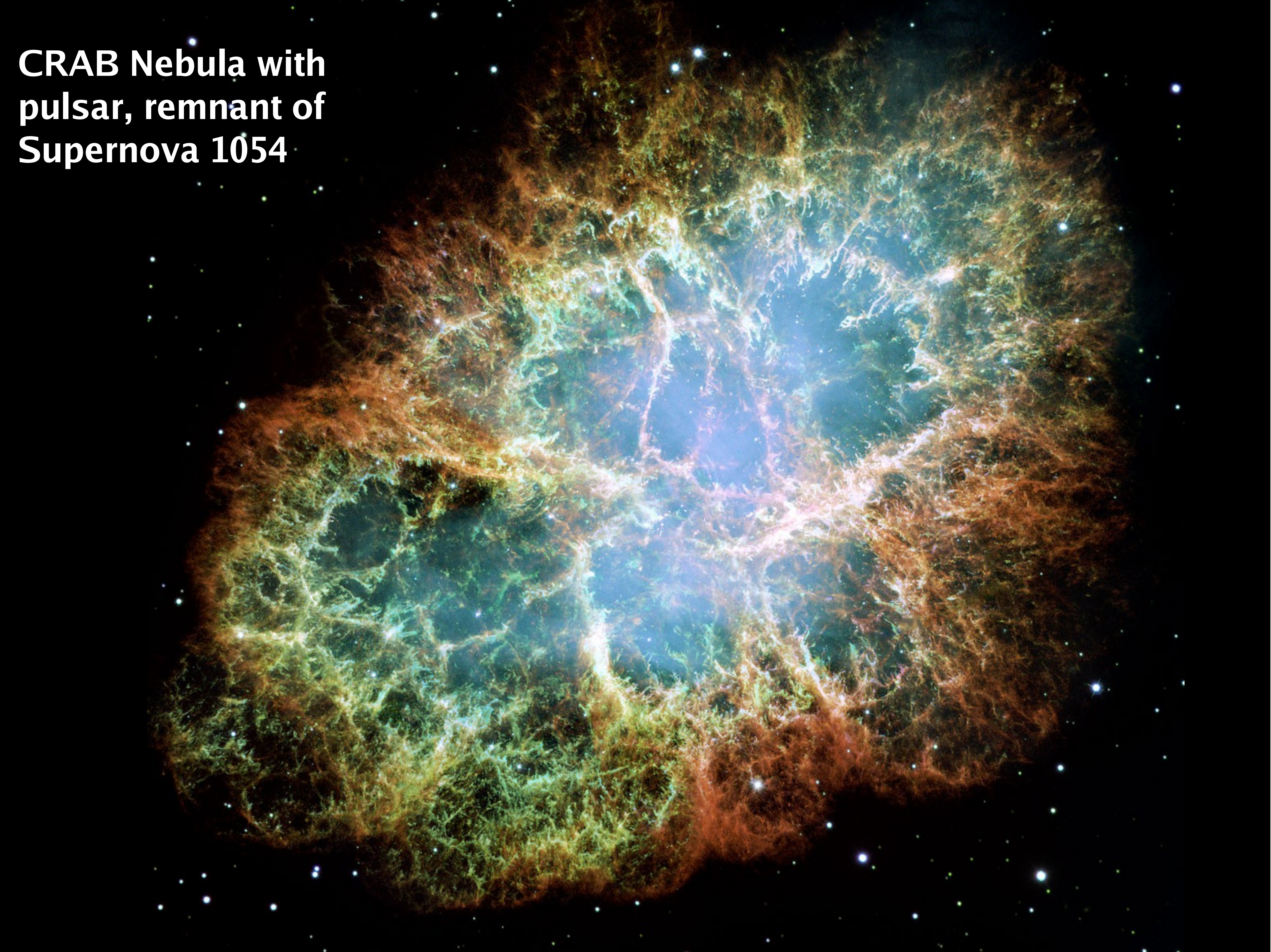
CRAB Nebula with
pulsar, remnant of
Supernova 1054

9 M_{sun} Fe-core SN

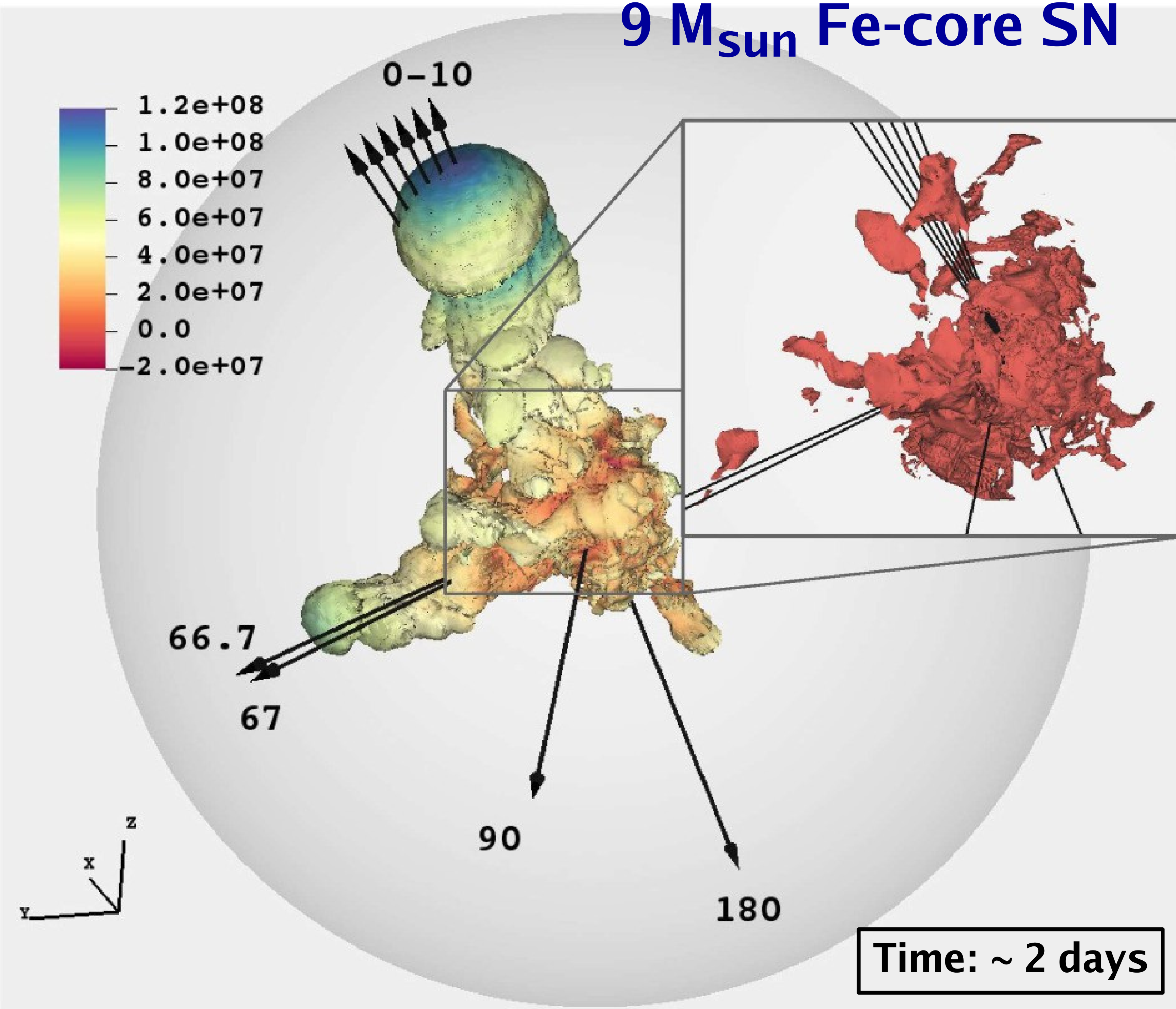

Time: ~ 2 days

(Stockinger et al., MNRAS 496 (2020) 2039
Kozyreva et al., MNRAS 514 (2022) 4173)

"Crab-like" Supernovae 2005cs & 2020cxd

Low-mass, low-energy supernovae from Fe-core progenitors

Multi-band light curves from 3D explosion models agree very well with observations!

Progenitor ~9 M_{sun} with Fe-core

- Explosion energy: ~7*10^{49} erg
- Ni+Fe mass: ~3*10^{-3} M_{sun}
- Ejecta mass: ~7.4 M_{sun}

Kozyreva et al., MNRAS 514 (2022) 4173

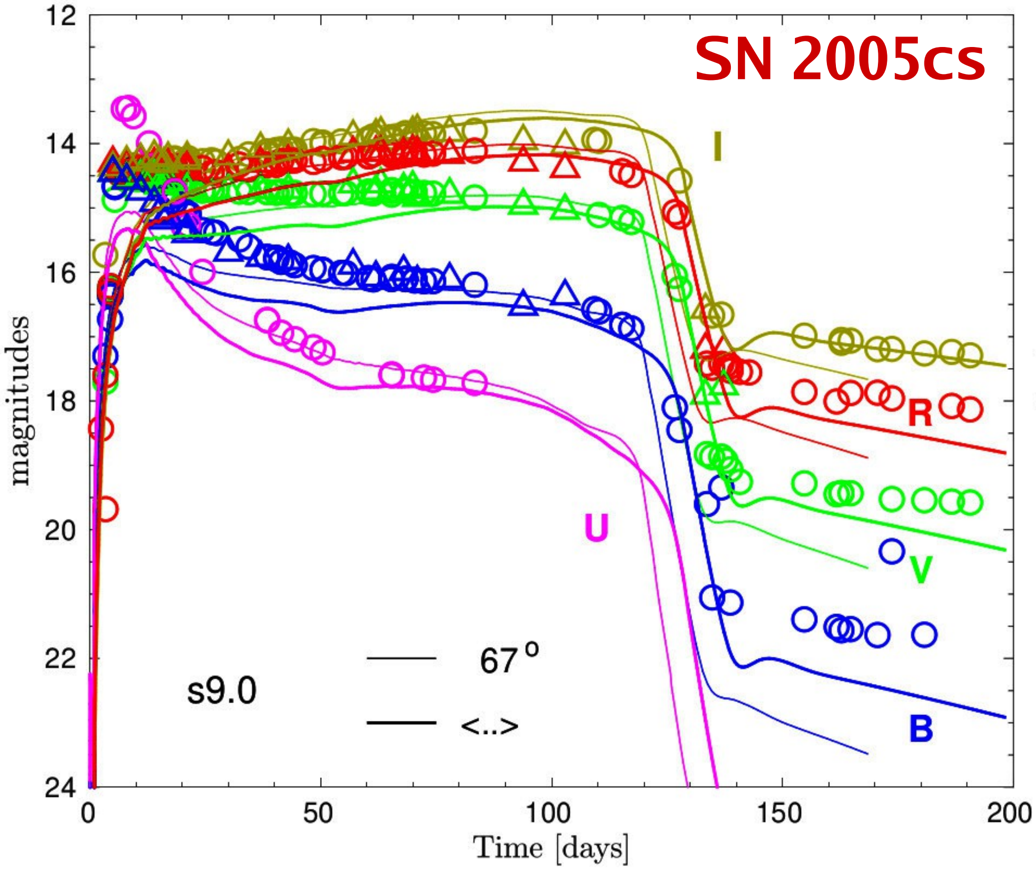

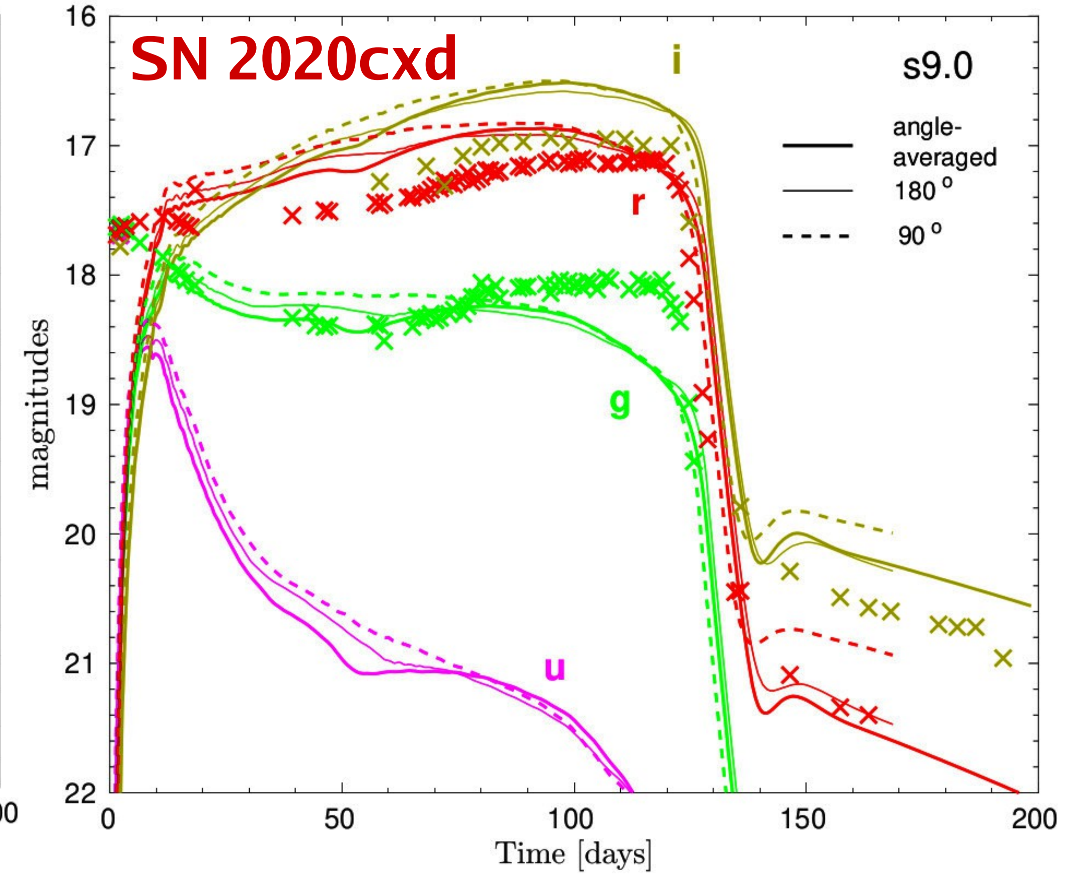

Nebular Spectra of Neutrino-driven Low-energy Explosion of 9.0 M_{sun} Fe-core Progenitor

Jerkstrand et al., MNRAS 475 (2018) 277

Spectra and line profiles of 1D explosion model:

Good agreement with SN 1997D and SN 2008bk; SN 2005cs unclear

All cases show clear O and He lines and no high ^{58}Ni/^{56}Ni ratio

ECSNe disfavored; explosions of low-mass Fe-core progenitors more likely

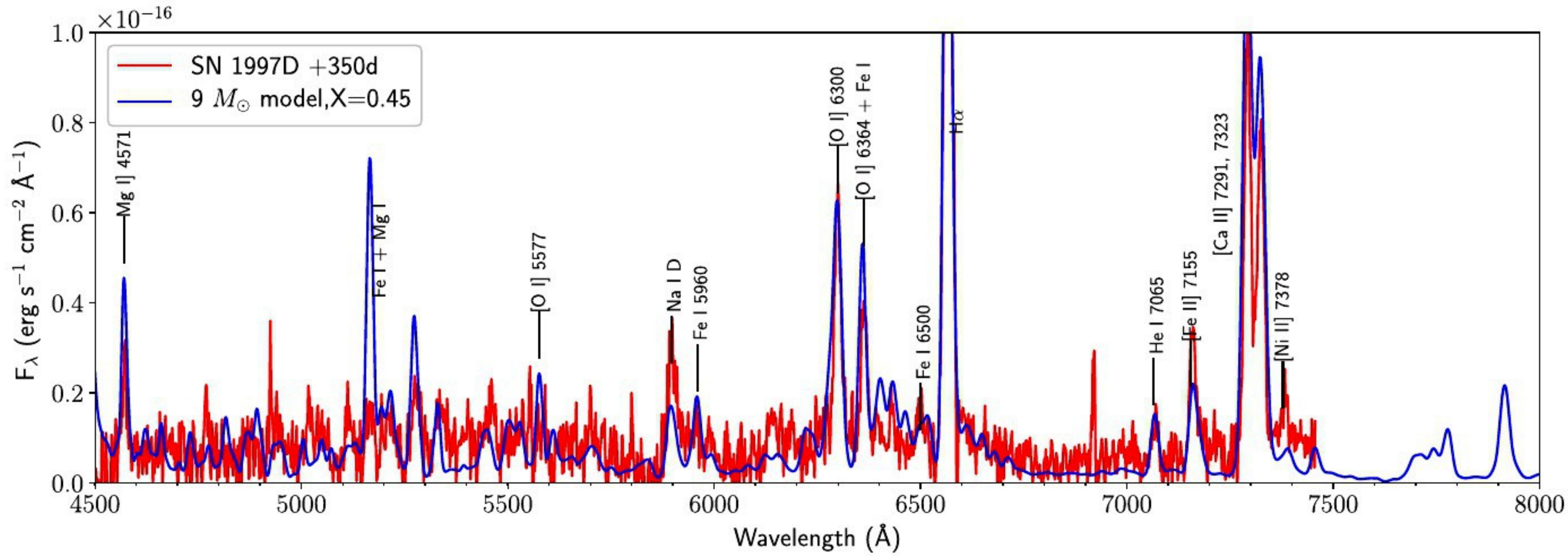

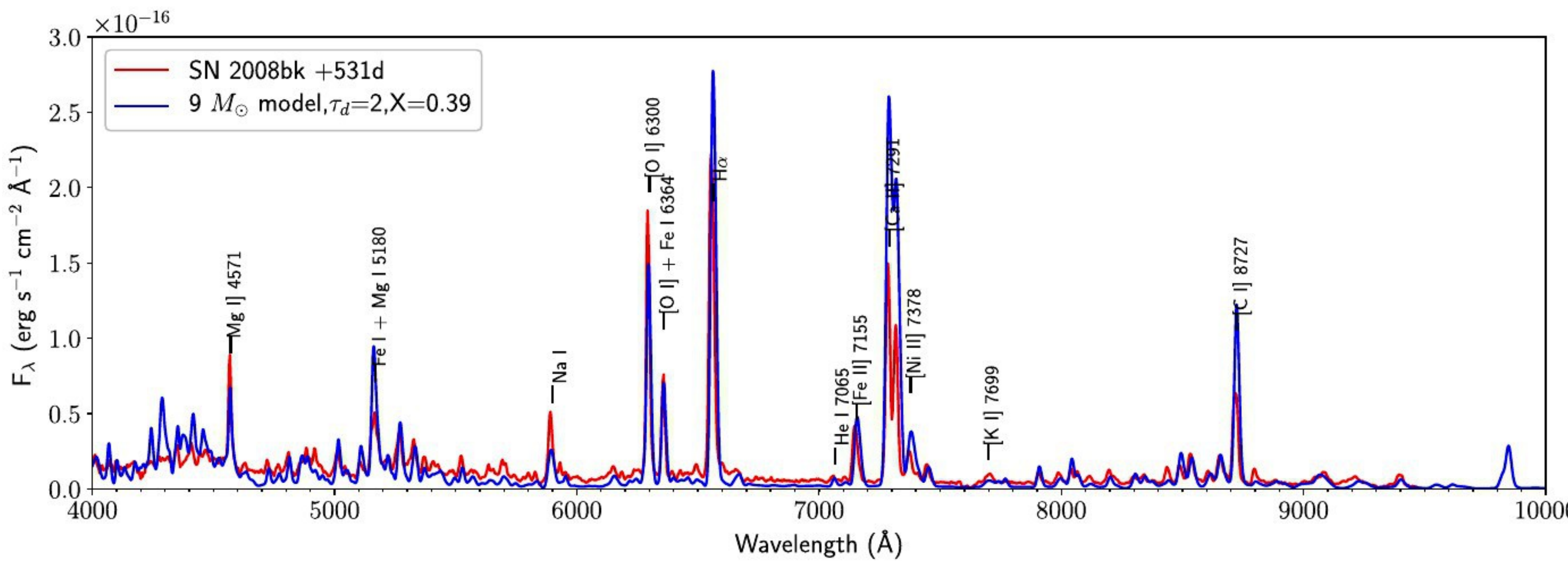

Low-energy Supernovae Constrain Radiative Particle Decays

Energy deposition by radiative decays of axion-like particles (ALPs) must not over-power low-energy, low-luminosity SNe

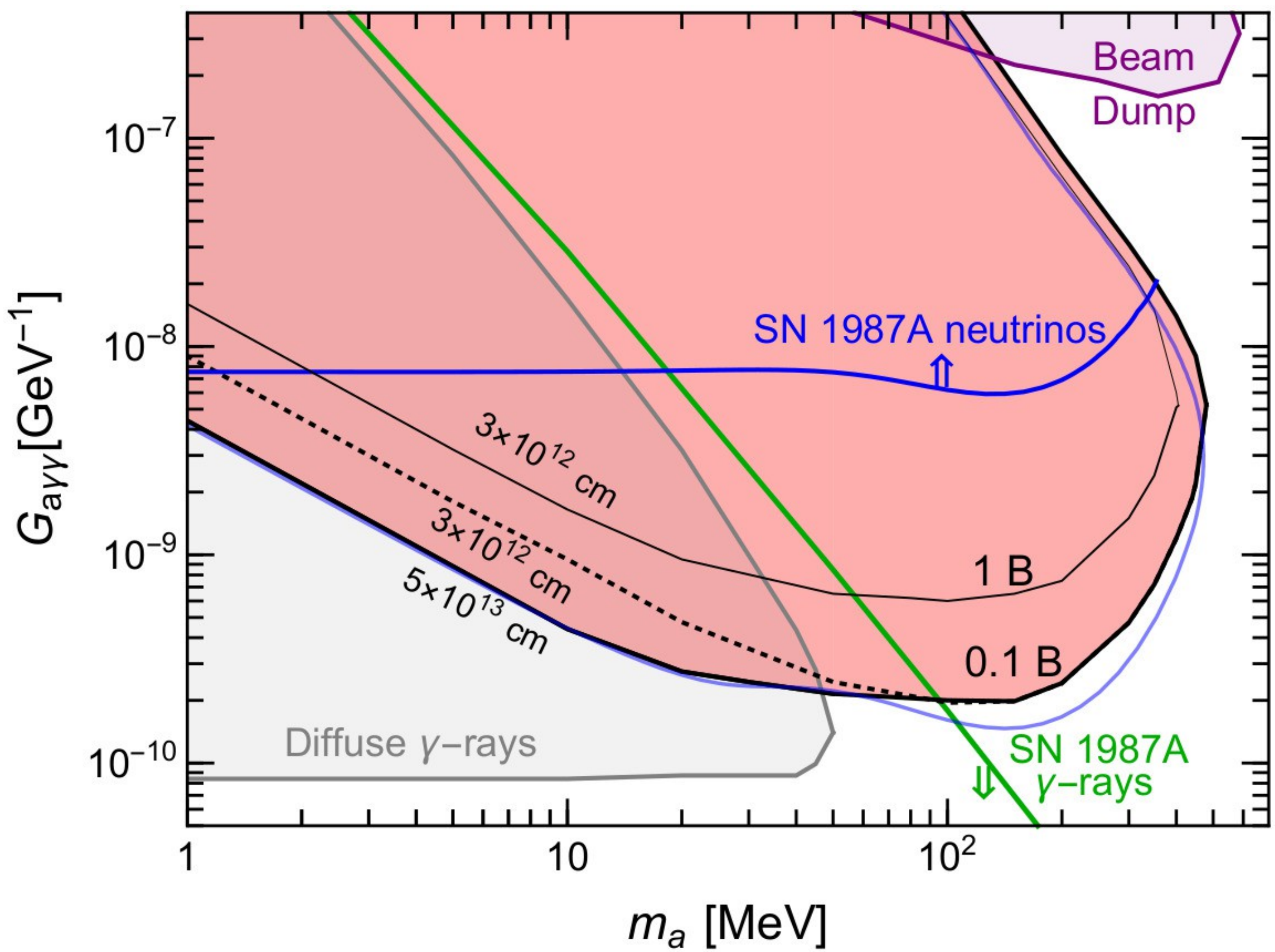

Caputo, THJ, et al., PRL 128 (2022) 221103

General overview of new physics and SN ν's: Manibrata Sen's talk of 05/29!

3D Neutrino-driven Explosion Models
Confronted with Observed Supernovae and Remnants

- Yield saturated explosion energies on time scales of seconds
- Match light curve and gamma-ray lines of SN 1987A
- Permit prediction of neutron star location in SN 1987A
- Explain multi-band light curves of low-energy SNe like Crab
- Reproduce 3D morphology and gamma-ray lines of Cas A

Conclusions

Neutrino-driven Explosions in Supernova Simulations

- Ab initio, self-consistent 2D and 3D simulations demonstrate viability of delayed neutrino-driven explosion mechanism

- Multi-D models of neutrino-driven explosions are sufficiently mature to test them against observations

- Problems and unsolved questions, e.g.:
  - * Results from different groups differ significantly
  - * Nuclear equation of state in (hot) neutron stars
  - * Neutrino flavor oscillations in dense environments
  - * Relevance of rotation and strong magnetic fields
  - * Progenitor-explosion systematics in 3D
  - * Effects of fallback and post-explosion accretion